

Cochleates: New insights into drug delivery system



seit 1558

Dissertation

To fulfill the requirements for the degree of

'Doctor rerum naturalium' (Dr. rer. nat.)

Submitted to

Council of the Faculty of Biology and Pharmacy of

Friedrich Schiller University Jena

Submitted by Kalpa Nagarsekar

Master of Pharmaceutical Sciences

Born on 25th December 1984 in Mumbai, India

Cochleates: New insights into drug delivery system



seit 1558

Dissertation

zur Erlangung des akademischen Grades

„*Doctor rerum naturalium*“ (Dr. rer. nat.)

vorgelegt dem Rat der Biologisch-Pharmazeutischen Fakultät

der Friedrich-Schiller- Universität Jena

von Kalpa Nagarsekar

Master of Pharmaceutical Sciences

Geboren am 25.12.1984 in Mumbai, Indien

Reviewers

Reviewer 1: Emeritus Prof. Dr. Alfred Fahr
Friedrich Schiller Universität Jena

Reviewer 2: Prof. Dr. Sylvio May
North Dakota State University

Reviewer 3: Emeritus Prof. Dr. Gerrit Scherphof
University of Groningen

Date of defense: 2nd March 2016

Acknowledgements

Foremost, I would like to express my sincere gratitude to my advisor Prof. Fahr for giving me opportunity to be part of his research group and this project. I would always be thankful to him for his endless support, patience, guidance and motivation in pursuing this research throughout my Ph.D. I could not have imagined having a better advisor and mentor.

My sincere thanks also goes to Phospholipid research center, Heidelberg especially to Dr. Rebmann and Dr. van Hoogevest, who provided funding for this research project. Without their precious and liberal support it would not be possible to conduct this research. I would like to thank Prof. May for his guidance and suggestions. I absolutely admire his passionate attitude towards physics which encouraged me and provided with different perspectives over my project. I am also grateful to Prof. Schacher for his kind help in SAXS analysis and suggestions during manuscript preparation. Many thanks to Prof. Jandt who kindly availed us the cryo-SEM facility.

I am extremely thankful to Jana Thamm, Frank Steiniger and Mr. Wagner for sharing their valuable expertise and constant support extended to me for microscopy studies. I would like to thank Christine Kämnitz, Susanne Linde, Walter Richter and Sandor Nietzsche from Electron microscopy center (EMZ), Jena for their kind help. Special thanks to Christine Steinbach, Ramona Brabetz, Alexander Mohn, Jessica Hiepe and Angela Herre for their help and support.

Heartfelt thanks to all my fellow labmates i.e. Erica D'Agvano, Stephan Holzschuh, Markus Rabenhold, Ronny Rüger, Gorge Pester, Maximillian Sperlich, Christiane Decker, Amaraporn Roopdee, Susann Schröder, Yaser Alkhatib, Kathrin Kaeß, Hossam Hefesha, Kewei Yang and Keda Zhang. Working in such multicultural and friendly environment was truly enjoyable and unforgettable experience. I also wish to thank Prof. Fischer's group and all current and past members of pharmaceutical technology department for wonderful times in lab and lunch breaks. Their discussions and insightful comments during lab meetings, conferences not only helped me understand my research more clearly but also allowed me to grow on personal level.

I would like to thank my family: my parents and my sister for their selfless and unconditional support throughout my life. Special thanks to my sister for trusting in me, even in times that I didn't. No words are probably enough to explain my gratitude to them.

Last but not the least, I will always be happily indebted to my husband/ part time colleague who kept me going, actively being my teacher, critic and friend, who stood by me for all difficult situations as my strength. Without him I wouldn't have achieved to be at this stage.

Table of contents

1	Introduction	1
1.1	Discovery of cochleates:	1
1.2	Materials for cochleate formation	2
1.3	Basic structure of cochleates:	2
1.4	Advantages of cochleates	4
1.5	Theoretical aspects of mechanism of drug release from cochleates	4
1.6	Methods for preparation of cochleates:	5
1.6.1	Trapping method:	5
1.6.2	Dialysis method:	6
1.6.3	Hydrogel isolation method	6
1.6.4	Emulsification-lyophilization method	6
1.6.5	Solvent injection method:	6
1.7	Characterization of cochleates:	7
1.7.1	Evaluation of morphology and dimensions of cochleates	7
1.7.2	Differential scanning calorimetry (DSC)	7
1.7.3	Fourier transform infrared (FT-IR) spectroscopy	8
1.7.4	X-ray analysis:	8
1.7.5	Nuclear magnetic resonance (NMR)	9
1.8	Applications of cochleates	9
1.8.1	Pharmaceutical industry	9
1.8.2	Food industry	10
1.8.3	Cosmetic industry	11
1.8.4	Perfume industry	11
1.9	Aim of the study	12
2	Publication overview	13
3	Publications	16
3.1	Publication 1:	16
3.2	Publication 2:	41
3.3	Publication 3	51
4	Discussion	81
4.1	General discussion:	81
4.1.1	Investigation on formation of cochleates:	81
4.1.2	Structural features of cochleates:	83
4.1.3	Effect of ethanol on formation of cochleates:	85
4.2	Conclusions and potential applications of this study	86

4.3	Future prospects of cochleates:	87
5	Summary	89
6	References.....	93
	List of Abbreviations.....	100
	Curriculum Vitae.....	101

1 Introduction

1.1 Discovery of cochleates:

The transition of negatively charged lipids from the liquid-crystalline to the gel state due to ionic interaction has been intensively investigated in past decades (Papahadjopoulos et al., 1973; Träuble and Eibl, 1974). This interaction leads to major morphological transformation into a rolled up cylindrical structure that were noted by Verkleij and coworkers during morphological evaluations in 1974 (Verkleij et al., 1974; Ververgaert et al., 1975). These cylindrical structures were also observed by Dr. D. Papahadjopoulos and co-workers while developing method for formulation of large vesicles (Papahadjopoulos and Kimelberg, 1974; Papahadjopoulos et al., 1975), at an intermediate stage, who named them 'cochleates' in 1975 (Papahadjopoulos, 1978). The term cochleate originates from Greek term for 'snail with spiral shell' which corresponds to the folding pattern of cylinders (Figure 1.1). Cochleates are formed due to self-assembly of negatively charged lipid bilayers and cations. Self-assembly at molecular level can be described as a process in which spontaneous arrangement of molecular subunits results into formation of ordered structures with properties unlike their precursors (Zhang, 2003). During cochleate formation positively charged binding agent and lipid head group interacts in order to form hierarchical superstructures (Poste et al., 1976). The interactions involved in this process are usually of non-covalent nature (e.g. electrostatic interactions, Van der Waals forces, hydrogen bonds, hydrophobic interactions etc.). This process finally results in formation of highly ordered cochleates from structures with less ordered states.

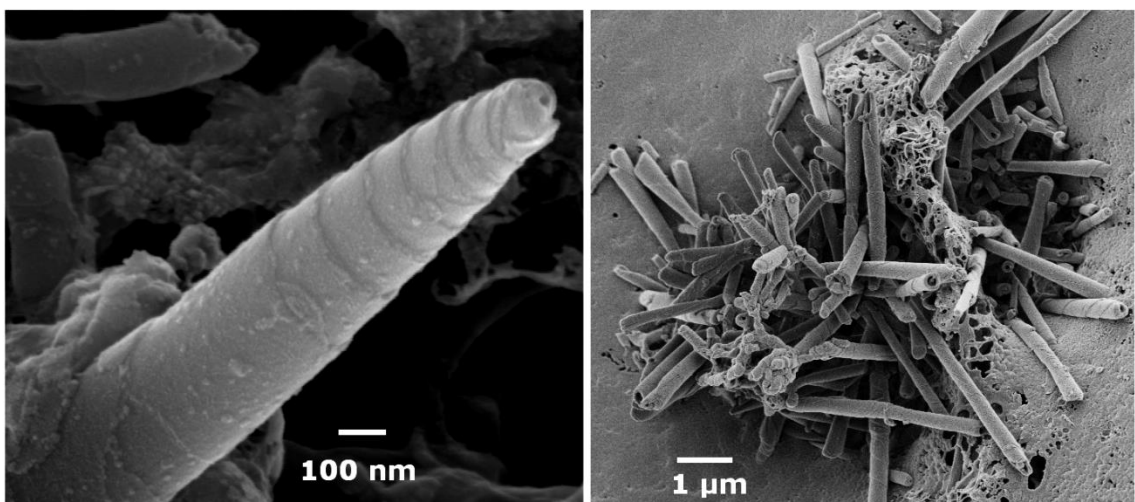


Figure 1.1: Cryo scanning electron micrograph of calcium cochleates of a) DMPS displaying folding pattern (figure from unpublished data) and b) DOPS showing cylindrical morphology (figure reported in article 1 of this thesis).

1.2 Materials for cochleate formation

Lipids: Naturally occurring phospholipids have often been used for preparation of cochleates. Most commonly used classes are anionic phospholipids e.g. Phosphatidic acid (Kouaouci et al., 1985), Phosphatidylethanolamine (Sarig et al., 2011), Phosphatidylinositol and Phosphatidylglycerol (Garidel et al., 2001), phosphatidylserines (PS) etc. Until the last two decades cochleate systems were mainly synthesized from mixtures of lipids viz bovine brain PS (Papahadjopoulos, 1978), Porcine brain PS, Soya PS (Zarif and Tan, 2003) etc. More recently pure synthetic lipids like 1,2-dioleoyl-*sn*-glycero-3-phospho-L-serine (DOPS) have been used in studies to incorporate drugs (Zarif et al., 2000). There are also reports regarding formation of cochleates from neutral lipids. Galactosylceramides (Kulkarni et al., 1999), sphingosines (Archibald and Mann, 1993) have been evaluated in past for their ability to produce cochleates. In 2010 cholesterol cochleates were synthesized by Harris et al. using ethanol injection method (Harris et al., 2011).

Binding Agents: Metal cations are commonly used as binding agents for cochleate formation. Divalent cations like Ca^{+2} , Mg^{+2} , Ba^{+2} and Zn^{+2} have been used in the past as binding agents with negatively charged phospholipids (Loomba and Scarabelli, 2013). Amongst these calcium is reported as most potent cation for cochleate formation (Papahadjopoulos et al., 1978). Monovalent ions like Na^{+} have also served as binding agents for cochleate formation from phosphatidylglycerols (Garidel et al., 2001). Organic cations like drugs or antimicrobial agents e.g. Oligo-acyl-lycyls (Sarig et al., 2011), 2,3,5,6-tetraaminopyrimidine, tobramycin, and polylysine have been employed for cochleate formation from anionic phospholipids (Jin, 2004). Cochleate formation from lipids like galactocerebroside in absence of binding agents has also been reported. In these cases the conversion of acyl chains to gel state and cochleation were initiated due to use of non-aqueous solvents and temperature fluctuations (Archibald and Yager, 1992).

1.3 Basic structure of cochleates:

Cochleates have a peculiar multilamellar structure (Figure 1.2) which imparts them extraordinary stability. Interaction of negatively charged bilayers with cations result in substantial structural rearrangement that causes aggregation and fusion of bilayers. This interaction triggers conversion of aliphatic acyl chains in lipid bilayer into gel state (Jacobson and Papahadjopoulos, 1975). The resulting planar bilayer sheets consist of lipid and binding agent in molar ratio of 2:1 (Bangham and Papahadjopoulos, 1966). These crystallized planar sheets further tightly fold upon to form cylindrical carpet roll like structure. Hence a typical cochleate is made up of sheets consisting alternating layers of binding agent and lipid bilayer (Rao et al., 2007).

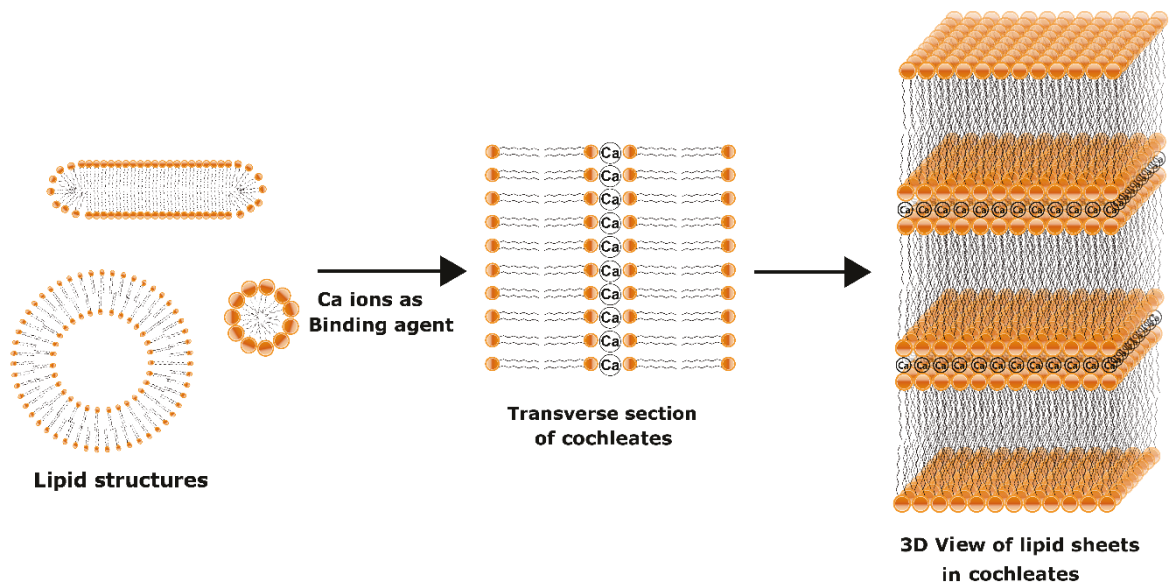


Figure 1.2: Diagrammatic representation of structure of cochleates, with close view of organization of lipid molecules before and after interaction with of calcium ions (binding agent)

Molecules with different properties viz. hydrophobic, hydrophilic, charged etc. are known to associate with cochleates and their incorporation into cochleates has been explained theoretically by Zarif et al. (2005). The schematic diagram in Figure 1.3 explains the possible embedding of molecules with different properties. As per this theory the hydrophobic molecules will get entrapped in lipid chains to minimize interaction with water (Figure 1.3a). Amphiphilic molecules may have higher probability to fit perfectly between bilayer with their hydrophobic and hydrophilic regions aligned with lipid molecules (Figure 1.3b). Whereas the charged molecules can partition into interbilayer domains (Figure 1.3c and d) since charged interactions with lipids and binding agent can promote the encapsulation.

Although entrapment of the molecule is highly defined by its nature the shape of molecule is also an important parameter. It has been observed that hydrophobic and linear molecules are best candidates to get incorporated in cochleates. Whereas small neutral hydrophilic molecules have lower chances of getting incorporated into cochleates considering hydrophobic nature of cochleates.

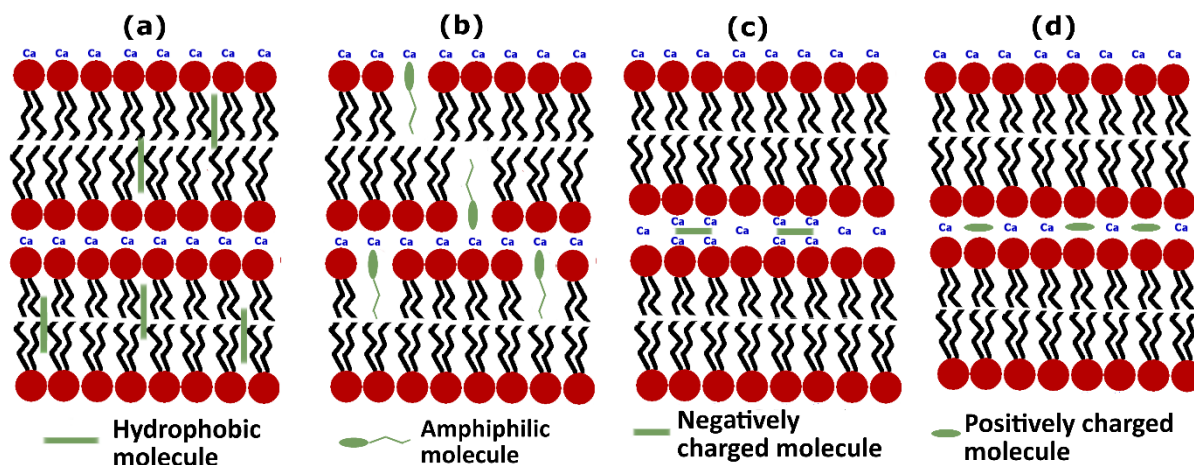


Figure 1.3: Diagrammatic representation of organization of A) hydrophobic B) amphiphilic C) negatively charged and D) positively charged drug molecules in cochleates based on their nature (reproduced from (Zarif, 2005)).

1.4 Advantages of cochleates

Cochleates are comprised of well tolerated and non-immunogenic excipients which are of natural origin (Ramasamy et al., 2009). The building blocks of cochleates such as phosphatidylserines impart additional benefits such as improved cognitive functions, better immune function and antiaging benefits (Sankar and Reddy, 2010). Repeated oral and intra-peritoneal doses of cochleates to mice have shown that cochleates are well tolerated, not toxic and non-inflammatory (Gibson et al., 2004; Zarif and Mannino, 2002). Condensed framework of cochleates can facilitate in protection of associated molecules from harsh conditions such as extreme pH, proteolytic enzymes etc. The extremely hydrophobic nature of cochleate surface and resistance to oxygen penetration protects the internalized moieties from oxidation. Multilamellar structure of cochleates imparts them potential for slow release of drugs. All these advantages are mainly favorable for establishing oral efficacy of drugs which are prone to degradation in gastric environment. Cochleates can easily be produced on large scale. They are very stable formulations with long shelf life. They can remain stable over a year at room temperature in absence of aqueous medium, or over 2 years when refrigerated at 4 °C (Rao et al., 2007). They can retain their structure, shape, and function even after being subjected to processes such as lyophilization. Hence solid structure of cochleates can provide chemical as well as mechanical stability (Bozo et al., 2015) and increase the shelf life of fragile susceptible molecules (Rao et al., 2007).

1.5 Theoretical aspects of mechanism of drug release from cochleates

Mechanism of action of cochleates is not completely understood at cellular or tissue level in biological systems. When administered in body, supramolecular and crystalline structure of the cochleates may

provide protection to the encochleated molecules from the hostile environments. This could facilitate the components within the interior of the cochleate to remain intact, even though the outer layers of the cochleate are exposed to degradation (Mannino and Gould-Fogerite, 1995). Hence, gradual digestion of cochleate may take place leading to slow release and enhanced absorption. In results of cell line studies, cochleates containing fluorescent probes have been shown to bind to the plasma membrane (Gibson et al., 2004). One of theories put forth for explanation of uptake studies considers phagocytic processes for cell internalization. Cochleates with smaller dimensions or their fragments may be taken up by endocytosis in active phagocytic cells and release the contents gradually in cell cytoplasm. In course of time concentration gradient between cochleate and endocytic vesicle may cause calcium to leach out facilitating release of the contents within the endocytic vesicle. Another theory for mechanism of action is based on the fact that calcium ions and phospholipids play pivotal roles in naturally occurring membrane fusion events. This probably increases chances of interaction between cell surface and calcium rich cochleates. During close encounter the outer layer, edge or end of the cochleate and the cell membrane might undergo fusion. As a result encochleated material may be transferred onto cell membranes and eventually be released into the cytoplasm of the cell. The cochleate could then separate from the cell and undergo another fusion event, with the same or another cell. Hence the contact of the cochleate system with the mucous membrane may facilitate in drug absorption (Rao et al., 2007).

1.6 Methods for preparation of cochleates:

1.6.1 Trapping method:

Papahadjopoulos reported preparation of PS-Ca cochleates by trapping method (Papahadjopoulos et al., 1975) i.e. simple mixing of aqueous suspension of lipid and binding agent in molar ratio of 2:1. Trapping method involves the formation of lipid dispersion viz liposomes, micelles etc. as initial step. This is followed by dropwise addition of a solution of binding agent like metal cations into lipid dispersion. Although it is a straight forward procedure it seldom offers narrow size distribution of the final product (Mannino et al., 2005; Zarif and Mannino, 2002). Some modifications such as solvent drip method have been used to improve the loading of active ingredients in cochleates. Briefly, in this modification the active ingredient is dissolved in solvents such as ethanol and added to liposomal suspension. This triggers transfer of active ingredient in higher concentration on liposomal bilayer and hence in cochleates precipitated from them (Mannino et al., 2014). In other modification, liposomes were prepared at higher pH by simple mixing of excipients and drug or by film hydration method in order to attain increase in entrapment. These liposomes were further subjected to cochleate formation by the trapping method (Zarif, 2005).

1.6.2 Dialysis method:

In this method cochleates are prepared by a process involving dialysis. First approach is called '*LC dialysis method*'. In this approach, small unilamellar vesicles are prepared from mixture of lipid and detergents using dialysis. These vesicles are then further subjected to a second dialysis step in presence of binding agent. The second approach is called '*DC dialysis method*'. In this approach, a mixture of detergent and lipids is directly dialyzed in the solution of binding agent. Both approaches necessitates use of detergent (e.g. Octyl β D glucopyranoside 2% w/v solution). Dialysis method forms cochleates with large dimensions (Gould-Fogerite and Mannino, 2000; Gould-Fogerite and Mannino, 1992; Papahadjopoulos, 1978; Zarif, 2002).

1.6.3 Hydrogel isolation method

Hydrogel isolation method utilizes a binary aqueous–aqueous emulsion system for producing small-sized cochleates from unilamellar vesicles. Liposomes are suspended in dispersed phase of an aqueous emulsion formed by immiscible polymer solution (e.g. Dextran-500000/PEG-8000). Further the solution of positively charged binding agent such as Ca^{2+} or Zn^{2+} is added to this emulsion. Slow diffusion of binding agent through polymer solution results in formation of cochleates with particle size in nano-range. The precipitate is then subjected to washing to get rid of polymers. This process can be used to produce cochleates containing drugs or biologically relevant molecules (Jin et al., 2001).

1.6.4 Emulsification-lyophilization method

This process involves formation of multiple emulsion. Briefly, lipid is dissolved in a solvent (viz. chloroform, cyclohexane) which is considered as the oil phase (O). A solution containing binding agent and cryoprotectant are used as the inner water phase (W1), and the buffer as the outer water phase (W2). At initial stage, a primary emulsion with submicron particle size is prepared with aid of probe sonicator using phase O: phase W1 in 3:1 ratio. This emulsion is further added as dispersed phase to five parts of aqueous phase (W2) and gently emulsified to form double emulsion of W1/O/W2. The resultant double emulsion is lyophilized and cochleates are formed on rehydration from lyophilized powder (Wang et al., 2014).

1.6.5 Solvent injection method:

Harris et al. and coworkers reported a method of preparation for cholesterol cochleates in 2011. In this study, ethanoic solution of cholesterol was rapidly injected and mixed with distilled water in ratio 1:9. Mixing was performed above room temperature (40°-75°C). Cochleates obtained by this procedure were hollow cylindrical structures of varying length. They were made up of tightly coiled

multi-bilayer cholesterol helices sometimes with one end closed. Some characteristic planar hexagonal microcrystals were also observed along with cylinders (Harris et al., 2011).

1.7 Characterization of cochleates:

1.7.1 Evaluation of morphology and dimensions of cochleates

Morphology of cochleates have often been evaluated by simple visualization (Miclea et al., 2007; Ramani and Balasubramanian, 2003; Zarif, 2005). Optical microscopy was used to evaluate success of cochleation by several working groups. This could be achieved by addition of EDTA solution to the cochleate suspension and observing formation of large vesicles arising from aggregated cochleates under optical microscope. Electron microscopy techniques such as TEM, SEM, AFM etc. have been mainly employed to study structural details of cochleates (Bozo et al., 2015). Amongst these freeze fracture TEM technique is argued to be most favorable to evaluate the morphology of cochleates (Papahadjopoulos-Sternberg, 2012; Zarif, 2005).

The dimensions of cochleates depend upon size of lipid particles (Liposomes, micelles etc.), final lipid concentration and rate of calcium addition (Zarif, 2005). Cochleates prepared by trapping method or dialysis method are in micron size. Images of cochleates in micron range acquired by electron microscopy (e.g. SEM) have been utilized for particle size determination (Zarif and Mannino, 2002). Such large cochleates have also been evaluated for particle size by incorporation of fluorescent probe and visualization using fluorescence microscope (Miclea et al., 2007). Particle size measurement of nanocochleate formulations prepared by techniques such as hydrogel isolation or emulsification-lyophilization have been reported based on photon correlation spectroscopy data (Pham et al., 2014; Wang et al., 2014).

1.7.2 Differential scanning calorimetry (DSC)

Differential scanning calorimetry has been used to measure a number of characteristic properties of cochleate samples especially in order to observe crystallization events during complexation of lipid and binding agent. The addition of binding agent to lipid dispersions induces the appearance of peak at higher temperature away from original transition peak of pure lipid (Portis et al., 1979; Silviu and Gagne, 1984; Takahashi et al., 1995). The ability of DSC to record transitions in heat capacity has been exploited in monitoring the effect of incorporation of various drugs in cochleate systems and the physicochemical properties of drug after incorporation (e.g. Ketoconazole cochleates)(Landge et al., 2013; Sarig et al., 2011).

1.7.3 Fourier transform infrared (FT-IR) spectroscopy

Fourier transform infrared spectroscopy was reported as effective technique to investigate the conformational changes that occur in lipid after conversion to cochleate phase by studying methylene vibrational bands. Methylene vibrational bands in spectral region 2919 and 2850 cm^{-1} correspond to antisymmetric and symmetric stretching CH_2 modes respectively. Cochleate phase showed symmetric stretching of CH_2 in acyl chains. Monitoring the frequencies in scissoring vibrations of the methylene and methyl groups can also shed some light on acyl chain packing. In this region cochleate phase with an orthorhombic subcell lattice (with molecules ordered all-*trans* acyl chains being arranged perpendicular to each other) gives rise to a splitting of band into two components at 1462 cm^{-1} and 1472 cm^{-1} (Garidel et al., 2000; Snyder, 1967). A marked narrowing of the band arising due to C=O ester stretching with band maximum to 1732 cm^{-1} is observed. Such narrow shape results from a reduced head group mobility, changes in the polarity or possible interfacial hydrogen bonding interactions (Garidel et al., 2000; Zhang et al., 1997). FT-IR studies of PS-Ca complex suggested that Ca^{2+} binds to the phosphate in head group and causes a dehydration of the phosphate ester (Dluhy et al., 1983; Flach and Mendelsohn, 1993). The data obtained from FT-IR supports observation that crystallization of the hydrocarbon chains takes place after complex formation (of lipid and binding agent) as explained in thermal analysis. The possibility of hydrogen bonding between the drug molecules and phospholipids in cochleate formulations have also been determined based on FT-IR studies (Chellampillai et al., 2014; Landge et al., 2013).

1.7.4 X-ray analysis:

X-ray analysis of cochleates revealed supporting data for DSC and FT-IR studies (Garidel et al., 2001; Hauser et al., 1977). The repeat distance obtained by small angle x ray scattering (SAXS) and wide angle x ray scattering (WAXS) indicate formation of a tight, anhydrous Ca-lipid chelate with crystalline hydrocarbon chains (Garidel et al., 2001; Hauser et al., 1977). The SAXS patterns of cochleates show multiple reflections suggesting the lamellar phase. The repeat distance of the cochleates can be calculated from the first reflection of highest intensity. This SAXS pattern remains constant below transition temperature of cochleate phase. When cochleates are heated above its transition temperature a hydrated lamellar phase is formed which exhibits completely different SAXS pattern with an increased lamellar repeat distance and broad diffraction peaks with almost similar intensities. Hydrated gel phase can also be differentiated from reflection pattern of cochleates. WAXS data reveals information about the packing of the acyl chains. The cochleate phase shows appearance of multiple sharp reflections in the wide angle scattering region which is indicative of the formation of a highly ordered chain lattice (Blaurock and McIntosh, 1986; Ruocco and Graham Shipley, 1982). Above transition of cochleate phases a very broad peak is observed, which is characteristic for the

liquid-crystalline phase with fluid acyl chains.(Blaurock, 1982; Tardieu et al., 1973). Hydrated gel state also shows a single broad WAXS band at lower repeat distance, indicating bilayer with tilted hydrocarbon chains (Ranck et al., 1974; Tardieu et al., 1973). Hence diffraction patterns of crystalline cochleate phase and other phases are characteristic and can be easily identified using x-ray analysis.

1.7.5 Nuclear magnetic resonance (NMR)

NMR studies on phosphatidylserine calcium cochleates were reported by Hauser et al. (1977). The ^2H -NMR spectra of aqueous lipid suspension in absence of binding agent consisted of a broad singlet. This can be explained by presence of excess free water giving rise to fast exchange between free and bound water of the hydration shells in bilayer lipids. In contrast, the complex of binding agent and lipid gave rise to sharper singlet in the ^2H -NMR spectra. This can be regarded to interaction of binding agent with lipid head group which can displace water molecules. The spectra remained constant even after freeze-drying. ^{31}P -NMR studies showed that the signal of lipid dispersion is completely broadened to the baseline on complex formation. This can be correlated with interaction of binding agent which leads to higher order and reduced segmental motion of the polar head group (Butler et al., 1970; Tocanne et al., 1974; Verkleij et al., 1974).

1.8 Applications of cochleates

1.8.1 Pharmaceutical industry

In last few decades considerable research has been devoted towards study of lipid based drug delivery systems amongst which cochleates are one of potential drug delivery system owing unique advantages. Cochleates have been investigated for the safe and effective delivery of number of therapeutically active molecules. Although hydrophobic or amphipathic molecules are usually preferred drug candidates, cochleates have been used as vehicles for different kinds of drugs (Zarif, 2005) as discussed below;

Cochleates showed potential to encapsulate number of antifungal agents. Many studies on oral delivery of cochleate-mediated amphotericin B (Amb), a potent antifungal drug have been reported. Amb cochleates proved efficient when orally administered in a murine model of systemic candidiasis (Santangelo et al., 2000). Delmas et al. investigated Amb cochleates in murine model of systemic aspergillosis which showed improved safety profile by oral route (Delmas et al., 2002). Other antifungal agents such as nystatin have also been incorporated into cochleate formulations (Mannino and Lu, 2014). Ketoconazole cochleates were characterized and evaluated for topical delivery (Landge et al., 2013).

Nanocochleates of Amb and miltefosine were developed for oral administration against visceral leishmaniasis (Pham et al., 2014). Efficacy of orally administered Amb cochleates against

leishmaniasis was confirmed by Wasan et al in hamster model (2009). Cochleates of aminoglycoside antibiotic amikacin have also shown positive results on oral and intra peritoneal administration in black mice infected by *Mycobacterium avium* complex (Lu and Mannino, 2014). Cochleate formulations of other antibiotics such as gentamicin, paromomycin have been evaluated to enhance their oral bioavailability. Clofazimine cochleates showed lower toxicity and improved bactericidal action during *in vitro* evaluation in anti-tubercular model (Popescu et al., 2001). Cochleates can be used to deliver antiviral drugs, such as acyclovir and nelfinavir (Gould-Fogerite and Mannino, 1999; Zarif et al., 2003). Bio Delivery Sciences Inc. (Morrisville, NC) has investigated the potential of cochleates to deliver anti-inflammatory agents (e.g. aspirin, ibuprofen, naproxen, acetaminophen) (Rao et al., 2007). Aspirin and acetaminophen cochleate formulations were found more effective than free drugs in inhibition of nitric oxide synthase in cell-culture studies. *In vivo* studies also showed cochleates to be beneficial in protecting the gastrointestinal tract from side effects such as gastric irritation, ulceration and bleeding (Delmarre et al., 2004b). Cochleates have been employed to deliver anticancer drugs such as paclitaxel, fisetin etc. (Chellampillai et al., 2014). Apart from this, cochleates can be used as a safe, non-viral approach in vaccine therapy. Cochleates have been proved efficacious mediators for induction of antigen-specific immune responses *in vivo* following intranasal (Del Campo et al., 2010), oral (Gould-Fogerite and Mannino, 1996) and intramuscular (Gould-Fogerite et al., 1998) administration. Evaluation of cochleate formulations containing antigens showed generation of strong, long-lasting, mucosal and circulating antibody responses in rodent models. Cochleates were also reported to be useful for delivery of plasmid DNA, gene and proteins (Rao et al., 2007).

1.8.2 Food industry

Cochleates can stabilize and protect an extended range of micronutrients. Hence nutraceutical cochleate formulations can be employed to increase the nutritional value of processed foods, baked goods, natural or artificial dairy products and ready to make products (Delmarre et al., 2004a). Domesticated animal chow, fish food, poultry feed can also be improved by using this approach. It has been evaluated as a strategy to deliver fragile nutrients which can be destroyed during food manufacturing or storage, e.g. quercetin, silibin, vitamins and lycopene. Using cochleates as vehicle such molecules could be efficiently added without affecting the color or taste of both nutraceutical and food (Jin et al., 2007). Cochleates of omega-3 fatty acids, beta carotene have been used in products such as cakes, muffins, pasta, soups and cookies without altering their taste or odor (Sankar and Reddy, 2010). Cochleates can be employed to incorporate one or more additional agents such as coloring agents, flavoring agents, edible acids, preservatives etc.

1.8.3 Cosmetic industry

Phospholipids are known to exhibit beneficial effects on the visual appearance of humans. The topical application of phospholipid lamellar systems offer a wide range of advantages such as increased moisturization, restoring action, biodegradability, biocompatibility and extended release. Their similarity with biological membranes allows better penetration into skin, compared with other delivery systems. Therefore, cochleates can be a favorable strategy to improve the topical delivery of cosmeceuticals (Lasic, 1997; Rahimpour and Hamishehkar, 2012).

1.8.4 Perfume industry

Perfumes are mixtures of fragrances which are chemicals with low molecular weight, lipophilic character and high vapor pressure. Their reactive functional groups (viz. ketones, aldehydes) make them susceptible to degradation by oxidation or hydrolysis (Cortial et al., 2015). For most perfumes as well as the essential oils used for insect repellants prolonged release of fragrance is more desirable than burst release (Nasir, 2010). Therefore, in order to improve the stability of fragrance, prevent evaporation and sustain hydrophilic environment the encapsulation in solid lipid delivery systems such as cochleates might be beneficial (Cortial et al., 2015; Delmarre et al., 2004a).

1.9 Aim of the study

Cochleates offer a high potential for several biomedical applications. Considering the advances of this system towards pharmaceutical industry many studies have focused on the feasibility of employing cochleates as drug delivery vehicles. However, further research is needed on relatively unexplored areas such as thermodynamic stability, formation pathway or structural features of cochleates as detailed understanding of this system may prove vital for formulation development. Another noteworthy challenge is polydispersity of cochleate formulations. Cochleate formation follows a continuous self-assembly process which includes unrestrained growth of particles (Kulkarni et al., 1999; Zarif, 2002). Hence controlling the morphology and the dimensions of individual particles in cochleate formulations is a difficult task. Also the coexistence of intermediate structures makes the purification of formulation a demanding affair. Traditional strategies for preparation of cochleates, such as simple mixing, dialysis etc. lack precise control over morphology of final product. Such structural diversity of formulation may cause unpredictable, non-reproducible and erratic drug release resulting in highly variable bio-availability of incorporated drugs. Therefore, there is a growing need for a strategy to address this issue. Although in past few decades improvements were made in cochleate formation protocols, these methods have limitations for large scale production. In view of all the above mentioned aspects our study was aimed at following goals:

- **To study formation mechanism of cochleates through detailed electron microscopy** in order to understand different intermediate and metastable structures. Motivation of this study arises from the fact that although formation of cochleate cylinders has been explained, specific aspects of formation process are not known.
- **To develop a theoretical model for estimation of dimensions of cochleates** and validate the model by comparing experimentally observed dimensions.
- **To develop simple, reproducible and economic procedure for formation of cochleates** which could be easily transformed to large scale production, reduce random particle aggregation and thereby decrease the size dispersity in cochleate systems.

2 Publication overview

2.1 Publication 1:

Understanding cochleate formation: Insights into structural evolution

Kalpa Nagarsekar, Mukul Ashtikar, Frank Steiniger, Jana Thamm, Felix Schacher, Alfred Fahr

Soft Matter, submitted on 12th June 2015, manuscript resubmitted after peer review

Abstract

Phosphatidylserines of different chain lengths (Viz. C8:0, C10:0, C14:0, C16:0, C18:1, C18:0) were evaluated for cochleate formation using calcium as binding agent. The chosen lipids in the present study exhibited transition temperatures in range of -11 to 68°C. During cochleate formation, process temperature was decreased to decelerate the self-assembly. Detailed electron microscopy study of these samples was carried out to investigate formation of array of structures during self-assembly of cochleates. Our observations suggested that variation in phosphatidylserine chain length did not have remarkable influence on the type of structures that evolved during formation process. During progression of cochleate formation structures such as ribbons, stacks and networks were identified in all lipid samples. Based on these findings from microscopy studies we have proposed revision in probable pathway for cochleate formation.

Own contribution to manuscript:

1. Experimental design
2. Preparation and evaluation of cochleates except for FFTEM, SEM and SAXS.
3. Data evaluation, interpretation and presentation of the results.
4. Preparation of the manuscript.

2.2 Publication 2:

Electron microscopy and theoretical modeling of cochleates

Kalpa Nagarsekar, Mukul Ashtikar, Frank Steiniger, Jana Thamm, Felix Schacher, Alfred Fahr and Sylvio May

Langmuir, 2014, 30 (44), pp 13143–13151 Published on October 28, 2014

Abstract

Cochleates of phosphatidylserine C18:0 and C18:1 were prepared using calcium ions as binding agent under identical conditions. Detailed structural analysis of cochleates from both lipids was carried out using different microscopy techniques. Our investigations confirmed presence of a continuous hollow channel in rolled-up bilayers stating that most of the cochleate particles formed from lipids under investigation are not like cigars as explained in past. The structure of cochleate was found to be variant along its long axis and tend to exhibit a pattern like an involute in most of the cases. Also the estimated dimensions of the internal channels appeared to be characteristic for building blocks. This knowledge was used for building a thermodynamic model based on minimizing phenomenological free energy for estimating optimal dimensions of a cochleate. Our calculations suggest that membrane bending and calcium induced bilayer–bilayer adhesion alone are insufficient to reproduce the observed experimental dimensions.

Own contribution to manuscript:

1. Experimental design
2. Preparation and evaluation of cochleates except for SAXS, SEM and cryo-electron tomography.
3. Data evaluation, interpretation and presentation of the results except for the theoretical model.
4. Preparation of the manuscript except for theoretical model.

2.3 Publication 3:

Micro-spherical cochleate composites: method development for monodisperse system

Kalpa Nagarsekar, Mukul Ashtikar, Frank Steiniger, Jana Thamm, Felix Schacher, Alfred Fahr

Journal of Liposome Research, submitted on 8th September 2015, manuscript under review.

Abstract

A new method was developed to fabricate cochleate composites with a simple microfluidic setup, by employing solvent effect. Product obtained from the proposed method was characterized using electron microscopy, small angle X-ray scattering and compared with those obtained by other established methodologies. These microspheres (3–5 μm in diameter) made of nanocochleates retain the basic advantages of cochleates. Our simple strategy eliminates elaborate preparation methods, is convenient and could easily be programmed to transform for large scale production. The results of current investigation illustrate this approach to be promising for preparing monodisperse cochleate system with analogous quality.

Own contribution to manuscript:

1. Experiment design
2. Preparation and evaluation of cochleate formulations except for SEM and SAXS.
3. Data evaluation, interpretation and presentation of the results.
4. Preparation of the manuscript.

3 Publications

3.1 Publication 1:

Understanding cochleate formation: Insights into structural evolution

Kalpa Nagarsekar, Mukul Ashtikar, Frank Steiniger, Jana Thamm, Felix Schacher, Alfred Fahr

Soft Matter, submitted on 12th June 2015,

Manuscript resubmitted after peer review

Soft Matter



Soft Matter

Understanding cochleate formation: Insights into structural evolution

Journal:	<i>Soft Matter</i>
Manuscript ID	SM-ART-06-2015-001469.R1
Article Type:	Paper
Date Submitted by the Author:	n/a
Complete List of Authors:	Nagarsekar, Kalpa; Friedrich Schiller Universität Jena, Institut für Pharmazie, Lehrstuhl für Pharmazeutische Technologie Ashtikar, Mukul; Friedrich Schiller Universität Jena, Institut für Pharmazie, Lehrstuhl für Pharmazeutische Technologie Thamm, Jana; Friedrich Schiller Universität Jena, Institut für Pharmazie, Lehrstuhl für Pharmazeutische Technologie Steiniger, Frank; Universitätsklinikum Jena, Elektronenmikroskopisches Zentrum Schacher, Felix; Friedrich Schiller University Jena, Institute of Organic and Macromolecular Chemistry Fahr, Alfred; Friedrich Schiller Universität Jena, Institut für Pharmazie, Lehrstuhl für Pharmazeutische Technologie

SCHOLARONE™
Manuscripts

Soft Matter

1

1 **Understanding cochleate formation: Insights into structural evolution**

2

3 Kalpa Nagarsekar^{1*}, Mukul Ashtikar^{1*}, Frank Steiniger², Jana Thamm¹, Felix Schacher^{3,4}, Alfred Fahr^{1**}

4

5 ¹ Lehrstuhl für Pharmazeutische Technologie, Institut für Pharmazie, Friedrich-Schiller-Universität Jena, Lessingstraße 8, 07743 Jena,
6 Germany

7 ² Elektronenmikroskopisches Zentrum, Universitätsklinikum Jena, Ziegmühlenweg 1, 07743 Jena, Germany.

8 ³ Institut für Organische Chemie und Makromolekulare Chemie Friedrich-Schiller-Universität Jena, Lessingstraße 8, 07743 Jena, Germany

9 ⁴ Jena Center for Soft Matter, Friedrich-Schiller-Universität Jena, Philosophenweg 7, 07743 Jena, Germany

10

11 *These authors have contributed equally in the preparation of this manuscript.

12 **Corresponding Author:

13 **Address:**

14 Lehrstuhl für Pharmazeutische Technologie,

15 Institut für Pharmazie,

16 Friedrich-Schiller-Universität Jena,

17 Lessingstraße 8,

18 07743 Jena, Germany

19 Phone: +49 3641 949901

20 Email: Alfred.Fahr@uni-jena.de

21

22

Soft Matter

2

23 **Abstract**

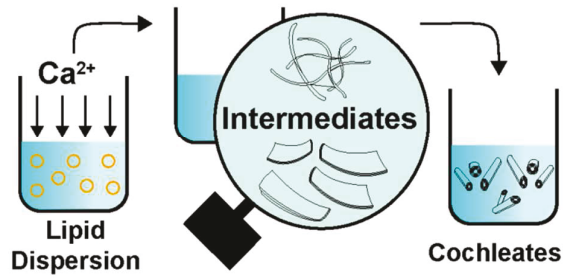
24 Understanding of cochleates, their structure and self-assembly process has become increasingly necessary
25 considering the advances of this drug delivery system towards pharmaceutical industry. It is well known that
26 the addition of cations like calcium to a dispersion of anionic lipids such as phosphatidylserines results in
27 stable, multilamellar cochleates through spontaneous assembly. In the current investigation we have studied
28 the intermediate structures generated during this self-assembly of cochleates. To attempt this, we have varied
29 the process temperature for altering the rate of cochleate formation. Our findings from electron microscopy
30 studies showed formation of ribbonlike structures, which with proceeding interaction associate to form lipid
31 stacks, networks and eventually cochleates. We also observed that variation in lipid acyl chains did not make a
32 remarkable difference to the type of structures evolved during formation of cochleates. More generally, our
33 observations provide a new insight into the self-assembly process of cochleates based on which we have
34 proposed a pathway for cochleate formation from phosphatidylserine and calcium. This knowledge could be
35 employed in using cochleates for a variety of possible biomedical applications in the future.

36 **Keywords:** Cochleates, phosphatidylserine, self-assembly, electron microscopy, intermediate structures

37

38 **Graphical abstract**

39



40

41

42 Introduction

43

44 Cochleates are lipid-based supramolecular assemblies which may show potential as advanced drug delivery
45 system¹. Cochleates have elongated shape and carpet roll like morphology invariably accompanied by tightly
46 packed bilayers.² Apart from being biocompatible, cochleates exhibit high stability which is attributed to their
47 unique compact structure³. Since discovery, there have been number of modifications in preparation methods
48 of cochleates in order to yield suitable structures for specific purposes, albeit not much has been explored
49 regarding the actual mechanism of cochleate formation. Hierarchical superstructures originating from
50 unrestrained self-organization impart impressive complexity to the cochleate system but it is accompanied by
51 higher degrees of polydispersity. This lack of homogeneity can be a prominent obstruction in large scale
52 production of cochleates. Due to the higher polydispersity, a tendency for aggregation, and peculiar geometry
53 cochleates have remained as one of the challenging systems for characterization by standard methods used for
54 nanoparticles. In order to overcome this challenge, thorough knowledge of all metastable species arising from
55 the involved building blocks is obligatory. Although the general concept for cochleate formation has been
56 established, there may be a scope to elaborate further and such information can be of assistance in the future
57 to predict properties of the resulting products or to maneuver the process towards an expected outcome.
58 Hence, it is important to study formation of cochleates closely in order to gain understanding of this drug
59 delivery system.

60 Many theories have been presented to explain formation of cochleate cylinders yet specific details remain
61 hidden. Transformations of lipid membrane into tubular structures have been thoroughly investigated in
62 theory, however, these theories are difficult to verify conclusively⁴⁻⁶. The most accepted theory describes that
63 binding of bilayer sheets results in formation of high axial ratio microstructures like helices which in turn due
64 to intrinsic bending of bilayers form structures like cochleates^{7,8}. For cochleate formation, interaction between
65 phospholipid headgroups and the cationic bridging agent is a pivotal step which is essential to trigger the
66 membrane fusion⁹. It is well documented that after addition of divalent cations the fusion between lipid
67 dispersion gives rise to extraordinarily stable high melting¹⁰, crystalline phases by dehydration and strong
68 immobilization of the serine headgroups¹¹⁻¹³. The resultant lipid complexes have aliphatic acyl chains in a
69 crystalline state¹⁴ which further results in stable cylindrical multilamellar superstructures⁸. Apart from this,
70 chirality may play an essential role in order to form cochleates¹⁵. As per theories based on molecular chirality,
71 chiral interactions result in packing of molecules with non-zero angle against neighboring molecules. This in
72 turn contributes to the twisting of bilayers leading to formation of a cylinder^{4, 16, 17}.

73 In the last decades many detailed studies have addressed the mechanistic understanding of bilayer fusion. The
74 most commonly encountered difficulty in such studies is to segregate the kinetics of bilayer fusion from
75 consecutive stages of destabilization¹⁸⁻²⁰. Characterization of such studies often depicts overlap of multiple
76 simultaneous events. Acquiring experimental evidence to affirm various steps and their order in cochleate
77 formation is a challenge as it is difficult to pace these stages during the course of the experiment. Conditions
78 that induce aggregation in anionic lipids have been studied extensively. Along with the concentration of the
79 bridging agent, temperature is a very important aspect affecting the rate of bilayer fusion^{21, 22}. We attempted
80 to use process temperature as a variable to observe gradual evolution of cochleates during the formation
81 process. Therefore, synthetic phosphatidylserines (PS) with varying phase transition temperatures (T_m) were
82 selected for this study.

83 PS are anionic phospholipids which have been repeatedly exploited for the preparation of cochleates. PS are
84 negatively charged over a wide pH range. They consist of a serine headgroup with three ionizable sites, i.e.
85 phosphate group, amino group and a carboxyl functionality. Both the carboxyl and phosphate groups in the
86 serine headgroup have a high inclination to bind with positively charged moieties^{23, 24}. This makes serine lipids

Soft Matter

87 one of the most eligible phospholipids to form cochleates. Apart from calcium, cations such as magnesium,
88 zinc etc have also been used to form PS cochleates in past^{25,26}. It should be noted that there are reports of
89 substances other than PS forming cochleates^{27, 28}. However for the purpose of this article we will only discuss
90 calcium PS cochleates. Further, by formulating cochleates using various PS with 8-18 carbon chains we
91 attempted to assess the influence of building blocks over characteristics of this drug delivery system. It would
92 be interesting to understand if alterations in chain length have any effect on the resulting structures.

93 In the current study, the basis of cochleate formation has been explored by investigating the observed peculiar
94 metastable microstructures and their coexistence with cochleates. In order to fathom intermediate stages of
95 cochleates we observed specimens multiple times during outset using electron microscopy as primary
96 characterization technique. In the past most of the investigations related to structural features or formation of
97 cochleates have relied strongly on freeze fracture techniques²⁹. In the current study along with Freeze Fracture
98 Transmission Electron Microscopy (FFTEM) we employed other EM techniques like cryo-SEM (Scanning
99 electron microscopy) or cryo-TEM (Transmission electron microscopy) to visualize cochleates from different
100 perspectives. Our morphological exploration was complemented by small angle X-ray scattering (SAXS). During
101 imaging studies we came across different intermediate metastable structures which may shed some light on
102 the underlying formation mechanism. We identified ribbonlike structures as an important subunit and report
103 their formation as alternative first stage, which is an unrecognized facet in phosphatidylserine cochleate
104 formation. Our results indicate that all selected PS displayed presence of similar intermediate structures some
105 of which can coexist with cochleates. Based on our findings we present details for possible pathways for
106 cochleate formation from phospholipid aggregate precursors.

107

108

Soft Matter

109 **Materials and Methods**110 **Materials :**

111 1,2-dioctanoyl-sn-glycero-3-phospho-L-serine [sodium salt] (DOctPS); 1,2-didecanoyl-sn-glycero-3-phospho-L-
 112 serine [sodium salt] (DDPS); 1,2-Dimyristoyl-sn-glycero-3- phospho-L-serine [sodium salt] (DMPS); 1,2-
 113 dipalmitoyl-sn-glycero-3-phospho-L-serine [sodium salt] (DPPS); 1,2-dioleoyl-sn-glycero-3-phospho-L-serine
 114 [sodium salt] (DOPS) and 1,2-distearoyl-sn-glycero-3-phospho-L-serine [sodium salt] (DSPS) were obtained
 115 from Avanti Polar Lipids Inc (Alabama, USA). Araldite LY 564 was obtained from HunTcan Advanced Materials
 116 GmbH (Switzerland). All other chemical reagents were of analytic grade and used as received without further
 117 purification. Ultrapure water (RiOs™ 8, Millipore, Eschborn, Germany) was used for all experiments.

118

119 **Preparation of cochleates**

120 Briefly, the lipid was dissolved in a mixture of chloroform:methanol (3:1) in a round bottom flask followed by
 121 removal of the organic solvents using a rotary evaporator (R-144 BÜCHI Labortechnik GmbH, Germany) to
 122 form a thin lipid film. The lipid film was further hydrated with 10 mM TRIZMA® [2-Amino-2-(hydroxymethyl)-
 123 1,3-propanediol] buffer above the T_m of the lipid. The dispersion was vortexed followed by extrusion through
 124 a polycarbonate membrane of 100 nm pore size to produce a homogenous dispersion of lipid. Cochleates were
 125 formed by slow (10 µl at a time) addition of calcium chloride (100 mM) to the lipid dispersion in TRIZMA®
 126 buffer (NaCl, 100 mM; TRIZMA®, 10 mM) under constant stirring above T_m of the lipid. The molar ratio of lipid
 127 to calcium was 1:1. Precipitated mixtures were then stored at 4 °C. Apart from these batches in order to study
 128 intermediate structures as explained above, batches of cochleates were also prepared at lower temperatures,
 129 see Table-1. All samples were evaluated immediately after preparation and periodically during incubation up
 130 to 12 months by electron microscopy (EM).

131

132 **Table 1:** Process temperatures used during preparation of various phosphatidylserine cochleates.

Phosphatidylserine	Transition Temperature	Process temperature
DOctPS (C8:0)	< 10 °C	4 °C and 20 °C
DDPS (C10:0)	< 10 °C	4 °C and 20 °C
DOPS (C18:1)	-11 °C	4 °C and 20 °C
DMPS (C14:0)	35 °C	20 °C and 40 °C
DPPS (C16:0)	54 °C	20 °C and 59 °C
DSPS (C18:0)	68 °C	20 °C, 50 °C and 73 °C

133

134 **Electron Microscopy:**

135 **Scanning Electron Microscopy:** A droplet of the cochleate sample was adhered for 5 min onto a perforated
 136 Formvar-coated copper grid (300 mesh, Quantifoil, Germany). Excess liquid was removed with a lint-free filter
 137 paper and examined in a LEO 1530 Gemini (Carl Zeiss, Germany) scanning electron microscope (SEM) at 4 kV
 138 acceleration voltage.

139 **Cryo-Scanning electron microscopy:** 10 µL of sample was adhered onto a gold stub (3 mm, Zeiss, Germany).
 140 Further, grid was quickly plunged in liquid ethane (-180 °C) and the sample was cryo-transferred with the help
 141 of the vacuum cryo-transfer system BALTEC BAF 060 (Baltec, Switzerland) in liquid nitrogen in order to knife-
 142 fracture the specimen. Further, temperature of the sample was raised to -80 °C to allow controlled
 143 sublimation of water in order to expose the particles. To improve contrast sample was then coated by 1.5 nm
 144 of tungsten. Images were acquired using a Zeiss Auriga 60 (Carl Zeiss, Germany) using the SEM imaging routine
 145 at 3 kV acceleration voltage and a working distance of 6 mm using a secondary electron detector.

146

Soft Matter

7

147 **Freeze fracture-transmission electron microscopy:** An aliquot of 5 μL of the dispersion was placed between
148 copper profiles and subjected to plunge freezing immediately using liquid ethane/propane mixture. Fracturing
149 and replication of the samples were carried out at -150°C in a BAF 400T freeze-fracture device (BAL-TEC,
150 Liechtenstein) equipped with electron guns and a film sheet thickness monitor. Samples were coated with 2
151 nm of Pt(C) under an angle of 35° , followed by perpendicular evaporation of C. The replicas were cleaned with a
152 chloroform-methanol mixture, and examined in an EM 902A (Carl Zeiss, Germany) electron microscope.

153 **Transmission electron microscopy:** An aliquot of 5 μL of the dispersion was placed onto a Formvar-coated
154 copper grid (300 mesh, Plano, Germany) for 4 minutes. Excess of liquid was removed with a lint-free filter
155 paper and the grid was air dried. TEM grids were investigated using Zeiss EM 902A (Carl Zeiss, Germany)
156 operated at 80 KV. Images were taken with a 1k x 1k FastScan-F114 CCD Camera (TVIPS GmbH, Germany). To
157 evaluate and compare dimensions of cochleates of high T_m lipids micrographs were analyzed using ImageJ
158 version 1.47³⁰.

159 **Cryo-Transmission electron microscopy:** 5 μL of Dispersion of sample was placed on carbon-coated copper grid
160 (R1.2/1.3 + 2 nm, Quantifoil Micro Tools GmbH, Germany). It was subjected to plunge freezing in liquid ethane
161 at -180°C . Grids were then transferred into a liquid nitrogen cooled ($T = -196^\circ\text{C}$) cryo-holder (Gatan Inc., USA)
162 and inserted into Philips CM 120 cryo-TEM (Philips CM 120, Netherlands) for evaluation. The images were
163 recorded with 1k CCD camera (FastScan F114 TVIPS, Germany).

164 **Investigation of Cross Section of Resin-Embedded stacks:** Embedding was carried out using same procedure as
165 described by *Nagarsekar et al.*². Briefly, sample was redispersed in 100 mM cacodylate buffer (pH 7.2)
166 containing 1% OsO₄ for 2 h. Sample was centrifuged again and rinsed in buffer before dehydration in ethanol
167 (50% v/v) for 15 min. It was further subjected for 1 h to 1% uranyl acetate solution to improve contrast. The
168 pellet was then redispersed in an epoxy resin Araldite (Agar Scientific, United Kingdom) used as embedding
169 medium. The mixture was polymerized and the polymer blocks were ultramicrotomed into thin (70–100 nm)
170 slices, using a diamond knife mounted on an Ultracut E device (Reichert Labtec, Germany) at room
171 temperature. The slices were then transferred to copper grids (Quantifoil, Germany) and examined by TEM.

172 **Small angle X-Ray scattering**

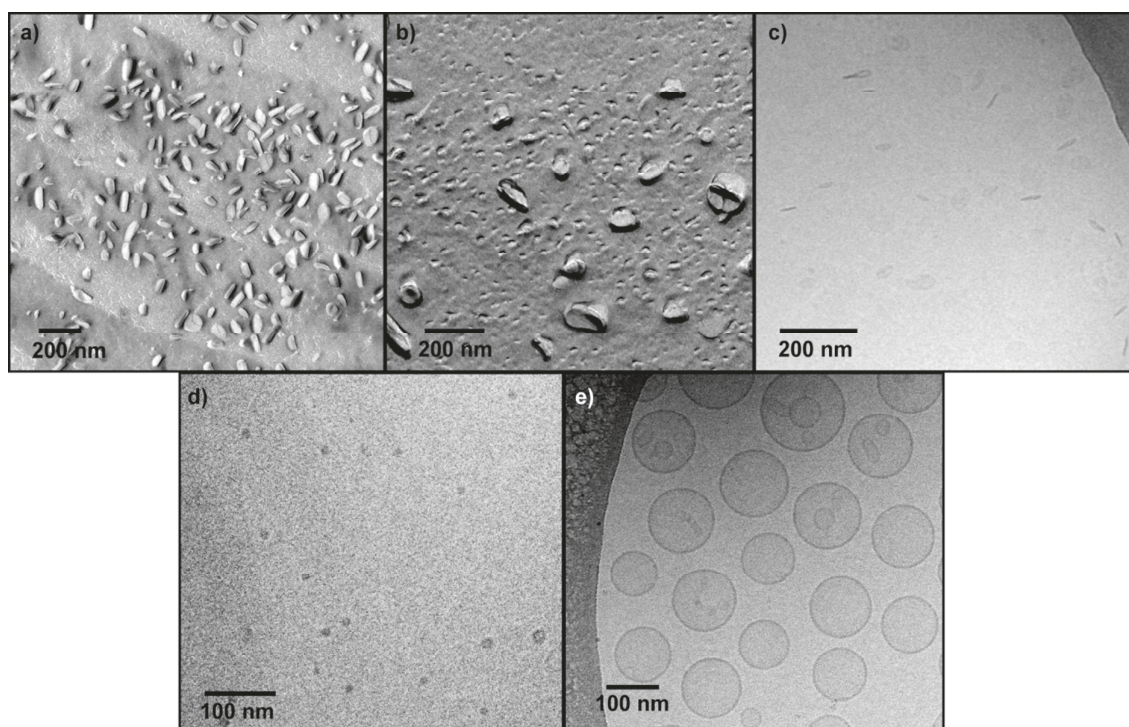
173 All samples were dialyzed and freeze dried before evaluation. SAXS measurements were performed on a
174 Bruker Nanostar (Bruker, Germany) equipped with a $1\mu\text{S}$ (IncoaTec, Germany) X-ray source, operating at
175 $\lambda=1.54\text{\AA}$. The sample-to-detector distance was 107 cm. Samples were mounted on a metal rack and fixed using
176 tape. All measurements were carried out at room temperature for 120 minutes, with a 2D position sensitive
177 detector Vantec 2000 (Bruker GmbH, Germany). The scattering patterns were corrected for the background
178 (Scotch Tape, Germany) prior to evaluations and radially integrated to obtain the scattering intensity as a
179 function of the scattering vector, $q=(4\pi/\lambda) \sin\theta$, with 2θ being the scattering angle and λ the X-ray wavelength.

180

181

182 **Results and Discussion**

183 To decrease the polydispersity, all lipid dispersions were subjected to extrusion before cochleate formation.
 184 Amongst chosen lipids, DOPS formed liposomes. DOPC and DDPS having strong surfactant properties formed
 185 micelles along with small vesicles. High T_m lipids like DSPS, DPPS and DMPS formed bilayer discs (Fig 1).
 186 Cochleates were formulated using simple trapping method contemplating the ease of control over process
 187 conditions. Considering the strong influence of process parameters on morphology of the final products, it was
 188 assured that during preparation all conditions were kept constant except the variable of interest i.e.
 189 temperature. Formulations were prepared at different temperatures to identify intermediates and determine
 190 the pathway of cochleate formation. Visually, during formulation all translucent lipid dispersions went turbid
 191 following precipitation upon addition of CaCl_2 solution. This observation was consistent for all process
 192 temperatures. White fluffy precipitate and a clear supernatant were formed in the samples which were
 193 prepared below the T_m of the respective lipid. However, the samples prepared above T_m showed a densely
 194 aggregated suspension. The change from opalescent to turbid suspension after addition of calcium was
 195 considered as an indication for binding processes taking place. The visual appearance of samples did not
 196 change with aging. The microstructures formed in all samples were explored using different electron
 197 microscopy techniques.



198

199 **Figure 1:** Electron micrographs showing discs of (a) DSPS and (b) DMPS by FFTEM. Cryo-TEM images of (c) DPPS
 200 discs, (d) DDPS micelles and (e) DOPS liposomes.

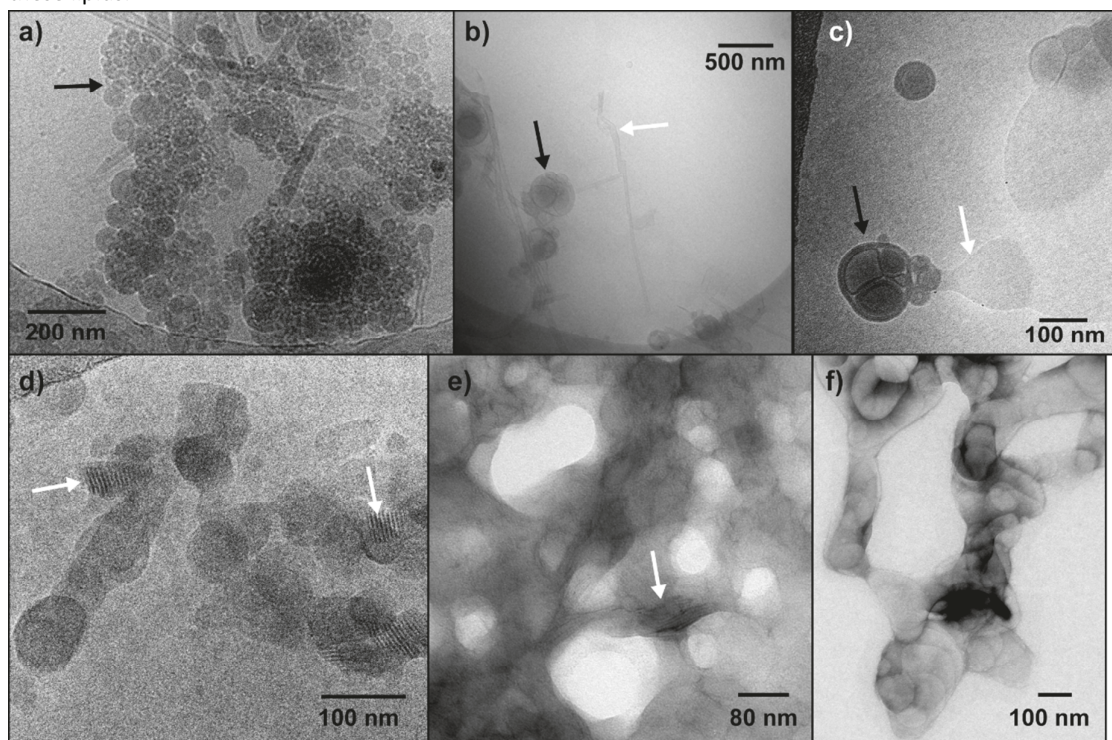
201 Although most cochleate samples observed under TEM and cryo-TEM could be visualized without staining, for
 202 better contrast aggregated bilayers and ribbons were visualized by negative staining with uranyl acetate in
 203 TEM. The drying of cochleate samples during electron microscopy did not affect the tubule structure, or cause
 204 collapsing of the internal hollow space. This was probably due to the rigid nature of the multilamellar system³¹.
 205 Nonetheless, no decomposition artifacts were generated as a result of electron dosage used to capture
 206 micrographs of the sample observed in the study. In order to confirm the findings multiple techniques such as
 207 SEM, cryo-SEM, cryo-TEM, FFTEM and resin-embedding were employed. Throughout the text, DOPC, DDPS
 208 and DOPS are referred to as low T_m lipids while DMPS, DPPS and DSPS are referred to as high T_m lipids.

Soft Matter

9

209 **Aggregation and formation of calcium chelated bilayers**

210 Aggregation is an inceptive step during cochleate formation which in turn leads to the generation of calcium
 211 chelated bilayers³². Literature suggests addition of calcium ions to PS vesicles triggers formation of array of
 212 intermediate structures such as discs, sheets and partially folded bilayers which finally give rise to cochleate
 213 cylinders⁸. Being nucleation-dependent, aggregation processes are usually characterized by a lag period, i.e.
 214 time required for the critical nuclei to form can be decelerated by reducing the process temperature³³. Since
 215 fusion processes and rates of morphological transitions are very fast (in milliseconds) in substrates with
 216 smaller or unsaturated carbon chain length, it is not easy to trap these initial intermediate structures.
 217 Consequently, few early intermediate structures could be observed during evaluation of cochleate samples of
 218 low T_m lipids. Apart from this some higher order intermediate structures also appeared simultaneously in
 219 these samples. We found that among selected PSs high T_m lipids were ideal candidates to trap early
 220 intermediate structures by this method since, these transformations could be prolonged more efficiently in
 221 these lipids.



222

223 **Figure 2:** Aggregation observed in cryo-TEM images of (a) DOctPS (b) DDPS and (c) DOPS samples prepared at 4
 224 °C. TEM images of samples prepared below T_m (d) DMPS, Cryo-TEM image (e) DSPS aggregates showing
 225 twisted bilayers and (f) DPPS aggregates. White arrows indicate formation of ribbonlike structures while dark
 226 arrows point at aggregated lipid bilayers. All micrographs were taken in 10 seconds after addition of calcium.

227 Samples prepared above the T_m of lipids mainly showed cochleates along with higher intermediate structures
 228 and did not show early intermediates e.g aggregates of liposomes, disc micelles etc. Cochleate samples
 229 prepared at lower process temperatures were evaluated immediately (10 seconds) by EM before incubation to
 230 visualize early intermediate structures. Samples of low T_m lipids prepared at 4 °C showed presence of
 231 aggregation structures along with ribbons or sheets. Aggregates observed in these samples varied in size and
 232 shape. These aggregates appeared to contain a large number of dense particles (as indicated by dark arrows in
 233 Fig. 2a-c). Multilamellar aggregates observed in samples of DOPS appeared largely dehydrated and revealed
 234 repeat distance of bilayer suggesting efficient binding of calcium ion. We presumed that such dense
 235 aggregates may be highly unstable as they displayed asymmetrical but closely packed lamellae. Such instability
 236 may result from destabilization of the outer monolayers during vesicle fusion as reported in the past³⁴.

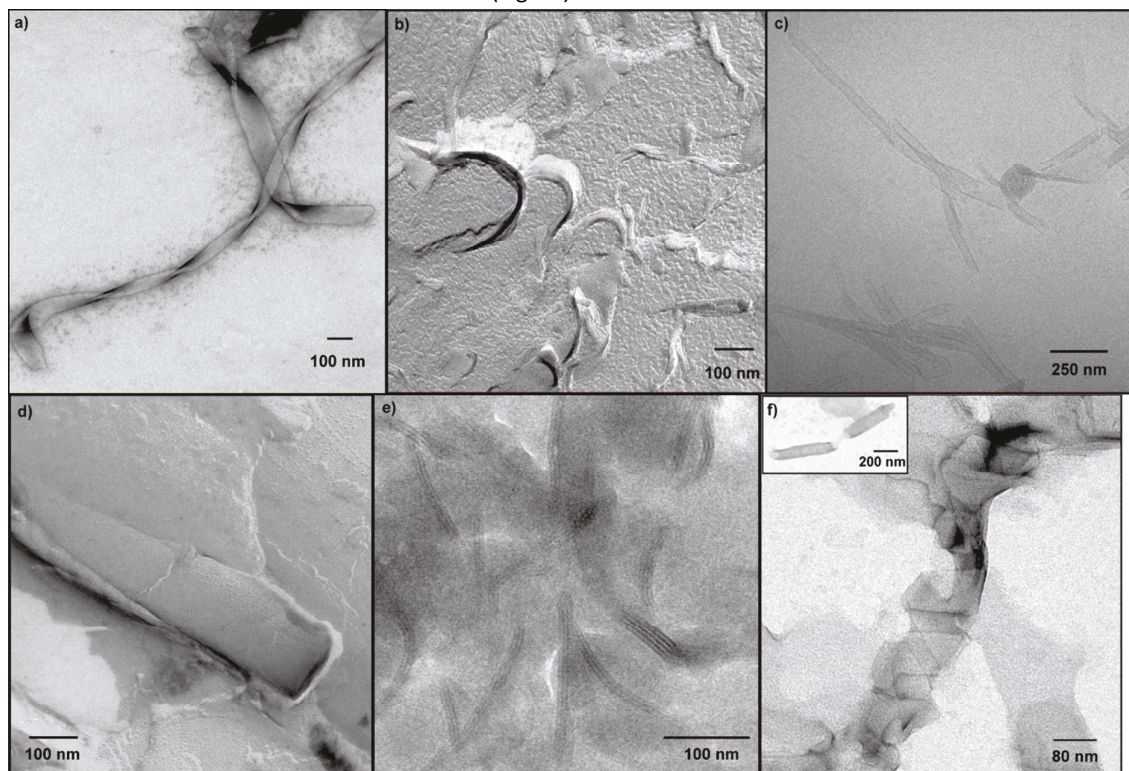
237 Previous investigations on calcium interaction with PS vesicles also reported deformation of primary structures
 238 following aggregation and possibility of rupture or fusion of the multilamellar aggregates which was in line
 239 with our observations³⁴⁻³⁶. DDPS and DoctPS samples revealed several such aggregates showing formation of
 240 ribbonlike structures (Fig. 2b). Similar patterns were observed in samples of DOPS which showed aggregates
 241 radiating broad ribbonlike structures (Fig. 2c). Though rare, few cochleate cylinders were also observed in
 242 DoctPs samples at this stage.

243 In high T_m lipid samples prepared at 20 °C, large fraction of agglomerated bilayers and ribbons appeared to
 244 coexist at the aggregation stage. No traces of cochleate cylinders were evident. In high T_m lipids, edges of
 245 bilayer discs probably fuse with a specific orientation to form ribbonlike silhouette giving rise to three
 246 dimensional rigid network. Chain-like morphology of aggregated discs in micron length were also observed
 247 (Fig. 2f). These three dimensional aggregated structures finally appear to evolve into ribbons (Fig. 2d), which
 248 were formed in abundance and was in micron range. The edges of bilayer discs in aggregated structures often
 249 appeared twisted indicating instability, which may be responsible for such transformation or fragmentation.
 250 Nucleation at the edges may also be preferred due to better accessibility and probability of orientation.

251

252 **Ribbons:**

253 EM images of all samples prepared at lower process temperatures revealed presence of ribbonlike bilayer
 254 strips. Fig. 3 shows images of ribbons from different lipids. The length of ribbons observed in samples were
 255 quite divergent. Although highly transparent all ribbons had well-shaped edges with thickness varying from 2-3
 256 bilayers as can be seen in cryo-TEM image of DSPS ribbons (Fig. 3e). Though few in number, ribbons were
 257 noticed in samples of low T_m lipids prepared at 4°C. DOctPS (Fig. 3d) and DOPS samples showed presence of
 258 ribbons within 10 seconds after addition of calcium. In case of DDPS, ribbons were observed in abundance
 259 within an hour after addition of calcium ions in (Fig. 3c).



260

261

262 **Figure 3:** Ribbons observed in samples prepared below T_m (a) TEM image of DSPS (b) FFTEM image of DPPS (e)
 263 Cryo-TEM of DSPS and (f) TEM of DMPS with occasionally observed helical ribbon and tubules inset. Ribbons
 264 observed in samples prepared at 4°C (c) Cryo-TEM of DDPS (d) FFTEM of DOctPS.

Soft Matter

11

265
266 The samples of high T_m lipids prepared at 20 °C also consisted of a large amount of ribbons that partially
267 overlapped (Fig. 3 a, b and e). Amongst these samples of DSPS and DPPS did not show any other higher order
268 intermediate structures. The main feature of ribbons observed in DSPS and DPPS samples (Fig. 3a and b)
269 prepared at 20 °C is that they did not evolve into closed aggregates or give rise to nanotubes. Even upon
270 prolonged incubation up to twelve months both DSPS and DPPS samples prepared at 20 °C showed only the
271 presence of aggregated ribbons. They formed structures that looked like loose networks (shown in Fig. 7b)
272 however failed to form cochleates. In case of DMPS samples prepared at 20 °C few helical ribbons and tubule
273 like structures formed from single ribbon were also observed (within 20 min after addition of calcium ions).
274 These tubule like structures (Fig. 2f inset) resembled nanotubes and seemed to lack the multilamellar structure
275 of a typical cochleate. As compared to other high T_m lipids the DMPS samples prepared at 20 °C showed
276 higher inclination towards formation of higher order structures in the hierarchy of cochleate formation. In
277 order to confirm that stack formation takes place after formation of ribbons, DSPS ribbons were heated up to
278 50 °C. EM evaluation of this sample showed a large number of stacks. Further heating of this DSPS sample,
279 above T_m gave rise to cochleates (data not shown).
280 Literature advocates that large lipid sheets condense and curl up to form a cylindrical structure³⁷. We presume
281 from our findings that ribbonlike fragments are probably formed at early stage during cochleate formation.
282 Initiation point for any supramolecular assembly would be the formation of a template by nucleation before
283 subsequent growth. Ribbons are also most repeatedly observed precursors of tubular structures³⁸. The Repeat
284 distance observed for ribbonlike structures is smaller as compared to that of bilayers without calcium
285 interaction (with reference to SAXS data). This suggest orientation and organization of lipid molecules
286 governed by interactions of their polar headgroups³⁹. Hence ribbon formation may be the outcome of the
287 dehydrated headgroups of lipid molecules sealing in a zipper effect due to divalent cations⁹.
288

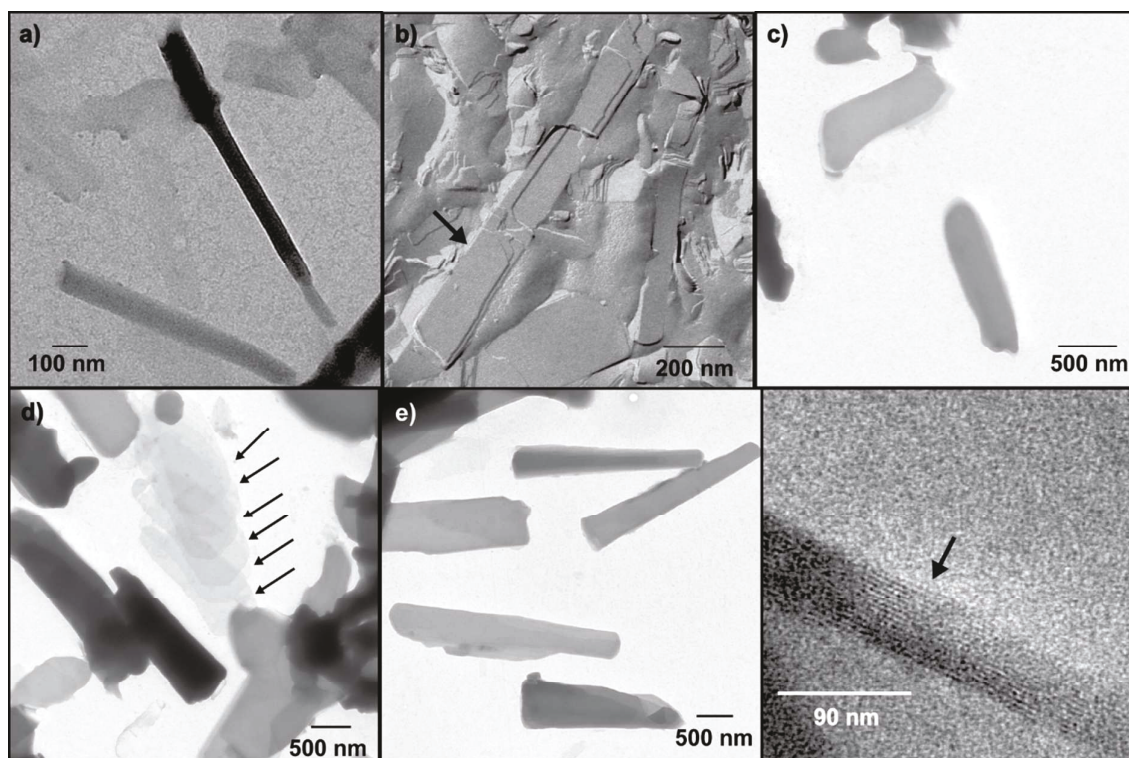
289 Stack formation

290 The contrast between ribbons and stacks due to variation of the packing density assisted in identification of
291 structures in EM analysis. No negative staining was required for evaluation of stacks in the samples unlike
292 ribbons. Fig. 4 shows the morphology of stacks which have a strong tendency to associate into multilamellar
293 aggregates (as highlighted in Fig. 4d). TEM images from embedding study (Fig. 4f) and cryo-SEM data (Fig. 5c)
294 also reveal multilamellarity of these lipid stacks. Interestingly, most of the stacks showed an elongated
295 trapezoidal shape. Some exhibited different morphology due to curling, aggregation, and possible fusion with
296 other stacks. Although our results of characteristic shape and multilamellarity of stacks are in line with
297 previous findings of the Blume workgroup²⁸ our data revealed that the dimensions of stacks varied
298 considerably in width, thickness and length (Fig. 5a & b). We observed that stacks were inclined to attach to
299 cochleates or fuse together to form larger stacks. Our EM data also indicated cochleate formation from
300 helically coiled stacks, which may be the result of curvature arising from packing frustration of the terminal
301 lipid molecules. In our previous work we have hypothesized that energy required for rolling of stacks comes
302 from a combined contribution of bending, adhesion and a frustration energy². Although formation of large
303 planar multilamellar sheets is considered as critical step before the formation of cylindrical cochleate
304 structures^{8, 40}, our findings suggested that it may not be essential. PS samples such as DOPS and DoctPS
305 prepared above T_m displayed large planar sheets in abundance as compared to others which showed larger
306 number of stacks and networks.

307 No stack formation was observed in the samples of DPPS and DSPS, which were prepared at 20 °C below the
308 T_m of the respective lipids. These samples did not form stacks or any cylindrical structures even upon
309 prolonged incubation for up to 12 months. In contrast, DMPS samples prepared below T_m showed presence of
310 lipid stacks within 1 hour after addition of calcium and gave rise to cochleates along with large amount of
311 networks after further incubation. This might be an indication that stack formation is an essential step in
312 formation of cochleate cylinders without which the process of cochleate formation cannot reach completion.

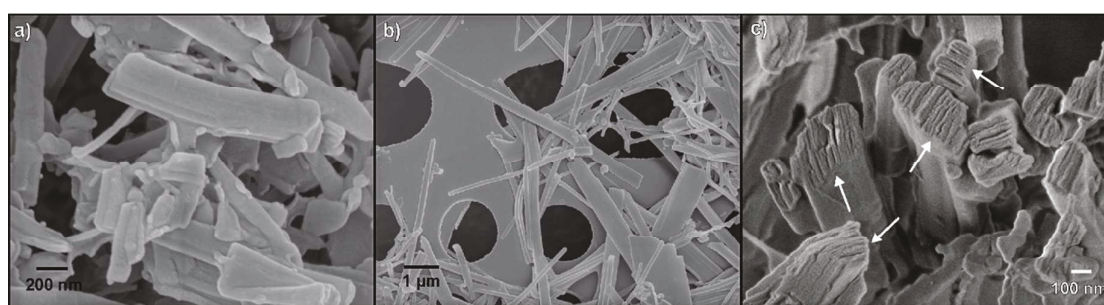
Soft Matter

12



313

314 **Figure 4:** Electron micrographs showing stack formation (a) TEM image of DOctPS, (b) FFTEM image of DMPS,
 315 (c) and (d) TEM of DPPS; arrows indicate multiple plates with similar outline. TEM of (e) DOPS, (f) DDPS sample;
 316 cross section by resin embedding technique. Samples of low T_m lipids were prepared at 4°C whereas DPPS
 317 and DMPS are prepared above T_m

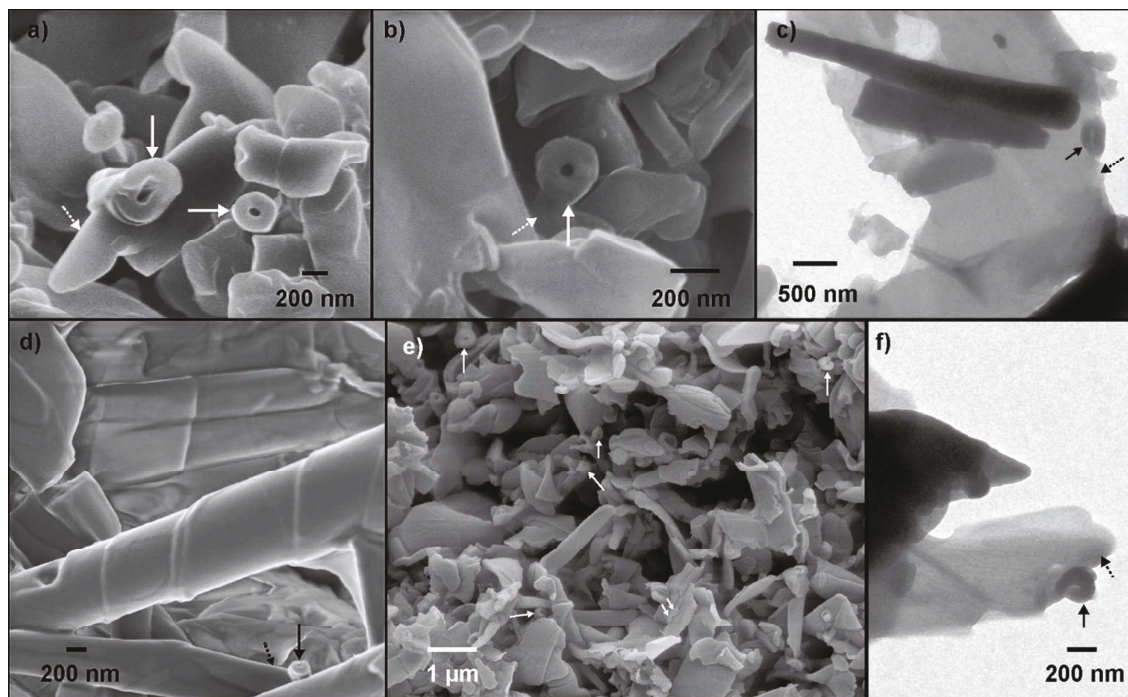


318

319 **Figure 5:** DDPS samples prepared at 4°C showing stacks (a) adhered to network-like structure in SEM image (b)
 320 with varying dimensions in SEM image and (c) displaying multilamellarity at the edges in a cryo-SEM image.

321 A peculiar ring like structure was observed on multiple occasions at the terminal edges of stacks (Fig. 6). EM
 322 data of all PS samples displayed this structure with an approximate diameter of 200-300 nm. It was more
 323 prominently observed in high T_m lipids. Such formations were mainly observed at the ends of lipid stacks or
 324 sheets. Due to breaks or irregularities at the boundaries of sheets or stacks the probability of ring formation
 325 may be enhanced. Although its function is not completely clear up to now, it could be an initiation point for
 326 cochleate formation. It is difficult to comment about immergence of such structure. One could suspect that
 327 this is a result of curling starting at the most vulnerable end of the lipid sheet, which may initiate formation of
 328 cylindrical structure and this kind of structure may serve as a support for another sheet. However, for this to
 329 work one can imagine that the axis of the ring must be parallel to the sheet that will eventually roll around the
 330 ring structure. Nevertheless, all the ring like structures we observed had its axis perpendicular to the stack.

331 Hence, it is difficult to conclude based on our findings if such structures attach to a stack and lead to further
 332 curling or if they have any other significance in the formation of cochleates. Ring formation was never
 333 observed in DSPS and DPPS samples prepared below T_m of lipid which displayed ribbons. This hints that such
 334 structure may have been formed after formation of stacks. We would like to stress that the ring formation was
 335 not completely understood as it was not possible to isolate these structures and further studies are needed to
 336 understand them completely.



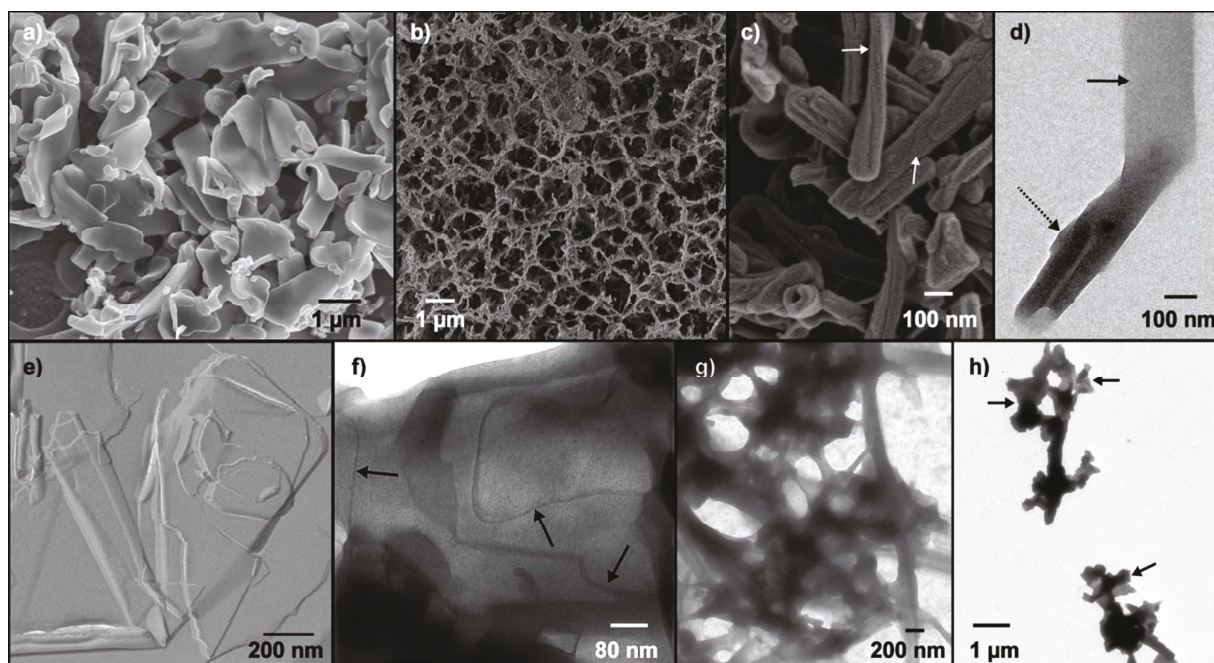
337

338 **Figure 6:** SEM images obtained from samples of (a) & (b) DPPS and (d) DOPS. (e) Overview of DPPS stacks with
 339 multiple sites showing ring formation in SEM image. TEM images of (c) DDPS and (f) DMPS, bilayer sheet
 340 attached to a ring. Dotted arrows indicate stacks/sheet and solid arrows indicate ring formation. All samples
 341 were prepared above T_m of respective lipids.

342 Networks

343 All samples prepared above T_m displayed the presence of networks of stacks as seen in Fig.7. The lateral
 344 dimensions of lamellae building network varied from a couple of bilayers to lipid stacks with coherent piling.
 345 Apparently, the process of network formation might be promoted due to unrestrained interactions between
 346 lipid stacks resulting in random attachment to one another (Fig. 7a). Occasionally, these convex-concave
 347 bilayers showed a continuous flattened regions. These regions in networks clearly showed outlines of lipid
 348 stacks at higher magnification (Fig. 7f). This suggests that formation of a nexus must be via continuous
 349 intercalation of bilayers on the host aggregate, which ultimately undergoes fusion in order to achieve
 350 thermodynamic equilibrium. However, for cochleate formation curling of stacks or sheets is a critical step,
 351 which may be hindered by uncontrolled formation of networks. The size and spatial distribution of these
 352 networks must have a strong influence on a fraction of stacks that undergo transformation into cylinders, as it
 353 directly correlates with the potential number of favorable interaction sites. Our observation suggests, samples
 354 of DMPS, DPPS and DSPS prepared above T_m had higher fraction of networks than low T_m lipids. These
 355 samples also exhibited a large number of cochleates attached to networks. TEM of these structures as seen in
 356 Fig. 7h shows fragments of curved lipid bilayers on what appears to be as pieces of incompletely formed
 357 cochleates. Although not abundant, presence of networks was also observed in samples of low T_m lipids (Fig.
 358 7g).

359



360

361 **Figure 7:** Networks observed in (a) SEM image of DPPS and (h) TEM image of DSPS sample, prepared above
 362 Tm. Networks observed samples prepared below the Tm b) Cryo-SEM image of DPPS (c) Cryo SEM image of
 363 DMPS. (g) TEM image of DDPS sample prepared at 4 °C. (d) TEM image of single stack forming a cochleate in
 364 sample of DMPS prepared below the Tm. Sheet formation observed in sample prepared above Tm in (e)
 365 FFTEM image of DPPS (f) TEM image of DSPS, image clearly shows outline of fused edges of lipid stacks. Solid
 366 arrows indicate stacks whereas dashed arrow indicates cochleate

367

368 Cochleate samples of DSPS, DPPS and DMPS prepared below Tm of lipids also showed formation of network
 369 like structures. Fig. 7b shows morphology of dense porous sponge like structures observed two month after
 370 formation of DPPS samples (prepared at 20 °C). This three-dimensional sponge like aggregates formed from
 371 the interaction of ribbons may be the result of physical gelation, a phenomenon often observed in
 372 concentrated lipid suspensions incubated for longer time⁴¹. From SEM images, the distribution of pores within
 373 the networks DSPS and DPPS samples appeared more homogeneous as compared to the networks observed in
 374 samples prepared above Tm. These network like structures never showed any presence of entangled
 375 cochleates. Morphology of these networks did not change significantly over the period except for DMPS
 376 samples prepared below Tm. In case of DMPS samples prepared at 20 °C presence of networks made of stacks
 377 was observed (Fig. 7c). These networks were different in appearance as compared to the one found in samples
 378 of DPPS and DSPS, prepared at 20 °C. In DMPS samples stacks varied in width and occasionally showed
 379 presence of cochleates (Fig. 7d) in detailed EM analysis. Fig. 7d shows cochleate forming from a single stack of
 380 DMPS in a sample prepared at 20 °C.

381 Cochleates

382 All the PSs used in this study formed cochleates when prepared above the respective Tm. Altering the length
 383 of acyl chains of PS significantly changed the aggregated structures. In samples prepared above Tm, DSPS,
 384 DPPS and DMPS showed the presence of intermediate structures along with the cochleates (Fig. 8) yielding to
 385 relatively higher polydispersity. Cochleates of high Tm lipids were often observed attached to stacks or
 386 networks (Fig. 8c). In contrast, DOPS, DOctPS and DDPS showed less intermediate structures along with
 387 cochleates and were less polydispersed. Fig. 8e shows a cochleate amidst a cluster of network and stacks.

Soft Matter

388 Although the shape of cochleates is usually reported as cylindrical, the shape of many particles in samples of
 389 low T_m lipids was rather like a truncated cone where one end was tapering away from a broad end. Cochleates
 390 of high T_m lipids appeared more cylindrical in shape.

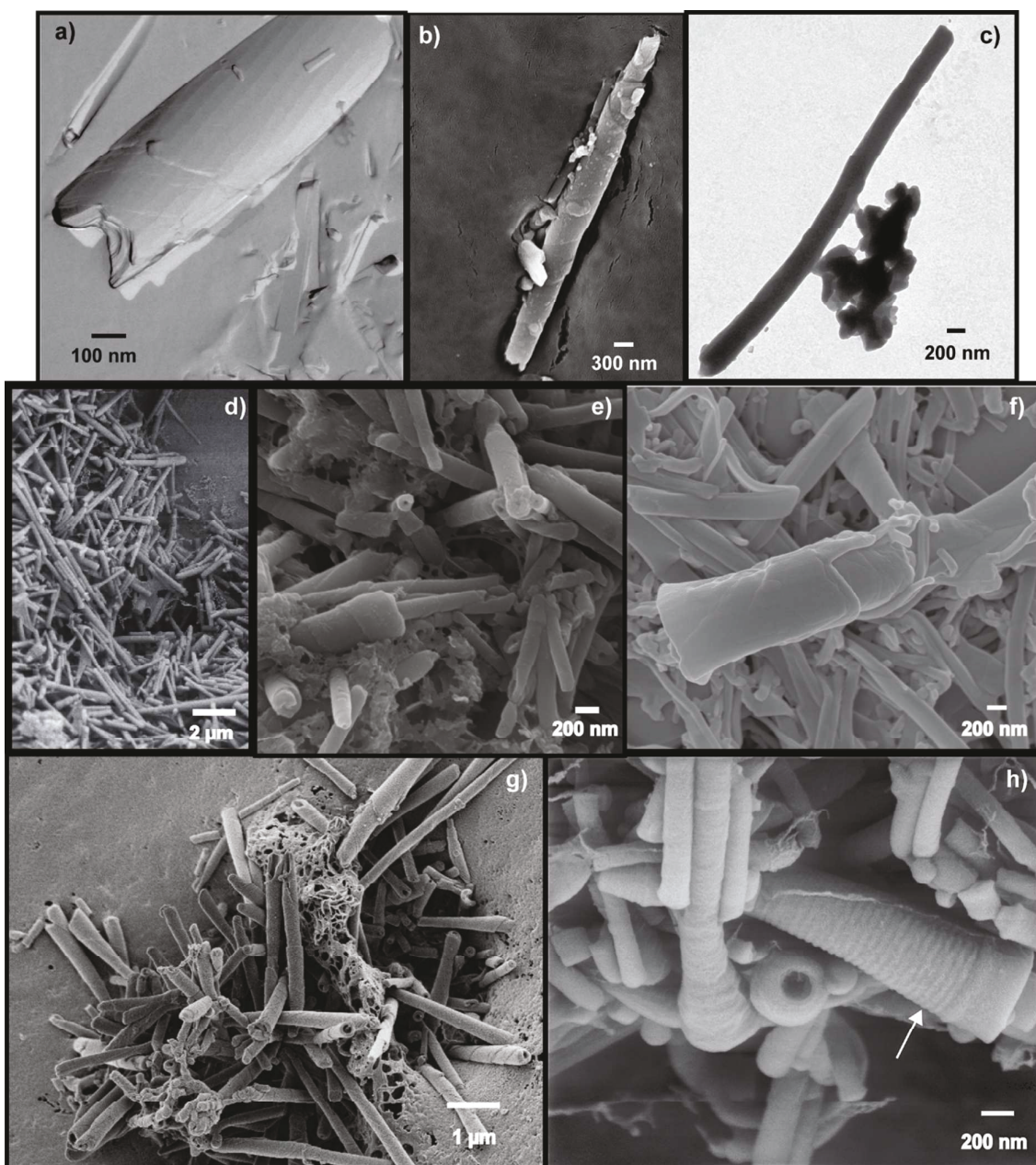
391 All samples of low T_m lipids prepared at 4 °C showed formation of cylindrical structures. DoctPS samples
 392 prepared at 4 °C showed cochleates within first 2 minutes after addition of calcium along with intermediate
 393 structures. However, samples observed 40 minutes after addition of calcium predominantly showed
 394 cochleates. In DDPS samples prepared at 4 °C cochleate formation was observed only one hour after addition
 395 of calcium. In case of DSPS and DPPS when cochleate formation was carried out below the T_m, the aggregation
 396 process seemed to stop at the formation of ribbons and there was no presence of any cochleates. This arrest
 397 may be attributed to low acyl chain mobility of these lipids below the T_m and hence highlights the importance
 398 of process temperature for the optimal cochleate formation⁴². One can anticipate the increased mobility of
 399 lipid molecules above T_m which would help the self-assembly into lamellar structures which would further
 400 enhance lamellar order by condensation. In case of DMPS few cochleates were observed when the samples
 401 were prepared at 20 °C

402 **Table 2:** Size Analysis of cochleates

Phosphatidylserine	Width (nm ± SE)	Length (nm ± SE)
DSPS (C18:0)	283.1±8.4 (n=352)	3190.7±106.3 (n=352)
DPPS (C16:0)	435.2±8.9 (n=490)	3137.4±84.8 (n=385)
DMPS (C14:0)	492.7±14.3 (n=385)	3294.7±98.9 (n=457)
DOPS (C18:1)	314.8±6.4 (n=224)	5156.8±156.4 (n=249)

403

404 To find out effect of acyl chains variation on the resulting cochleates, we studied dimensions of cochleates
 405 formed in samples prepared above T_m. We evaluated over 1500 TEM images to measure width and length of
 406 DSPS, DPPS, DMPS, and DOPS cochleates (Table 2). When plotted against number of carbon atoms in lipid
 407 chain, the width of cochleates of DMPS, DPPS and DSPS reveals a negative linear association with a fair value
 408 of the correlation coefficient ($r^2 = 0.9364$). This suggests that cochleates get slender with increase in carbon
 409 chain length. It is well known that transition of the lipid molecules from the liquid crystalline to the gel state
 410 results in a decrease of area per molecule⁴³. In the past we have proposed that the extent of this decrease may
 411 affect the size of the inner channel of cochleates when acyl chain length is constant². This could explain
 412 difference in widths between DMPS, DPPS and DSPS cochleates. It is however of interest to note that the mean
 413 length in cochleates of high T_m lipids did not differ much with variation in carbon chain of saturated fatty
 414 acids. Samples of low T_m lipids showed inclination towards the production of cochleates with larger
 415 dimensions. It is noteworthy that an unsaturation in fatty acyl chain in case of DOPS (C18:1) led to formation of
 416 longer cochleates (5.1 μm) as compared to completely saturated DSPS (3.2 μm).



417

418 **Figure 8:** Cochleates observed in different samples prepared above their respective T_m . (a) FFTEM image of
 419 DDPS, (b) Cryo-SEM image of DPPS, (c) TEM image of DSPS; image showing cochleates tangled with network of
 420 lipid stacks, (d) SEM image of DOctPS, (e) cryo-SEM image of DMPS; showing attached networks (f) SEM image
 421 of DDPS, stacks building cochleate cylinder g) cryo-SEM image of DOPS and h) SEM image of DOctPS; arrow
 422 showing cochleate having a ridge like pattern.

423 In DOctPS samples SEM images of some cochleate particles revealed regular striations on the entire surface
 424 (Fig. 8h). These structures were observed only in DOctPS cochleate samples. We did not come across any
 425 reference of such structures in the literature for cochleates. The angle of the striations was approximately
 426 perpendicular as compared to the length of cochleates indicating the structures to be periodic decorations.
 427 These structures may result from self-assembly of free amphiphilic molecules on the hydrophobic surface as
 428 previously suggested by Ke *et al.*⁴⁴. Adsorption of surfactants at interfaces in aqueous environment is
 429 commonly observed and is a phenomenon that can create a distribution of charges on particles⁴⁵. According to

Soft Matter

430 the model put forth by *Islam et al.*, it is also possible that surfactant hemimicelles are chemically adsorbed on
431 the hydrophobic surfaces⁴⁶. The fact that these structures were only observed for DOctPS, which is the most
432 surfactant like PS in this study, points toward hydrophobic interactions between cochleate surface and
433 surfactant molecules. At this moment, we can only speculate on these structures and a further detailed
434 investigation would be required before origins of such structures can be explained in detail.

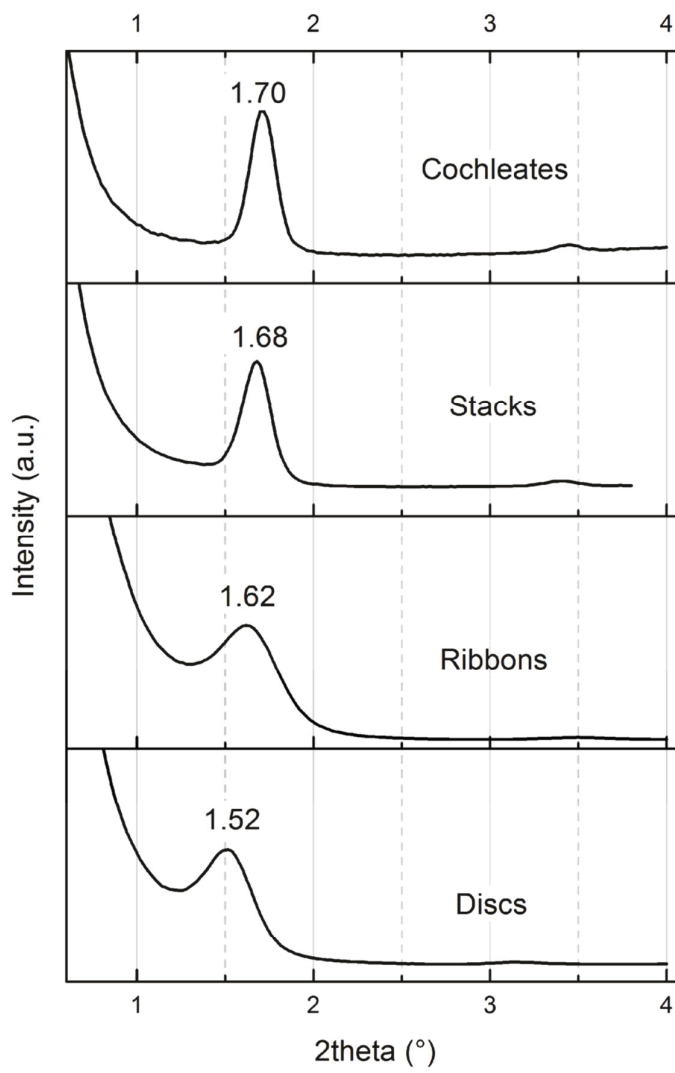
435

436 SAXS studies

437 Small angle X-ray scattering (SAXS) was employed as an alternative approach for further characterization and
438 to understand distinguishing characteristics of the intermediate structures. DSPS was the choice of lipid for this
439 study since it does not allow stack or cochleate formation when prepared at 20 °C allowing for evaluation of
440 sample with single morphology. Prior to SAXS studies, the dialyzed-freeze dried samples were evaluated under
441 electron microscope to make sure the samples contained the desired structures, which were of interest. The
442 SAXS data of DSPS for four structures i.e. bilayers before calcium interaction (discs), bilayers after calcium
443 interaction at 20 °C (ribbons), stacks prepared just below the T_m at 50 °C and cochleates formed above the T_m
444 are shown in Fig. 9. According to SAXS, the inter-lamellar repeat distance for all four structures was calculated.
445 DSPS bilayers without calcium revealed the repeat distance of 5.7 nm whereas the corresponding repeat
446 distance for ribbons, stacks, and cochleates was 5.4 nm, 5.2 nm, and 5.1 nm, respectively. Dissimilar SAXS
447 values for discs and ribbons are indicative of a strong interaction between calcium ions and the serine
448 headgroups taking place even below T_m of the lipid. Gradual reduction in the repeat distances from discs to
449 cochleates may be indicative of the increase in degree of condensation in different intermediate structures
450 during cochleate formation. Despite the same basic molecular subunits the degree of disorder and
451 polydispersity may also establish differences in SAXS patterns of different intermediates. Hence being
452 organized molecular assemblies, physical properties of cochleates are not solely indicated by their molecular
453 nature but are also strongly influenced by their ensemble.

Soft Matter

18



454

455 **Figure 9:** SAXS spectra for DSPS discs, ribbons, stacks and cochleates.

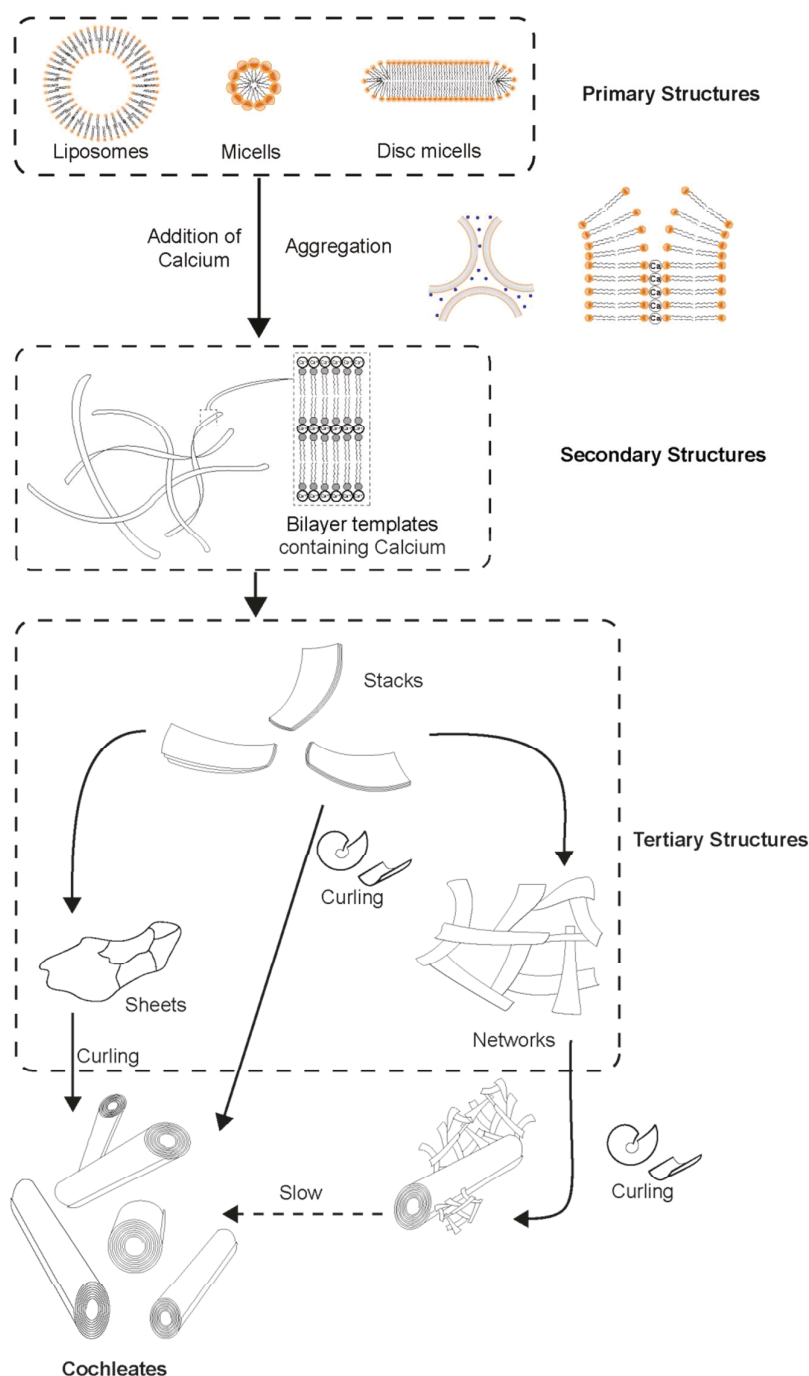
456

457

Soft Matter

19

458 Possible mechanism of cochleate formation:



459

460 **Figure 10:** Schematic showing probable order for evolution of microstructures during formation of cochleates

461 In the current article we have mainly focused on understanding various intermediate structures involved in the
 462 formation mechanism of cochleates. The mechanism of cochleate formation from PS has been briefly
 463 discussed previously by Papahadjopoulos⁸. Some further investigations on intermediates arising during
 464 interaction of PS vesicles with calcium ions were reported which mention fusion or violent rupture of vesicles
 465 and formation of flattened structures^{35,36}. Studies on this scheme have exercised use of video-enhanced
 466 microscopy³⁵, rapid mixing³⁴ and freezing device³⁶ etc in past. In the current study we have focused on the

Soft Matter

467 process temperature and effect of its variation on rate of cochleate formation. Cochleate formation being a
468 polymorphous process may have more than one secondary pathways due to uncontrolled interaction of
469 calcium and PS headgroups. In this section we have summerized the sequence of morphological changes
470 obseved during this investigation to put forth the probable formation mechanism.

471 We have classified structures under primary, secondary and tertiary structures (Fig. 10). Cochleate formation
472 involves two main stages: first, rapid nucleation which acts like a template followed by aggregation and
473 association of templates to assist in growth of the final superstructures. During growth cochleate formation
474 pathway most likely evolves through rearrangement and oriented attachment⁴⁷. Primary structures are the
475 starting materials and represent liposomes, discs or micelles of PS without calcium. Addition of calcium to
476 primary structures triggers the mutual adhesion, deformation, fusion and formation of precipitates or
477 aggregates of intrinsically ordered fragments³⁵. Our observations showed that the multilamellar intermediate
478 structures observed immediately after aggregation give rise to secondary bilayer fragments (which we named
479 ribbons). We interpret that these structures may result due to bilayer destabilization or rupture due to high
480 tension in intermediate multilamellar aggregates^{48, 49}. These resulting ribbonlike templates of lipids containing
481 cations are secondary structures. Tendency of a system to minimize free energy probably promotes further
482 aggregation and particle growth. The two possible reasons may include reduction in surface area and
483 regulation of high energy surfaces. Because ribbons would have larger energetically unfavorable surfaces they
484 may undergo curling, adhesion or fusion comparatively faster in order to give rise to complex multilamellar
485 structures.

486 We speculate that ribbons undergo fusion to form an array of tertiary structures most characteristic of which
487 are stacks. These structures had also been identified by *Garidel et al.* as bands in DMPG cochleate samples and
488 were suggested to form cochleates²⁸. Stacks are multilamellar and generally have elongated trapezoidal shape.
489 Our results highlight that stack formation may be an essential step in order to form cochleates. Stacks can
490 form cochleates without undergoing further aggregation. It was observed that stacks can also undergo fusion
491 to form broad sheets which are irregular in shape and roll up to form cochleates. Our study points to the
492 possibility that generation of ring like structures may play a part in cochleate formation by initiating curling of
493 stacks, sheets etc. Intermediates observed throughout the cochleate formation process are non-stoichiometric
494 and occur due to transformations precursors undergo before forming cochleates. Cochleates are carpet-roll
495 like structures with hollow central channel and open ends, which can further undergo aggregation. Complete
496 absence of tertiary structures was seldom observed in samples of cochleates prepared from PS. Reason being
497 various steps may take place simultaneously during cochleate formation such as curling, branching,
498 agglomeration, rearrangement etc and these complex interactions may give rise to diverse tertiary structures
499 which can further form networks of tertiary structures and/or cochleates. Complex architectures composed of
500 fused lipid networks, sheets and cochleates may be the final result of thermodynamic equilibrium during
501 formation process. Such tertiary structures appear to be stable and may coexist with cochleates. Hence rate of
502 conversion of tertiary structures to cochleates is an important parameter which would influence polydispersity
503 of the final cochleate formulation, which in turn would be of great interest to a formulation scientist.

504

505

Soft Matter**506 Conclusion**

507

508 Current research was undertaken on various pure PSs with a goal to understand fundamental mechanisms of
509 cochleate formation. It was found that the samples prepared at lower process temperatures allowed a glimpse
510 into intermediate structures as compared to those prepared above the T_m . This could probably be a result of
511 decreased rate of cochleate formation at lower temperatures, however more studies with focus on kinetics
512 and calorimetry are required for further understanding of this aspect. It is noteworthy that the inability to
513 form stacks in samples prepared below T_m resulted in failure to form cochleate structures. Hence, the
514 proposed formation mechanism has identified the generation of stacks as an essential stage in the cochleate
515 formation. Current investigation also showed that saturation and chain length of PS fatty acids have a strong
516 influence on final morphology of cochleates. Despite the variation in lipid acyl chains, similar intermediate
517 structures were observed during formation of cochleates from all phosphatidylserines. Our findings
518 ascertained that cochleate formation is not by simple accretion of monomers, but through evolution of well-
519 defined hierarchical structures like ribbons, stacks, networks, sheets which leads to stable cochleates. Hence
520 for the development of a desired cochleate system, monitoring reciprocity of several processes, whose relative
521 rates determine the final outcome, may be a necessity. We believe our effort will provide better
522 understanding regarding formation of cochleates which may present future scientists with ability to modulate
523 formulation by making rational alterations and could eventually aid to design and characterize a product for
524 pharmaceutical applications.

525 Acknowledgement

526 K. N. and A. F. would like to thank Phospholipid Research Centre, Heidelberg, Germany for financial support. F.
527 H. S. is grateful to the Thuringian Ministry for Education, Science, and Culture (TMBWK; #B515-11028, SWAXS-
528 JCSM) for financial support.

529

Soft Matter

530 References

- 531 1. R. Rao, E. Squillante, 3rd and K. H. Kim, *Critical reviews in therapeutic drug carrier systems*,
532 2007, **24**, 41-61.
- 533 2. K. Nagarsekar, M. Ashtikar, J. Thamm, F. Steiniger, F. Schacher, A. Fahr and S. May,
534 *Langmuir*, 2014, **30**, 13143-13151.
- 535 3. L. Zarif, in *Methods in Enzymology*, ed. D. Nejat, Academic Press, 2005, vol. Volume 391, pp.
536 314-329.
- 537 4. J. V. Selinger and J. M. Schnur, *Physical review letters*, 1993, **71**, 4091-4094.
- 538 5. W. Helfrich, *The Journal of Chemical Physics*, 1986, **85**, 1085-1087.
- 539 6. J. S. Chappell and P. Yager, *Chemical Physics*, 1991, **150**, 73-79.
- 540 7. A. S. Goldstein, A. N. Lukyanov, P. A. Carlson, P. Yager and M. H. Gelb, *Chemistry and physics*
541 *of lipids*, 1997, **88**, 21-36.
- 542 8. D. Papahadjopoulos, W. J. Vail, K. Jacobson and G. Poste, *Biochimica et biophysica acta*,
543 1975, **394**, 483-491.
- 544 9. M. Roux and M. Bloom, *Biophysical journal*, 1991, **60**, 38-44.
- 545 10. H. Hauser, *Chemistry and physics of lipids*, 1991, **57**, 309-325.
- 546 11. M. J. Hope and P. R. Cullis, *Biochemical and biophysical research communications*, 1980, **92**,
547 846-852.
- 548 12. C. P. S. Tilcock and P. R. Cullis, *Biochimica et Biophysica Acta (BBA) - Biomembranes*, 1981,
549 **641**, 189-201.
- 550 13. H. L. Casal, H. H. Mantsch, F. Paltauf and H. Hauser, *Biochimica et biophysica acta*, 1987, **919**,
551 275-286.
- 552 14. K. Jacobson and D. Papahadjopoulos, *Biochemistry*, 1975, **14**, 152-161.
- 553 15. F. Giulieri and M. P. Krafft, *Journal of colloid and interface science*, 2003, **258**, 335-344.
- 554 16. W. Helfrich and J. Prost, *Physical review. A*, 1988, **38**, 3065-3068.
- 555 17. P. Nelson and T. Powers, *Journal de Physique II*, 1993, **3**, 1535-1569.
- 556 18. R. P. Rand, B. Kachar and T. S. Reese, *Biophysical journal*, 1985, **47**, 483-489.
- 557 19. P. S. David, in *The Structure of Biological Membranes, Second Edition*, CRC Press, 2004, DOI:
558 doi:10.1201/9781420040203.ch8.
- 559 20. B. Kachar, N. Fuller and R. P. Rand, *Biophysical journal*, 1986, **50**, 779-788.
- 560 21. S. T. Sun, E. P. Day and J. T. Ho, *Proceedings of the National Academy of Sciences*, 1978, **75**,
561 4325-4328.
- 562 22. J. R. Silvius and J. Gagne, *Biochemistry*, 1984, **23**, 3232-3240.
- 563 23. A. Martin-Molina, C. Rodriguez-Beas and J. Faraudo, *Biophysical journal*, 2012, **102**, 2095-
564 2103.
- 565 24. P. T. Vernier, M. J. Ziegler and R. Dimova, *Langmuir*, 2009, **25**, 1020-1027.
- 566 25. C. R. Flach and R. Mendelsohn, *Biophysical journal*, 1993, **64**, 1113-1121.
- 567 26. L. Loomba and T. Scarabelli, *Ther Deliv*, 2013, **4**, 1179-1196.
- 568 27. H. Sarig, D. Ohana, R. F. Epanand, A. Mor and R. M. Epanand, *FASEB journal : official publication*
569 *of the Federation of American Societies for Experimental Biology*, 2011, **25**, 3336-3343.
- 570 28. P. Garidel, W. Richter, G. Rapp and A. Blume, *Physical Chemistry Chemical Physics*, 2001, **3**,
571 1504-1513.
- 572 29. B. Papahadjopoulos-Sternberg, *Biophysical journal*, 2012, **102**, 290a.
- 573 30. W. S. Rasband, *U. S. National Institutes of Health, Bethesda, Maryland, USA*, 1997-2014.
- 574 31. T. Bozo, R. Brecka, P. Grof and M. S. Kellermayer, *Langmuir*, 2015, **31**, 839-845.
- 575 32. D. Papahadjopoulos, W. J. Vail, C. Newton, S. Nir, K. Jacobson, G. Poste and R. Lazo,
576 *Biochimica et Biophysica Acta (BBA) - Biomembranes*, 1977, **465**, 579-598.
- 577 33. J. Wilschut, N. Duzgunes, D. Hoekstra and D. Papahadjopoulos, *Biochemistry*, 1985, **24**, 8-14.
- 578 34. R. P. Rand, B. Kachar and T. S. Reese, *Biophysical journal*, 1985, **47**, 483-489.
- 579 35. B. Kachar, N. Fuller and R. P. Rand, *Biophysical journal*, 1986, **50**, 779-788.

Soft Matter

23

- 580 36. D. C. Miller and G. P. Dahl, *Biochimica et Biophysica Acta (BBA)-Biomembranes*, 1982, **689**,
581 165-169.
- 582 37. L. Zarif, J. R. Graybill, D. Perlin, L. Najvar, R. Bocanegra and R. J. Mannino, *Antimicrobial*
583 *Agents and Chemotherapy*, 2000, **44**, 1463-1469.
- 584 38. J. H. Fuhrhop and W. Helfrich, *Chemical Reviews*, 1993, **93**, 1565-1582.
- 585 39. C. Fong, T. Le and C. J. Drummond, *Chemical Society reviews*, 2012, **41**, 1297-1322.
- 586 40. V. R. Sankar and Y. Reddy, *International Journal of Pharmacy and Pharmaceutical Sciences*
587 2010, **2**, 220-223.
- 588 41. S. Svenson and P. B. Messersmith, *Langmuir*, 1999, **15**, 4464-4471.
- 589 42. P. Yager, P. E. Schoen, C. Davies, R. Price and A. Singh, *Biophysical Journal*, 1985, **48**, 899-
590 906.
- 591 43. M. C. Blok, E. C. van der Neut-Kok, L. L. van Deenen and J. de Gier, *Biochimica et biophysica*
592 *acta*, 1975, **406**, 187-196.
- 593 44. P. C. Ke, *Physical chemistry chemical physics : PCCP*, 2007, **9**, 439-447.
- 594 45. C. Richard, F. Balavoine, P. Schultz, T. W. Ebbesen and C. Mioskowski, *Science*, 2003, **300**,
595 775-778.
- 596 46. M. F. Islam, E. Rojas, D. M. Bergey, A. T. Johnson and A. G. Yodh, *Nano Letters*, 2003, **3**, 269-
597 273.
- 598 47. R. L. Penn and J. F. Banfield, *Science*, 1998, **281**, 969-971.
- 599 48. E. A. Evans and V. A. Parsegian, *Annals of the New York Academy of Sciences*, 1983, **416**, 13-
600 33.
- 601 49. E. Evans and R. Kwok, *Biochemistry*, 1982, **21**, 4874-4879.
- 602

3.2 Publication 2:

Electron microscopy and theoretical modeling of cochleates

Kalpa Nagarsekar, Mukul Ashtikar, Frank Steiniger, Jana Thamm, Felix Schacher, Alfred Fahr and Sylvio May

Langmuir, 2014, 30 (44), pp 13143–13151 Published on October 28, 2014

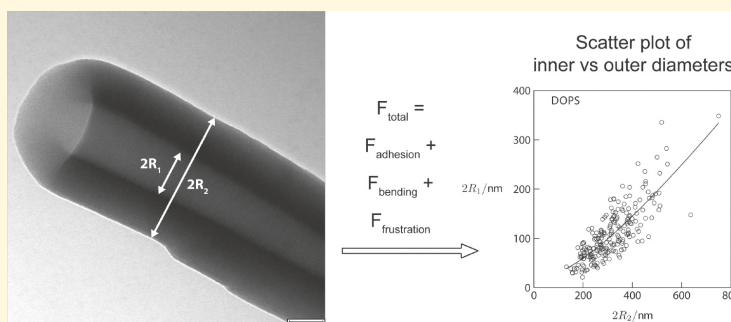
Electron Microscopy and Theoretical Modeling of Cochleates

Kalpa Nagarsekar,[†] Mukul Ashtikar,[†] Jana Thamm,[†] Frank Steiniger,[‡] Felix Schacher,[§] Alfred Fahr,[†] and Sylvio May^{*,||}

[†]Lehrstuhl für Pharmazeutische Technologie, Institut für Pharmazie, and [§]Institut für Organische Chemie und Makromolekulare Chemie und Jena Center for Soft Matter, Friedrich-Schiller-Universität Jena, Lessingstraße 8, 07743 Jena, Germany

[‡]Elektronenmikroskopisches Zentrum, Universitätsklinikum Jena, Ziegelmühlenweg 1, 07743 Jena, Germany

^{||}Department of Physics, North Dakota State University, Fargo, North Dakota 58108-6050, United States



ABSTRACT: Cochleates are self-assembled cylindrical condensates that consist of large rolled-up lipid bilayer sheets and represent a novel platform for oral and systemic delivery of therapeutically active medicinal agents. With few preceding investigations, the physical basis of cochleate formation has remained largely unexplored. We address the structure and stability of cochleates in a combined experimental/theoretical approach. Employing different electron microscopy methods, we provide evidence for cochleates consisting of phosphatidylserine and calcium to be hollow tubelike structures with a well-defined constant lamellar repeat distance and statistically varying inner and outer radii. To rationalize the relation between inner and outer radii, we propose a theoretical model. Based on the minimization of a phenomenological free energy expression containing a bending, adhesion, and frustration contribution, we predict the optimal tube dimensions of a cochleate and estimate ratios of material constants for cochleates consisting of phosphatidylserines with varied hydrocarbon chain structures. Knowing and understanding these ratios will ultimately benefit the successful formulation of cochleates for drug delivery applications.

INTRODUCTION

Since their discovery in 1975 by Papahadjopoulos and co-workers,¹ cochleates have attracted considerable interest, both because of their remarkable structural properties² and because of their potential use as drug delivery vehicles. Cochleates are elongated spiral rolls that consist of phospholipid and divalent (or higher-valent) cation complexes. Their highly condensed solidlike structure imparts protection to incorporated molecules³ and potential for slow release. This together with stability, ease of production, and biocompatibility renders cochleates promising candidates for the delivery of a wide range of drugs and fragile molecules such as proteins and peptides.^{4,5} Until now, cochleates have been successfully utilized for the delivery of multiple active ingredients such as antifungal agents,⁶ DNA, and vaccines.⁷

The building blocks of cochleates are negatively charged phospholipids with either saturated or unsaturated hydrocarbon chains. Several natural phospholipids such as phosphatidylserine,⁸ phosphatidylglycerol,⁹ and phosphatidic acid¹⁰ have been used as precursors for cochleates. Their interactions with divalent or higher-valent cationic condensing agents result in

the formation and precipitation of stacks of bilayer sheets. Interbilayer attraction and expulsion of water molecules are believed to originate from bridging of the condensing agent between opposed lipid layers, thus forming a compact aggregate with a concomitant increase in the value of the endothermic transition temperature.¹¹ Bending of the condensate into a cylindrical structure appears to be thermodynamically more favorable than the formation of other supramolecular structures, including a planar bilayer stack.

The past few decades have witnessed substantial improvements of protocols to form cochleates.^{12,13} In addition, the usage of drug molecules as condensing agents instead of metal cations has been explored. One of the reported strategies employing multivalent cationic drugs utilizes tobramycin as the bridging agent.¹⁴ We would like to point out that most previous studies have focused on the feasibility of using cochleates as drug delivery vehicles rather than on investigating

Received: July 15, 2014

Revised: September 16, 2014

Published: October 15, 2014

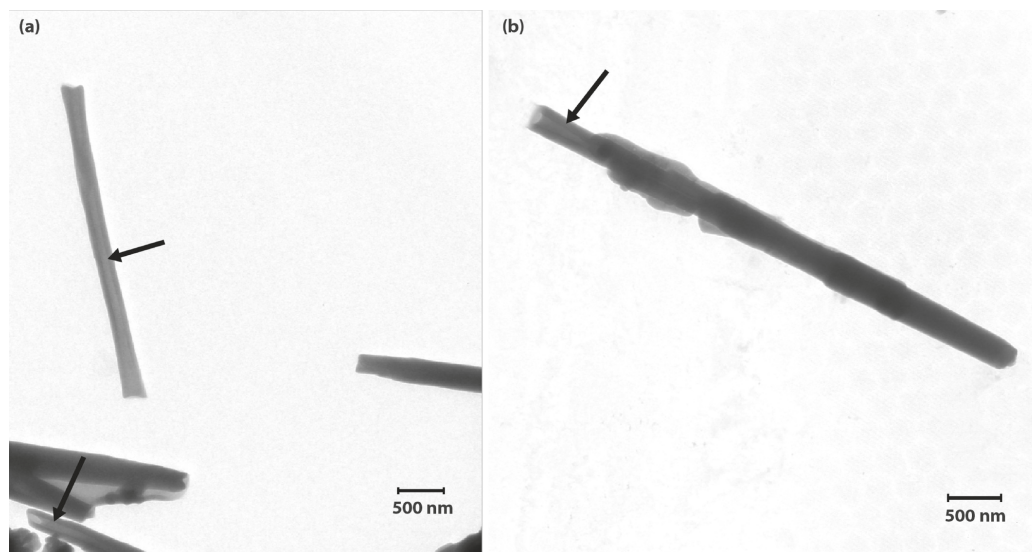


Figure 1. Transmission electron micrographs of (a) DOPS-Ca cochleates and (b) DSPS-Ca cochleates. Positions marked by arrows indicate the tubelike hollow cochleate structure.

their structure and stability. As a result, structural features, thermodynamic stability, and formation pathways of cochleates have remained largely unexplored. Our study addresses some of these aspects in a combined experimental and theoretical approach. By employing electron microscopy we demonstrate that both DOPS (dioleoylphosphatidylserine) and DSPS (distearoylphosphatidylserine) cochleates prepared with Ca^{2+} as bridging agent contain an aqueous inner channel. We quantify both the inner and outer radii of cochleate tubes consisting of calcium and phosphatidylserine with varying degree of chain saturation. In an attempt to rationalize the measured distribution of tube radii, we propose a theoretical model. Based on a phenomenological free energy expression, the model enables us to estimate the optimal dimensions of a cochleate. The model accounts for the degree to which cochleates are rolled up in thermal equilibrium and establishes a relation between the inner and outer radii. The model suggests that the sum of bilayer bending energy and calcium-mediated bilayer–bilayer adhesion energy alone is insufficient to explain the experimentally observed size distribution of cochleates. However, our data can be rationalized if we further add a mismatch contribution to the free energy that originates from an incomplete lipid relaxation during bending of an initially planar membrane stack into a tubular structure.

EXPERIMENTAL SECTION

Materials. Dioleoylphosphatidylserine and distearoylphosphatidylserine were obtained from Avanti Polar Lipids Inc. (USA). For embedding studies, Araldite LY 564 was obtained from Huntman Advanced Materials GmbH (Switzerland). All buffers and other chemical reagents were of analytical grade and were obtained from Sigma-Aldrich GmbH (Germany).

Preparation of Cochleates. Cochleates were prepared by a trapping method.⁶ Briefly, lipid was dissolved in a mixture of chloroform:methanol (3:1) in a round-bottom flask followed by removal of the organic solvents using a rotary evaporator (R-144 BUCHI Labortechnik GmbH, Germany) to form a thin lipid film. The lipid film was further hydrated with 10 mM TRIZMA [2-amino-2-(hydroxymethyl)-1,3-propanediol] buffer above the transition temper-

ature. The suspension was vortexed and extruded through a polycarbonate membrane of 100 nm pore size (Avestin, Canada) to produce a homogeneous lipid dispersion. Cochleates were formed by addition of calcium chloride (100 mM) to the lipid dispersion in buffer (NaCl, 100 mM; TRIZMA, 10 mM) under constant stirring above the lipid transition temperature. The molar ratio of lipid to calcium was 1:1. The precipitated dispersions were then stored at 4 °C.

Scanning Electron Microscopy. An aliquot of 5 μL of the cochleate dispersion was adhered for 5 min onto a perforated Formvar-coated copper grid (300 mesh, Quantifoil, Germany). Excess of liquid was removed with a lint-free filter paper. Further, the grid was quickly plunged in liquid propane–ethane ($-180\text{ }^\circ\text{C}$), freeze-dried in a BAL-TEC BAF 060 (Baltec, Liechtenstein) and examined in a LEO 1350 Gemini (Carl Zeiss, Germany) scanning electron microscope (SEM) at 3 kV acceleration voltage and working distance of 6 mm using a secondary electron detector.

Transmission Electron Microscopy. Cochleate dispersion was air-dried on a Formvar-carbon coated copper grid (300 mesh, Plano, Germany). Grids were investigated using a Zeiss EM 902A (Carl Zeiss, Germany) transmission electron microscope (TEM) operated at 80 kV. Images were acquired with a $1\text{k} \times 1\text{k}$ FastScan-F114 CCD Camera (TVIPS GmbH, Germany).

Cryo-electron Tomography. Sample Preparation. Cochleate dispersion was added to a carbon-coated copper grid (R1.2/1.3 + 2 nm, Quantifoil Micro Tools GmbH, Germany). After excess liquid was blotted from the sample, it was subjected to plunge freezing in liquid ethane at $-180\text{ }^\circ\text{C}$ as described by Dubochet et al.¹⁵ The grid was freeze-dried at $-90\text{ }^\circ\text{C}$ for 1 h in a Philips CM 120 cryo-TEM (Philips, Netherlands). Further, the grid was gold labeled by placing 3 μL of 5 nm colloidal gold clusters (Sigma, USA) for subsequent alignment purposes. The grids were then transferred into a liquid nitrogen cooled ($T = -196\text{ }^\circ\text{C} \pm 70^\circ$ tilt cryo-holder (Gatan Inc., USA) and inserted into the cryoelectron microscope.

Preparation of Tomographic Tilt Series. Tomographic tilt series were collected under low-dose conditions with an increment of 3° within a tilt range from -65 to $+65^\circ$ using a TEM operating at 120 kV and a $1\text{k} \times 1\text{k}$ FastScan-F114 CCD Camera (TVIPS GmbH, Germany). The defocus level was typically around $-3\text{ }\mu\text{m}$. Data acquisition was fully automated as described previously.¹⁶ The pixel size at the specimen level was between 1.08 and 1.7 nm.

Image Processing and Visualization. The projection images were aligned and back-projected, resulting in a three-dimensional (3D)

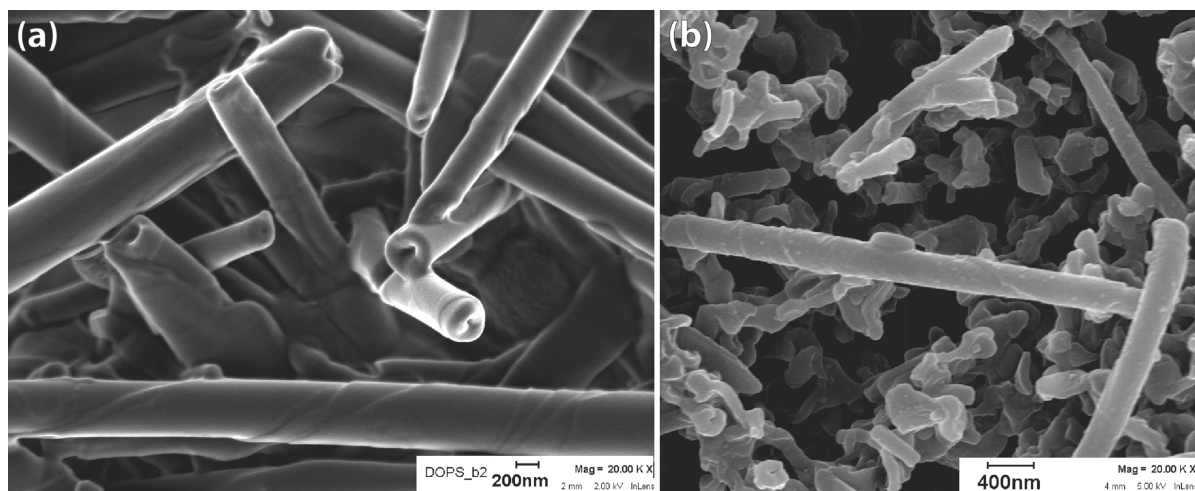


Figure 2. Scanning electron micrographs of (a) DOPS-Ca cochleates and (b) DSPS-Ca cochleates.

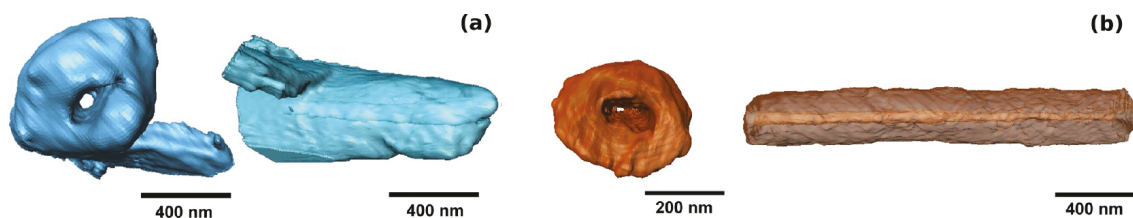


Figure 3. Three-dimensional reconstruction of (a) DOPS-Ca cochleates and (b) DSPS-Ca cochleates showing the inner channel from different perspectives.

reconstruction with a resolution of about 10 nm.¹⁷ The IMOD software package (University of Colorado, USA) was used for 3D processing and visualization.

Investigation of Cross Section of Resin-Embedded Cochleates. Cochleates were centrifuged and the pellet was redispersed in 100 mM cacodylate buffer (pH 7.2) containing 1% OsO₄ for 2 h. Cochleates were centrifuged again and the pellet was rinsed in buffer and dehydrated in ethanol (50% v/v) for 15 min. It was further subjected for 1 h to 1% uranyl acetate solution to improve contrast. The pellet was then dispersed in an epoxy resin Araldite LY 564, used as the embedding medium. The mixture was polymerized in a closed mold for 2 days at 60 °C. The polymer blocks were microtomed into thin (70–100 nm) slices, using a diamond knife mounted on an Ultracut E device (Reichert Labtec, Germany) at room temperature. The slices were then transferred to copper grids (Quantifoil, Germany) and examined by TEM.

Small Angle X-ray Scattering (SAXS). Cochleate samples were dialyzed using Spectra/Por CE dialysis tubing, 10 000 molecular weight cutoff (Spectrum Medical Industries, USA) and freeze-dried (Christ Epsilon 2-4 LSCPlus, Martin Christ Gefriertrocknungsanlagen GmbH, Germany) before evaluation. SAXS measurements of cochleate samples were performed on a Bruker Nanostar (Bruker, Germany), equipped with a microfocus X-ray source (Incoatec I μ S Cu E025, Incoatec, Germany), operating at $\lambda = 1.54$ Å. A pinhole setup with 750, 400, and 1000 μ m (in the order from source to sample) was used, and the sample-to-detector distance was 107 cm. Samples were mounted on a metal rack and fixed using tape. All measurements were carried out at room temperature for 120 min, with a two-dimensional position-sensitive detector, Vantec 2000 (Bruker GmbH, Germany). The scattering patterns were corrected for the beam stop and the background prior to evaluations and radially integrated to obtain the scattering intensity as a function of the scattering vector $q = (4\pi/\lambda) \sin \theta$, with 2θ being the scattering angle and λ the X-ray wavelength.

RESULTS AND DISCUSSION

Assessment of Cochleate Formation. Following the procedure outlined in the Experimental Section, DOPS and DSPS cochleates were prepared with Ca²⁺ as bridging agent by the trapping method.⁶ Samples were first observed by TEM and SEM. The presence of cylindrical structures indicated successful cochleate formation for both lipids. Figure 1 shows TEM micrographs of cochleate particles. In TEM analysis, cochleates appeared like elongated cylinders with the occasional appearance of bilayer patterns at higher magnification. Most importantly, at higher accelerating potentials, a hollow tube within the cochleates (highlighted in Figure 1 by arrows) was evident despite poor contrast due to the electron-dense nature of the system. SEM micrographs in Figure 2 also indicate channels inside the cylindrical particles, corroborating our TEM findings. All the samples were prepared in triplicate. The freeze-dried samples were also analyzed by electron microscopy to evaluate changes in their structure. The morphology of lyophilized cochleates was not altered, which can be attributed to the negligible water content associated with the bilayers.⁴ All the samples were confirmed to have formed cochleates before they were subjected to any further characterization.

Cochleate Structure Studied by Cryoelectron Tomography. The self-assembly of cochleates is characterized by a compact packing of lipid bilayers. Consequently, electrons cannot pass through the cochleate easily thus resulting in an image with poor contrast. Hence, TEM is not the method of choice for obtaining specific information about the internal cochleate structure, as most of the particles appear dark against

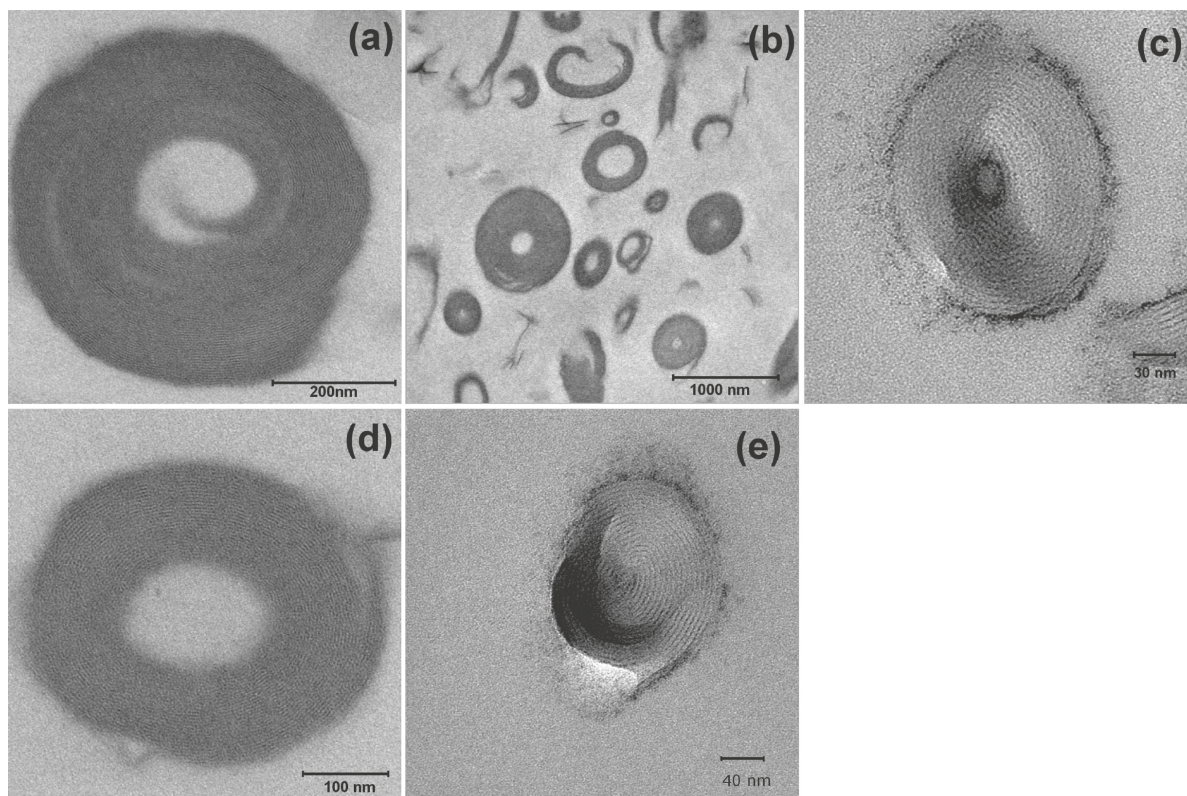


Figure 4. TEM of transverse sections of (a and b) DOPS-Ca and (c) DSPS-Ca cochleates obtained from resin-embedded samples showing inner cavities, (d) DOPS-Ca cochleate with concentric bilayers and inner cavity, and (e) DSPS-Ca cochleate with lack of inner cavity and bilayer representing a rolled-up structure.

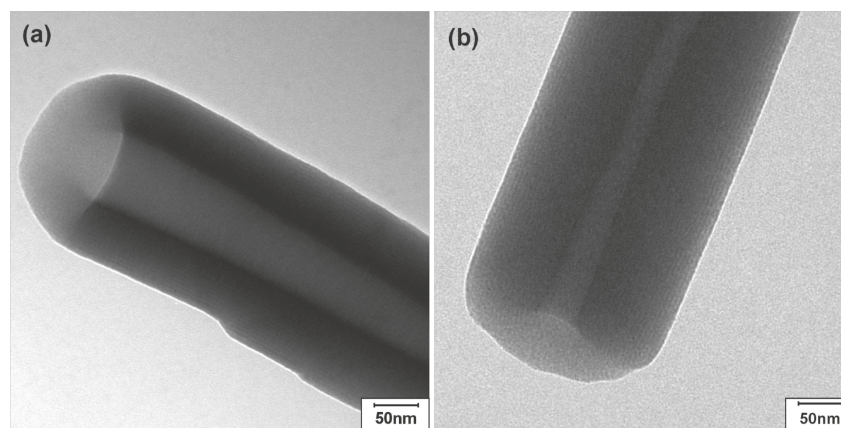


Figure 5. TEM images of (a) DOPS-Ca and (b) DSPS-Ca cochleates at medium magnification with clearly visible inner tubules.

a bright background. Electron tomographic techniques can be more useful in providing detailed information about the inner structure of cochleates. We performed a 3D reconstruction of a cochleate particle from acquisition and postacquisition processing of several TEM projection series for both DOPS-Ca and DSPS-Ca cochleates. Figure 3 shows the corresponding reconstructions viewed at two different angles for cochleate microstructures corresponding to each of the two lipids. The 3D reconstruction revealed a dense and uniformly packed

bilayer stack adopting a cylindrical geometry with a channel spanning the entire structure. No sample damage was observed during measurements.

In the past, cochleates have been described employing predominantly freeze–fracture microscopy as cigar-shaped structures.^{18–20} Some studies also suggested the possible presence of a luminal opening.^{9,21} In our microscopic investigations we observed virtually all cochleate particles to exhibit a continuous central channel that spans the entire

structure, with an opening at each terminus of a cochleate. In aqueous dispersions the central channel would be filled with water. On the basis of the prevalence of a central channel in cochleates, we suggest referring to its morphology as “carpet roll” rather than “cigarlike”, as cigars usually have a dense core. The central channel in a cochleate may be of relevance in pharmacokinetics due to its possible influence on the release kinetics of active ingredients trapped inside the particle.

Investigation of Cross Section of Resin-Embedded Cochleates. TEM micrographs of cross sections of resin-embedded DOPS-Ca and DSPS-Ca cochleates (Figure 4) display the presence of hollow tubules inside the particles. The majority of investigated particles exhibit cross sections of multilamellar scrolls folding into a compact, rolled-up structure. However, this is not discernible from all images as some micrographs displayed lipid bilayers arranged in a concentric manner. The tubules inside the particles were filled with epoxy resin, which most likely entered via the open ends of the central channel in the particle. Particles without any voids were also found, although their occurrence was very rare. During microscopy some fields also revealed bilayer stacks attached to the cochleate cylinders. The orientation of cochleate cylinders within the resin matrix could not be controlled in this technique, and as a result not all cross sections were perpendicular to the long axis of the cochleates.

Evaluation of Dimensions of the Cochleates. Unlike liposomes or microemulsions, cochleates cannot be adequately characterized with the help of dynamic light scattering due to their complex cylindrical shape. Hence we decided to analyze 479 TEM micrographs with the help of ImageJ version 1.45s²² for determining dimensions of cochleates. Specifically, we measured the outer and inner diameters for an ensemble of cochleate tubes at randomly selected positions. In the TEM micrographs (for an example, see Figure 5) the boundaries of the inner channel can clearly be discerned at high accelerating potentials. For a given single tube, both outer and inner diameters were measured at the same point. The results for the average outer and inner diameters (and their ratio) are listed in Table 1. The difference between the ratios for DOPS-Ca and

Table 1. Average Dimensions for DOPS-Ca and DSPS-Ca Cochleates^a

lipid	mean outer diam (nm) ± SE	mean inner diam (nm) ± SE	ratio ± SE
DOPS (<i>n</i> = 224)	314.7 ± 6.4	108.1 ± 3.6	3.3 ± 0.07
DSPS (<i>n</i> = 255)	203.6 ± 4.3	35.5 ± 1.6	7.4 ± 0.2

^aSE = standard error of the mean; *n* = number of samples.

DSPS-Ca cochleates is apparent and statistically significant. Below, in Figure 7, we also show the individual diameters in a scatter plot. Data obtained from these measurements are used in the section Theoretical Modeling to motivate a theoretical model.

According to the summary of our data in Table 1, unsaturation in the lipid chain resulted in the formation of cochleates with wider inner tubules as compared to the saturated lipid.

SAXS. The SAXS patterns of DOPS-Ca and DSPS-Ca cochleate samples (Figure 6) exhibit an intense reflection along with further weak reflections of higher order, characteristic of a lamellar structure.²³ The first reflection peak in the diffraction

pattern corresponds to the characteristic domain spacing in the sample, i.e., the bilayer thickness together with an interbilayer space containing the bridging agent.²⁴ Both diffractograms of DOPS-Ca and DSPS-Ca cochleates yielded an identical interlamellar repeat distance of 5.1 nm. The magnitude of the repeat distance obtained from SAXS studies agrees well with that measured geometrically using TEM micrographs (data not shown).

Theoretical Modeling. Our electron microscopy results demonstrate cochleates to be tubelike structures with an inner aqueous channel running through the particle. Visual inspection of our TEM images suggests a statistical distribution of tube sizes with significant differences between DOPS and DSPS. To quantify these differences, we have plotted the inner diameter $2R_1$ and outer diameter $2R_2$ of more than 200 randomly selected cochleate tubes (Figure 7), where R_1 and R_2 denote the corresponding radii.

Despite the large scatter in the measured tube sizes, there appears to be a systematic lipid-dependent relation between the inner and outer diameters, $2R_1$ and $2R_2$. In the following we discuss possible mechanisms that may give rise to this relation. To this end, we propose a theoretical model in which we assume the cochleate to be a cylindrically symmetric multilamellar vesicle—of sufficiently large extension L so that end effects can be neglected—with inner and outer radii R_1 and R_2 , respectively, and a bilayer repeat distance h . Because it is invariant along its axis of symmetry, we need to consider only the cochleate's free energy per unit length of the cylinder, F/L . We first account for two contributions to the total free energy $F = F_b + F_a$, a bending energy F_b of the lipid multilayer structure and a calcium-mediated bilayer–bilayer adhesion energy F_a between each pair of neighboring lipid bilayers in the cochleate.

The bending energy of a single cylindrically curved bilayer in a cochleate tube that is at distance r from the axis of cylindrical symmetry is $f_b = A_{bl}\kappa^2/2$, where $A_{bl} = 2\pi rL$ is the lateral area of this bilayer and $c = 1/r$ is its curvature. The constant κ denotes the bending energy of a single bilayer. Integrating the result, $f_b = \pi L\kappa/r$, over all bilayers of the cochleate yields the total bending energy per unit length of the cochleate:

$$\frac{F_b}{L} = \frac{1}{Lh} \int_{R_1}^{R_2} dr f_b(r) = \frac{\pi\kappa}{h} \int_{R_1}^{R_2} \frac{dr}{r} = \frac{\pi\kappa}{h} \ln \frac{R_2}{R_1} \quad (1)$$

We point out that the integration in eq 1 treats the individual bilayers as a continuum. Yet this is an excellent approximation as becomes evident by comparing the continuum expression $F_b/(L\pi\kappa) = \ln(R_2/R_1)/h$ with the discrete version $F_b/(L\pi\kappa) = \sum_{i=1}^n 1/[R_1 + h(i - 1/2)]$, where $n = (R_2 - R_1)/h$ is the number of bilayers crossed along the radial direction of the cochleate. For example, choosing the representative case $h = 5$ nm, $R_1 = 20$ nm, and $R_2 = 70$ nm yields $F_b/(L\pi\kappa) = 0.2505/\text{nm}$ for the continuum approximation and $F_b/(L\pi\kappa) = 0.2501/\text{nm}$ for the discrete version.

The adhesion energy can be expressed by assigning an energy penalty to the water-exposed innermost and outermost bilayers. Denoting this free energy penalty per unit area by σ , we can write for the adhesion energy of the innermost bilayer $2\pi R_1\sigma L$, and analogously $2\pi R_2\sigma L$ for the outermost bilayer. Hence, the total adhesion energy penalty per unit length of the cochleate is $F_a/L = 2\pi\sigma(R_1 + R_2)$. Combining the expressions for F_b and F_a leads to the total free energy:

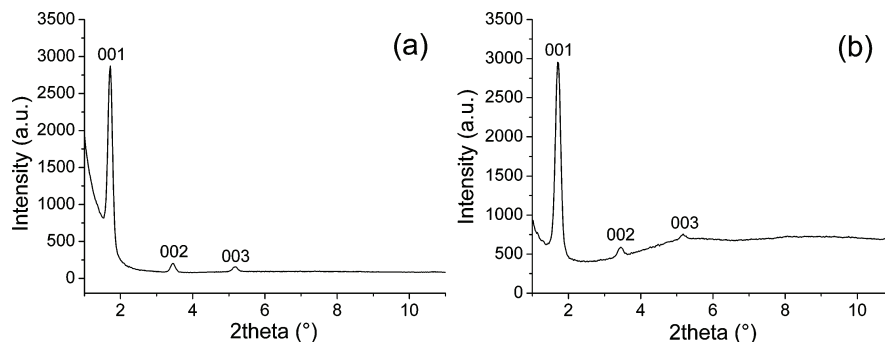


Figure 6. SAXS patterns of (a) DOPS-Ca and (b) DSPS-Ca cochleates exhibiting a primary peak (001) followed by higher order peaks (002) and (003).

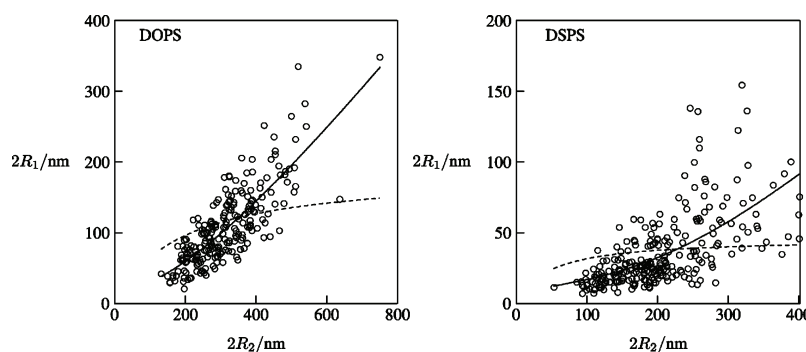


Figure 7. Scatter plots of inner and outer diameters, $2R_1$ and $2R_2$, of randomly selected cochleate tubes of DOPS ($n = 255$, left) and DSPS ($n = 224$, right). Dashed and solid lines are best fits of eqs 4 and 7, respectively.

$$\frac{F}{L} = \frac{F_b}{L} + \frac{F_s}{L} = \frac{\kappa\pi}{h} \ln \frac{R_2}{R_1} + 2\pi\sigma(R_1 + R_2) \quad (2)$$

$$R_1 = \frac{R_2}{1 + 2R_2 h \frac{\sigma}{\kappa}} \quad (4)$$

Note that, for the model in eq 2 to apply, it is irrelevant if we assume the cylindrical cochleate to be multilamellar (that is, with $(R_2 - R_1)/h$ individual bilayers) or a rolled-up structure, which consists only of one single bilayer that is wound upon itself. The latter can be modeled, mathematically, as the involute of a circle $x(s) = (h/2s)[\cos(s) + s \sin(s)]$ and $y(s) = (h/2s)[\sin(s) + s \cos(s)]$, which maintains a fixed bilayer-bilayer distance everywhere. The rolled-up cochleate has a local curvature $c = 2\pi/(hs)$, which (as a simple calculation shows) leads to the same free energy as for the multilamellar structure as long as the inner diameter is significantly larger than the repeat distance h . We assume the cochleate consists of a fixed number of lipids, each with constant cross-sectional area. The cochleate then has a fixed total bilayer area $A = Ll$, written here as the product of the cochleate tube length L and the total contour length

$$l = \frac{2\pi}{h} \int_{R_1}^{R_2} dr r = \frac{\pi}{h} (R_2^2 - R_1^2) \quad (3)$$

of all bilayers that appear in the cochleate's cross section. For any fixed l , the two radii R_1 and R_2 are no longer independent. Hence, the total free energy $F(R_1, R_2)$ adopts its minimum in thermodynamic equilibrium with respect to R_1 and R_2 , subject to l being kept constant. The minimization can be carried out conveniently using the Lagrangian multiplier method, which gives rise to the relation

A least-squares fit of the relation in eq 4 to the data in Figure 7 yields $h\sigma/\kappa = 0.0054/\text{nm}$ for DOPS and $h\sigma/\kappa = 0.022/\text{nm}$ for DSPS. The corresponding relation between R_1 and R_2 according to eq 4 is shown in Figure 7 as a dashed line in each diagram. Note that eq 4 predicts a saturation of the inner cochleate radius R_1 with growing outer radius R_2 . The predicted saturation is a result of the membrane's bending energy penalty which makes the decrease of the inner tube radius R_1 below a value of about $\kappa/(2h\sigma)$ very costly. Since no such penalty affects the outer radius R_2 , eq 4 predicts the cochleate to increase radius R_2 with only minor concomitant changes of R_1 . However, our experimental data in Figure 7 do not support the prediction of an essentially constant radius R_1 . What they suggest, instead, is that R_1 continues to grow with R_2 .

Membrane bending and calcium-mediated membrane-membrane adhesion alone cannot rationalize the data in Figure 7. The question arises, what other physical mechanism is able to keep R_1 and R_2 growing together? In the following, we discuss an additional free energy contribution that is able to account for the joint growth of R_1 and R_2 . Consider the bending of a planar membrane stack into a multilamellar cylindrical vesicle. Note that this hypothetical bending scenario merely compares the two states prior and after bending; it does not imply that the actual formation of a cochleate proceeds this way. If all individual bilayers of the initially planar stack are of the same lateral area, then an elastic stretching/compression deformation of the bilayers is required for a multilamellar tube

to form. Specifically, the outer bilayers must stretch and the inner ones must compress in order to compensate for the changes in circumference of the bilayer's cross section after bending. The energy cost F_m per unit length L of the cochleate of this area mismatch-compensating deformation depends on the area compressibility modulus K of a bilayer (which typically is on the order²⁵ of $K = 50 k_B T / \text{nm}^2$, where k_B is the Boltzmann constant and T is the absolute temperature) and can be expressed as

$$\frac{F_m}{L} = \frac{1}{h} \int_{R_1}^{R_2} dr 2\pi r \frac{K}{2} \left(1 - \frac{r}{\bar{r}}\right)^2 = \frac{K\pi}{6h} \frac{(R_2 - R_1)^3}{R_2 + R_1} \quad (5)$$

where $\bar{r} = (R_1 + R_2)/2$ is the mean radius of the cochleate tube. Note that eq 5 assumes there is no lipid exchange between the bilayers during the bending deformation. Indeed without lipid exchange bending deformations would imply large stretching and compression deformations, especially of the outer and inner bilayers, of the cochleate. For example, a cochleate with an outer radius twice the inner one (which is not an unusual case; see Figure 7) the relative stretching of the outer bilayer would be 33%, which would lead to membrane rupture. However, a large degree of lipid exchange will substantially reduce the degree of stretching. A reduction to about 0.3% of the stretching/compression values without any lipid relaxation is, in fact, what we find below from the analysis of our experimental data.

The presence of lipid exchange can approximately be accounted for by replacing \bar{r} with $\bar{r} + \eta(r - \bar{r})$ in the integral of eq 5, where η is a relaxation parameter. The relaxation parameter adopts the value $\eta = 0$ if no lipid exchange takes place and $\eta = 1$ for complete lipid exchange. In the latter case lipids rearrange during the bending deformation such that all area mismatch is removed, implying $F_m = 0$. If η is only slightly smaller than 1, we can still use eq 5, yet with K replaced by the effective area compressibility modulus $\bar{K} = K(1 - \eta)$. We will use \bar{K} instead of K in the following and justify this choice a posteriori. Adding F_m/L to the total free energy in eq 2 and performing the minimization, again subject to fixing l , yields

$$2h \frac{\sigma}{\kappa} = \frac{1}{R_1} - \frac{1}{R_2} + \frac{2\bar{K}}{3\kappa} \frac{(R_2 - R_1)^3}{(R_2 + R_1)^2} \quad (6)$$

Equation 6 has two unknown parameters: $h\sigma/\kappa$ and \bar{K}/κ . For $\bar{K} = 0$ (or, equivalently, $\eta = 1$, where the bilayer stretching/compression deformation is absent and thus does not incur an energy penalty) the model reduces to that in eq 4. Note that eq 6 cannot conveniently be expressed explicitly as $R_1 = R_1(R_2)$. Still, we can calculate R_1 numerically and then find the best fit of eq 6 to the data in Figure 7. The result is shown as the solid line in each of the two diagrams of Figure 7. The fit yields $h\sigma/\kappa = 0.0318/\text{nm}$ and $\bar{K}/\kappa = 0.00295/\text{nm}^2$ for DOPS, as well as $h\sigma/\kappa = 0.0691/\text{nm}$ and $\bar{K}/\kappa = 0.00299/\text{nm}^2$ for DSPS. We first point out that the model in eq 6 is able to reproduce the joint growth of R_1 and R_2 . The reason is that the energy penalty of the stretching/compression deformation energy in eq 5 grows quadratically with the ratio R_2/R_1 of the two radii. Hence, this free energy contribution tends to keep the difference $R_2 - R_1$ small. For a cochleate with a large number of lipids (and thus a large contour length l), it is favorable to form a larger tube (with a larger inner diameter), despite the less favorable membrane–membrane adhesion energy. More specifically, for a sufficiently large cochleate, the radii R_2 and R_1 become

independent of the bending stiffness κ , and the relative difference of the two radii turns smaller with growing R_1 .

$$\frac{R_2 - R_1}{R_1} = \left(\frac{6h\sigma}{R_1\bar{K}}\right)^{1/3} \quad (7)$$

Recall that the repeat distance $h = 5.1$ nm is known from our SAXS experiments and is the same for both lipids. Hence, we obtain an estimate for the ratio between the calcium-mediated adhesion energy σ and the bending stiffness κ , namely $\sigma/\kappa = 0.0062/\text{nm}^2$ for DOPS and $\sigma/\kappa = 0.0135/\text{nm}^2$ for DSPS. Neither one of the individual material constants is known from experiment. Generally, the order of magnitude for the bending stiffness of lipid bilayers^{26,27} in their fluid state is $10 k_B T$. We only know of one single experimental determination of κ involving phosphatidylserine. It was reported for a DOPS/DOPE mixture residing in the inverse-hexagonal phase using X-ray diffraction and applying osmotic stress,²⁸ yielding $\kappa = 11 k_B T$, largely independent of composition. However, cochleates involve millimolar calcium concentrations at which the lipids are condensed, with highly ordered alkyl tails and a loss of lipid-associated water,²⁹ and likely a significantly larger bending stiffness. Indeed κ can increase by an order of magnitude when transitioning from the liquid to the gel state.³⁰ Comparing DOPS with DSPS, it is likely that for DSPS κ is equally large or larger because its saturated lipid chains tend to be more condensed. It is thus remarkable that DSPS—a lipid with likely not a smaller bending stiffness than DOPS—forms cochleates with a smaller tube diameter. Let us assume, as an order-of-magnitude estimate, $\kappa = 50 k_B T$ for the membranes in both cochleate types. This would give rise to $\sigma = 0.31 k_B T / \text{nm}^2$ for DOPS and $\sigma = 0.67 k_B T / \text{nm}^2$ for DSPS, amounting to an energy gain on the order of a few tenths of a $k_B T$ per lipid associated with the calcium-mediated bilayer–bilayer adhesion. The fact that calcium mediates a bridging interaction between phosphatidylserine in apposed lipid bilayers was already proposed long ago²⁹ and is supported by recent molecular dynamics simulations³¹ (using, however, phosphatidylcholine instead of phosphatidylserine). The 2 times larger value of σ/κ for DSPS as compared to DOPS likely reflects a stronger calcium-mediated bilayer–bilayer interaction. What is the reason for the difference, given that the headgroups of DOPS and DSPS are of identical chemical structure? Recent work that combines experimental investigations with atomistic computer simulations provides insights into the interactions of calcium with phosphatidylserine or mixed phosphatidylserine/phosphatidylcholine bilayers.^{32,33} Specifically, Boettcher et al.³² find calcium to order and rigidify the phosphatidylserine headgroup, thereby favoring two major headgroup conformations and exerting only a minor influence on the mobility of the acyl chains. A dehydrating effect of calcium as well as preferential binding to the phosphate and carboxyl moieties of the phosphatidylserine headgroup were identified by Martin-Molina et al.³³ Endothermic membrane binding of calcium is also an indication for the liberation of water molecules³⁴ and a concomitant membrane dehydration. All this evidence supports a calcium-induced ordering and dehydration of the phosphatidylserine headgroups in each bilayer. Spatially more ordered headgroups in apposed bilayers facilitate calcium to mediate a bridging interaction. Hence, we expect the calcium-mediated bilayer–bilayer interaction to depend sensitively on how hydrocarbon chain packing affects the degree of headgroup ordering. The more ordered DSPS chains can be expected to

allow for a larger degree of headgroup order as compared to DOPS, thus facilitating the bridging interaction and increasing σ .

The estimate for the parameter $\bar{K}/\kappa = (1 - \eta)K/\kappa = 0.003/\text{nm}^2$ from the fit of eq 6 to the data in Figure 7 is the same for both DOPS and DSPS. Although neither K nor κ is known, their orders of magnitude are very roughly $K = 50 k_B T/\text{nm}^2$ and $\kappa = 50 k_B T$, implying $\eta = 1 - (\kappa/K)(0.003)/\text{nm}^2 = 0.997$. As we had assumed (see the discussion after eq 5), η is very close to 1. That is, our model prediction is consistent with a very minor degree of area mismatch for the lamellae in the cochleate. Yet, this small mismatch is still sufficient to cause the inner cochleate radius R_1 not to saturate as the model in eq 4 would predict. Varying degrees of η may also contribute to the large size variations of cochleates, namely the occurrence of a variety of outer radii R_2 at fixed R_1 .

We finally discuss a possible structural implication of having a relaxation parameter η close to 1. Recall that $\eta = 1$ corresponds to complete lipid relaxation, thus removing any stretching/compression deformations upon bending a multilamellar sheet from an initially planar state to a cylinder-like cochleate. In fact, there is a simple structural mechanism that allows for complete lipid relaxation: the multilamellar sheet may close after bending such that sheet n connects with sheet $n + 1$, thus forming a cochleate that consists of a single rolled-up bilayer. Because a rolled-up cochleate consists of only one single bilayer, it can more easily relax internal stress as compared to a multilamellar cochleate, where the relaxation would require fission and fusion or lipid transfer from one bilayer to another. Hence, our estimate of η being very close to 1 suggests that the cochleates consist predominantly of rolled-up bilayers and not of a multilamellar sheet.

CONCLUSION

We have used electron microscopy to study the structure of cochleates that consist of calcium as binding agent and phosphatidylserines with either saturated or unsaturated hydrocarbon chains. For both lipid types we demonstrate cochleates to be tubules where a stack of cylindrically curved bilayers encloses an inner aqueous channel. The inner and outer radii of a cochleate vary statistically, yet with characteristic differences for the two lipids. Specifically, the unsaturated lipid tends to form cochleates with larger dimensions, and the diameter of the inner tube does not saturate as the outer diameter of the cochleate grows. To rationalize these findings, we have proposed a theoretical model that is based on minimizing a phenomenological free energy expression. Our calculations suggest that membrane bending and calcium-induced bilayer–bilayer adhesion alone are insufficient to reproduce the observed relation between inner and outer cochleate tube radii. Yet, we can reproduce it by considering an additional free energy contribution that accounts for an area compression/expansion of the lipid bilayers within the cochleate. Our modeling approach yields predictions for ratios of material constants, namely the ratio between the area compressibility and the bending modulus as well as the ratio between the bilayer adhesion energy and the bending modulus. Although our model contains approximations (such as the neglect of the end-cap energy of the cochleate), it is likely that it captures some of the underlying principles of cochleate stability and thus may prove valuable for the design and understanding of cochleates as drug delivery vehicles.

AUTHOR INFORMATION

Corresponding Author

*E-mail: sylvio.may@nds.u.edu. Tel.: (701) 231-7048.

Notes

The authors declare no competing financial interest.

ACKNOWLEDGMENTS

We would like to acknowledge the Phospholipid Research Center, Heidelberg, Germany, for financial support. Felix Schacher is grateful to the FCI for a fellowship and also to the Thuringian Ministry for Education, Science and Culture (TMBWK, Grant B514-09051, NanoConSens, and Grant B515-11028, SWAXS-JCSM) for financial support.

REFERENCES

- Papahadjopoulos, D.; Vail, W. J.; Jacobson, K.; Poste, G. Cochleate lipid cylinders: formation by fusion of unilamellar lipid vesicles. *Biochim. Biophys. Acta* **1975**, *394*, 483–491.
- Zarif, L.; Graybill, J.; Perlin, D.; Mannino, R. J. Cochleates: New Lipid-Based Drug Delivery System. *J. Liposome Res.* **2000**, *10*, 523–538.
- Morishita, M.; Peppas, N. A. Is the oral route possible for peptide and protein drug delivery? *Drug Discovery Today* **2006**, *11*, 905–910.
- Ramasamy, T.; Khandasamy, U.; Hinabindhu, R.; Kona, K. Nanocochleate—A new drug delivery system. *FABAD J. Pharm. Sci.* **2009**, *34*, 91–101.
- Rao, R.; Squillante, E., 3rd; Kim, K. H. Lipid-based cochleates: a promising formulation platform for oral and parenteral delivery of therapeutic agents. *Crit. Rev. Ther. Drug Carrier Syst.* **2007**, *24*, 41–61.
- Zarif, L.; Graybill, J. R.; Perlin, D.; Najvar, L.; Bocanegra, R.; Mannino, R. J. Antifungal activity of amphotericin B cochleates against *Candida albicans* infection in a mouse model. *Antimicrob. Agents Chemother.* **2000**, *44*, 1463–1469.
- Acevedo, R.; Callico, A.; del Campo, J.; Gonzalez, E.; Cedre, B.; Gonzalez, L.; Romeu, B.; Zayas, C.; Lastre, M.; Fernandez, S.; Oliva, R.; Garcia, L.; Perez, J. L.; Perez, O. Intranasal administration of proteoliposome-derived cochleates from *Vibrio cholerae* O1 induce mucosal and systemic immune responses in mice. *Methods* **2009**, *49*, 309–315.
- Tan, F.; Zarif, L. Cochleates made with purified soy phosphatidylserine. World Patent WO 2003082209 A3, 2004.
- Garidel, P.; Richter, W.; Rapp, G.; Blume, A. Structural and morphological investigations of the formation of quasi-crystalline phases of 1,2-dimyristoyl-sn-glycero-3-phosphoglycerol (DMPG). *Phys. Chem. Chem. Phys.* **2001**, *3*, 1504–1513.
- Garidel, P.; Blume, A. Calcium Induced Nonideal Mixing in Liquid-Crystalline Phosphatidylcholine–Phosphatidic Acid Bilayer Membranes. *Langmuir* **1999**, *16*, 1662–1667.
- Papahadjopoulos, D.; Poste, G. Calcium-induced phase separation and fusion in phospholipid membranes. *Biophys. J.* **1975**, *15*, 945–948.
- Zarif, L. Elongated supramolecular assemblies in drug delivery. *J. Controlled Release* **2002**, *81*, 7–23.
- Zarif, L.; Jin, T.; Segarra, I.; Mannino, R. J. Hydrogel-isolated cochleate formulations, process of preparation and their use for the delivery of biologically relevant molecules. World Patent WO 2000042989, 2003.
- Syed, U. M.; Woo, A. F.; Plakogiannis, F.; Jin, T.; Zhu, H. Cochleates bridged by drug molecules. *Int. J. Pharm. (Amsterdam, Neth.)* **2008**, *363*, 118–125.
- Dubochet, J.; Adrian, M.; Chang, J. J.; Homo, J. C.; Lepault, J.; McDowell, A. W.; Schultz, P. Cryo-electron microscopy of vitrified specimens. *Q. Rev. Biophys.* **1988**, *21*, 129–228.
- Mastronarde, D. N. Automated electron microscope tomography using robust prediction of specimen movements. *J. Struct. Biol.* **2005**, *152*, 36–51.

- (17) Kremer, J. R.; Mastrorarde, D. N.; McIntosh, J. R. Computer visualization of three-dimensional image data using IMOD. *J. Struct. Biol.* **1996**, *116*, 71–76.
- (18) Zarif, L. Cochleates as Nanoparticulate Drug Carriers. In *Nanoparticulates as Drug Carriers*; Torchilin, V., Ed.; World Scientific: Singapore, 2006; pp 349–366.
- (19) Ravi Sankar, V.; Dastagiri Reddy, Y. Nanocochleate—A new approach in lipid drug delivery. *Int. J. Pharm. Pharm. Sci.* **2010**, *2*, 220–223.
- (20) Zarif, L. Drug delivery by lipid cochleates. *Methods Enzymol.* **2005**, *391*, 314–329.
- (21) Kodama, M.; Aoki, H.; Miyata, T. Effect of Na(+) concentration on the subgel phases of negatively charged phosphatidylglycerol. *Biophys. Chem.* **1999**, *79*, 205–217.
- (22) Schneider, C. A.; Rasband, W. S.; Eliceiri, K. W. NIH Image to ImageJ: 25 years of image analysis. *Nat. Methods* **2012**, *9*, 671–675.
- (23) Hamley, I. W.; Castelletto, V. Small-angle scattering of block copolymers: in the melt, solution and crystal states. *Prog. Polym. Sci.* **2004**, *29*, 909–948.
- (24) Ortiz, A.; Teruel, J. A.; Espuny, M. J.; Marques, A.; Manresa, A.; Aranda, F. J. Interactions of a bacterial biosurfactant trehalose lipid with phosphatidylserine membranes. *Chem. Phys. Lipids* **2009**, *158*, 46–53.
- (25) Marsh, D. *Handbook of Lipid Bilayers*, 2nd ed.; CRC Press, Taylor & Francis Group: Boca Raton, FL, 2013.
- (26) Marsh, D. Elastic curvature constants of lipid monolayers and bilayers. *Chem. Phys. Lipids* **2006**, *144*, 146–159.
- (27) Nagle, J. F. Introductory Lecture: Basic quantities in model biomembranes. *Faraday Discuss.* **2013**, *161*, 11–29.
- (28) Fuller, N.; Benatti, C. R.; Rand, R. P. Curvature and bending constants for phosphatidylserine-containing membranes. *Biophys. J.* **2003**, *85*, 1667–1674.
- (29) Portis, A.; Newton, C.; Pangborn, W.; Papahadjopoulos, D. Studies on the mechanism of membrane fusion: evidence for an intermembrane Ca²⁺-phospholipid complex, synergism with Mg²⁺, and inhibition by spectrin. *Biochemistry* **1979**, *18*, 780–790.
- (30) Lee, C. H.; Lin, W. C.; Wang, J. All-optical measurements of the bending rigidity of lipid-vesicle membranes across structural phase transitions. *Phys. Rev. E: Stat., Nonlinear, Soft Matter Phys.* **2001**, *64*, 020901.
- (31) Issa, Z. K.; Manke, C. W.; Jena, B. P.; Potoff, J. J. Ca(2+) bridging of apposed phospholipid bilayers. *J. Phys. Chem. B* **2010**, *114*, 13249–13254.
- (32) Boettcher, J. M.; Davis-Harrison, R. L.; Clay, M. C.; Nieuwkoop, A. J.; Ohkubo, Y. Z.; Tajkhorshid, E.; Morrissey, J. H.; Rienstra, C. M. Atomic view of calcium-induced clustering of phosphatidylserine in mixed lipid bilayers. *Biochemistry* **2011**, *50*, 2264–2273.
- (33) Martin-Molina, A.; Rodriguez-Beas, C.; Farado, J. Effect of calcium and magnesium on phosphatidylserine membranes: experiments and all-atomic simulations. *Biophys. J.* **2012**, *102*, 2095–2103.
- (34) Sinn, C. G.; Antonietti, M.; Dimova, R. Binding of calcium to phosphatidylcholine–phosphatidylserine membranes. *Colloids Surf., A* **2006**, *282–283*, 410–419.

3.3 Publication 3

Micro-spherical cochleate composites: method development for monodisperse system

Kalpa Nagarsekar, Mukul Ashtikar, Frank Steiniger, Jana Thamm, Felix
Schacher, Alfred Fahr

Journal of Liposome Research, submitted on 24th August 2015,

Manuscript under review.

Journal of Liposome Research



**Micro-spherical cochleate composites: method development
for monodisperse system**

Journal:	<i>Journal of Liposome Research</i>
Manuscript ID:	Draft
Manuscript Type:	Original Paper
Date Submitted by the Author:	n/a
Complete List of Authors:	Nagarsekar, Kalpa; Friedrich Schiller Universität Jena,, Pharmaceutical Technology Ashtikar, Mukul; Friedrich Schiller Universität Jena, Pharmaceutical Technology Steiniger, Frank; Universitätsklinikum Jena, Elektronenmikroskopisches Zentrum Thamm, Jana; Friedrich Schiller Universität Jena,, Pharmaceutical Technology Schacher, Felix; Friedrich Schiller Universität Jena, Institut für Organische Chemie und Makromolekulare Chemie Fahr, Alfred; Friedrich Schiller Universität Jena,, Pharmaceutical Technology
Keywords:	Cochleates, Phosphatidylserine, Microfluidics, Electron microscopy, Solvent effect

SCHOLARONE™
Manuscripts

URL: <http://mc.manuscriptcentral.com/llpr> Email: Y.Perrie@aston.ac.uk

1
2
3
4
5
6
7
8
9
10
11
12
13
14
15
16
17
18
19
20
21
22
23
24
25
26
27
28
29
30
31
32
33
34
35
36
37
38
39
40
41
42
43
44
45
46
47
48
49
50
51
52
53
54
55
56
57
58
59
60

1 **Micro-spherical cochleate composites: method development for**
2 **monodispersed cochleate system**

3 Kalpa Nagarsekar^{1*}, Mukul Ashtikar^{1*}, Frank Steiniger², Jana Thamm¹, Felix H. Schacher^{3,4}, Alfred Fahr^{1**}

4
5 ¹ Lehrstuhl für Pharmazeutische Technologie, Institut für Pharmazie, Friedrich-Schiller-Universität
6 Jena, Lessingstraße 8, 07743 Jena, Germany

7 ² Elektronenmikroskopisches Zentrum, Universitätsklinikum Jena, Ziegmühlenweg 1, 07743 Jena,
8 Germany

9 ³Institut für Organische Chemie und Makromolekulare Chemie, Friedrich-Schiller-Universität Jena,
10 Lessingstraße 8, 07743 Jena, Germany

11 ⁴ Jena Center for Soft Matter, Friedrich-Schiller-Universität Jena, Philosophenweg 7, 07743 Jena,
12 Germany

13 *These authors have contributed equally in this study and in the preparation of this manuscript.

14 **Corresponding Author:

15 **Prof Dr Alfred Fahr,**
16 Lehrstuhl für Pharmazeutische Technologie,
17 Institut für Pharmazie,
18 Friedrich-Schiller-Universität Jena,
19 Lessingstraße 8,
20 07743 Jena, Germany
21 Phone: +49 3641 949901
22 Email: Alfred.Fahr@uni-jena.de

23
24 **KEYWORDS**

25 Cochleates, phosphatidylserine, microfluidics, solvent effect, electron microscopy
26

1
2
3
4
5
6
7
8
9
10
11
12
13
14
15
16
17
18
19
20
21
22
23
24
25
26
27
28
29
30
31
32
33
34
35
36
37
38
39
40
41
42
43
44
45
46
47
48
49
50
51
52
53
54
55
56
57
58
59
60

27 **ABSTRACT**

28 Cochleates have been of increasing interest in pharmaceutical research due to their extraordinary
29 stability. However the existent techniques used in the synthesis of cochleates still need significant
30 improvements to achieve monodispersed formulations. In this study, we report a simple method for
31 the synthesis of spherical composites (3–5 μm in diameter) made up of nanocochleates from
32 phosphatidylserine and calcium. Products obtained from the proposed method were evaluated with
33 electron microscopy and small angle X-ray scattering and compared with those obtained by the
34 established cochleate preparation techniques. In this method, a lipid solution in an organic solvent,
35 ethanol and aqueous solution of a binding agent is subjected to rapid and uniform mixing with a
36 microfluidic device. The presence of high concentration of organic solvent promotes the formation of
37 composites made of nanocochleates. This simple methodology eliminates elaborate preparation
38 methods, while providing a monodisperse cochleate system with analogous quality.

39

1
2
3
4
5
6
7
8
9
10
11
12
13
14
15
16
17
18
19
20
21
22
23
24
25
26
27
28
29
30
31
32
33
34
35
36
37
38
39
40
41
42
43
44
45
46
47
48
49
50
51
52
53
54
55
56
57
58
59
60

40 INTRODUCTION

41 Cochleates are cylindrical particles featuring a rolled up carpet-like morphology made up of multiple
42 stacked layers of negatively charged phospholipids bound by a positively charged binding agent such
43 as calcium (Nagarsekar et al., 2014). Cochleates represent a potential delivery system with remarkable
44 advantages being non-immunogenic, highly stable and with the ability to impart safety to
45 incorporated active ingredients (Zarif, 2002). Cochleates have a hollow central channel and little or no
46 internal aqueous space in the lipid sheets (Zarif, 2005, Nagarsekar et al., 2014). In past few decades
47 cochleates are being explored for a number of possible applications thanks to their exceptional
48 properties. The know-how of cochleates has been employed to improve delivery of drugs (Zarif et al.,
49 2000, Syed et al., 2008), genes (Zarif and Mannino, 2000), flavoring agents (Mannino and Gould-
50 Fogerite, 2002), and antigens (Gould-Fogerite and Mannino, 2000). Cochleates of various lipids such
51 as phosphatidylserines, sphingolipids, and phosphatidylglycerols have been synthesized by groups
52 around the world. Cochleates are also found to be structurally more divergent if compared to lipid
53 tubules or nanotubes (Zarif, 2005, Kulkarni et al., 1999, Sarig et al., 2011, Kulkarni et al., 1996, Garidel
54 et al., 2001). Cochleates are accepted to be well suited for intramuscular (Gould-Fogerite et al., 2000)
55 and oral delivery (Delmas et al., 2002) however, being prone to aggregation they are not ideally
56 suitable for intravenous or ocular administration (Wang et al., 2014).

57 Different strategies have been developed for the preparation of cochleates. The conventional
58 preparation strategies such as trapping method or dialysis method are known to form aggregated
59 cochleates with variable and large particle sizes (Sankar and Reddy, 2010). This is mainly due to the
60 uncontrolled and continuous aggregation between the bilayer sheets. During the last decade research
61 was focused on synthesis strategies to form nanocochleates mainly by isolating or limiting the number
62 of building blocks that come in close contact. The development of methods such as hydrogel isolation
63 (Zarif et al., 2003) and emulsion-lyophilization (Wang et al., 2014) have opened up a new field of
64 application based research for various biomolecules using cochleates with sizes in the sub-micrometer

1
2
3
4
5
6
7
8
9
10
11
12
13
14
15
16
17
18
19
20
21
22
23
24
25
26
27
28
29
30
31
32
33
34
35
36
37
38
39
40
41
42
43
44
45
46
47
48
49
50
51
52
53
54
55
56
57
58
59
60

65 range. However, these are multistep methods which commonly involve formation of colloidal
66 structures such as liposomes or micelles as the first step, and subsequently form the cochleates
67 (Huerdo et al., 1997, Jin et al., 2001). These processes often involve complex and time consuming steps
68 such as multiple emulsions, washing off polymers etc., which tend to be difficult to scale up and might
69 also cause regulatory issues. Although these methods were successful in preparing sub-micron
70 cochleates, they often form cochleates with a broad particle size distribution, a problem that has
71 seldom received attention. These limitations can critically limit suitability of cochleates as drug
72 delivery systems in the pharmaceutical market (Zayas et al., 2013). Hence, an economical method
73 which could easily be translated into mass production needs to be developed for the formation of
74 monodisperse cochleate systems.

75 Cochleate formation follows a continuous self-assembly process which includes unrestrained
76 nucleation and growth of particles (Kulkarni et al., 1999, Zarif, 2002), this makes it difficult to control
77 either morphology or the dimensions of individual particles. In conventional cochleate formation,
78 bilayers or micelles of an acidic phospholipid in presence of a cationic binding agent undergo an
79 aggregation step to form planar bilayer stacks. These stacks further aggregate to form larger sheets
80 which eventually undergo curling to form cochleates with a carpet roll like morphology (Poste et al.,
81 1976). Also the intermediate structures that could coexist with the cochleates make the purification
82 of cochleate system a challenging task (reference: manuscript under review). Hence, the development
83 of a formation strategy should mainly focus on limiting uncontrolled interactions after nucleation.
84 Moreover, such a novel methodology for attaining monodispersity in case of natural lipids might also
85 render a cost effective system.

86 Recently we came across a very interesting solvent effect where phosphatidylserines (PS) formed
87 much smaller stacks during precipitation from ethanol compared to precipitation in water. In this
88 study we have utilized this solvent effect towards formulation development. We tried to exploit this
89 finding with the aim of reducing random particle aggregation and thereby decreasing size dispersity

1
2
3 90 in cochleate systems. We have developed one-step, simple, reproducible and economic procedure
4
5 91 where emulsification or polymers are not required prior to the formation of cochleates. In this case,
6
7
8 92 we exploit precipitation by solvent displacement. Nanoprecipitation is an attractive choice as the
9
10 93 process parameters such as rate of mixing or the concentration of reactants allow the control of size,
11
12 94 shape, and encapsulation efficiency of the final product. In order to precisely control the mixing rate
13
14 95 and mixing ratios we decided to employ a microfluidic reactor. A reactor with fast and reproducible
15
16 96 mixing has proven to be an excellent tool for creating a monodisperse system of multiple particles
17
18 97 with varied morphologies (Nie et al., 2006). Recently, the area of microfluidics has been explored for
19
20 98 synthesis and scale-up of various nanoparticles, where a final product with small and uniform
21
22 99 dimensions can be easily achieved by precision controlled fast mixing, dominated by diffusion or
23
24
25 100 convection (Whitesides, 2006, Kastner et al., 2014, Belliveau et al., 2012).

26
27
28
29 101 In this study, we report the formation of novel microparticles with spherical morphology made up of
30
31 102 nano-sized cochleate subunits using a microfluidic device. Throughout this manuscript we have
32
33 103 referred to these novel particles as 'cochleate composites'. We have demonstrated that controlled
34
35 104 mixing provided by the microfluidic device enabled us to fine-tune the cochleate composites. Products
36
37 105 obtained from the proposed method have been characterized and compared with those obtained
38
39 106 from conventional methodologies. Our method eliminates elaborate preparation procedures, while
40
41 107 providing a unique monodispersed cochleate system with analogous qualities.
42
43
44

45
46 108

47 109 **MATERIALS AND METHODS**

48 110 **Materials**

49
50
51 111 1, 2-dioleoyl-sn-glycero-3-phosphatidylserine (DOPS) was purchased from Avanti Polar Lipids, Inc
52
53 112 (Alabama, USA). Araldite® LY 564 used for embedding studies was obtained from HunTcan Advanced
54
55 113 Materials GmbH (Switzerland). Absolute ethanol used to prepare lipid solutions was purchased from
56
57
58 114 VWR International GmbH (Germany). All other chemical reagents were of analytic grade and were
59
60

1
2
3 115 used as received. Buffers used in the study were prepared using ultrapure water (Milli-Q® Direct-Q™
4
5 116 System, Merck-Millipore, Germany).
6
7 117
8
9
10 118 **Preparation of cochleates**
11
12 119 To achieve spherical morphology with desired particle size and to obtain a stable dispersion of
13
14 120 cochleate composites, the effect of different process variables was investigated during preparation.
15
16 121 To optimize the organic phase, various organic solvents which could dissolve DOPS i.e. ethanol,
17
18 122 methanol, chloroform, dichloromethane and DMSO were studied for preparation of cochleates.
19
20 123 Ethanol was selected as organic phase based on preliminary screening for all further experiments.
21
22
23
24 124
25
26 125 Using microfluidics:
27
28
29 126 Modified nanoprecipitation method was employed for preparation of cochleate composites. Ethanolic
30
31 127 solution of DOPS was prepared with the aid of bath sonication. 60 mM CaCl₂ solution in 10 mM Tris
32
33 128 buffer was used as source of binding cations. Formulations were prepared using a benchtop
34
35 129 NanoAssemblr™ instrument (Precision NanoSystems Inc., Canada) employing Poly (dimethyl siloxane)
36
37 130 micromixer chips (Precision NanoSystems Inc., Canada). The micromixer chips had molded channels
38
39 131 which were 200 µm in width and 79 µm in height and a series of herringbone features of 50 × 31 µm
40
41 132 (Kastner et al., 2014). Disposable 1 mL syringes (B-D Disposable Syringes, Luer-Lock Tips) attached at
42
43 133 the two inlet streams to the chip served as the reservoir of reactor solutions viz. organic lipid solution
44
45 134 and aqueous CaCl₂ solution. The syringe pumps allowed for a precise control of the flow rates and the
46
47 135 solvent phase ratios between the two inlet streams. The resulting suspensions were collected from
48
49 136 the outlet stream. To understand the effect of mixing rate on morphology of the particles, the ratio of
50
51 137 the aqueous phase : organic phase was varied from 1:1 to 1:9 (with constant flow rate of 12 ml/min).
52
53 138 In a different set of experiments the flow rate was varied from 1 ml/min to 18 ml/min (with constant
54
55 139 flow rate ratio of 1:9). Concentration of lipid was kept constant at 1 mg/ml for both experiments.
56
57 140 Further, to understand the effect of lipid concentration, the amount of DOPS was varied from 0.1
58
59
60

1
2
3 141 mg/mL to 1mg/mL keeping the ratio of aqueous phase : organic phase (1:9) and flow rate (12 mL/min)
4
5 142 constant. All samples were prepared in triplicate and the effect of changing parameters on the
6
7
8 143 morphology of formulation was assessed using electron microscopy (EM).
9

10 144

11
12
13 145 Modified trapping method:

14
15 146 To understand the influence of microfluidic device on the morphology, cochleate composites were
16
17 147 also prepared using T-25 Ultra-Turrax® homogenizer maintaining the 1:9 CaCl_{2(aqueous)} : DOPS_(ethanolic)
18
19 148 ratio. Cochleate composites were formed by slow (10 µl at a time) addition of aqueous calcium
20
21 149 chloride (60 mM in 10 mM Tris) to an ethanolic DOPS solution under constant stirring. Addition of
22
23 150 calcium chloride solution was carried out at a constant 13500 rpm with T-25 Ultra-Turrax®
24
25 151 homogenizer (IKA, Germany) stirring was continued for another five minutes after complete addition
26
27 152 of calcium chloride. Mixture was then stirred continuously up to 1 hour using a magnetic stirrer (RCT
28
29 153 Basic-Ika, Staufen, Germany). The molar ratio of lipid to calcium was 1:1. At the end of 1 hours
30
31 154 precipitated mixtures were collected and stored at 4 °C. All samples were prepared in triplicate and
32
33 155 evaluated by EM.
34
35
36
37

38 156

39
40 157 Preparation of cochleates by conventional methods:

41
42 158 Conventional cochleates were prepared in order to evaluate the difference in SAXS patterns and size
43
44 159 distribution with respect to cochleate composites. For the preparation of conventional cochleates,
45
46 160 DOPS liposomes were prepared by thin-lipid film hydration method. In brief, DOPS was dissolved in a
47
48 161 mixture of chloroform : methanol (3:1) in a round bottom flask and was subjected to a rotary
49
50 162 evaporator (R-144 BÜCHI Labortechnik GmbH, Germany) to form a thin lipid film. The lipid film was
51
52 163 hydrated with 10 mM Tris buffer and the resultant dispersion was subjected to extrusion through a
53
54 164 polycarbonate membrane of 100 nm pore size to produce uniform dispersion of liposomes. Cochleates
55
56 165 were formed by slow (10 µl at a time) addition of calcium chloride (60 mM) to the liposomes under
57
58
59
60

1
2
3
4 166 constant stirring using a magnetic stirrer at room temperature. The molar ratio of lipid to calcium was
5
6 167 1:1. Precipitated mixtures were then stored at 4°C. All samples were prepared in triplicate.
7
8 168
9
10 169 Preparation of nano cochleates by hydrogel isolation method:
11
12 170 Nano cochleates were prepared by hydrogel isolation method as described previously by Jin et al.
13
14 171 (2001). DOPS liposomes were formed as described above in section 2.2.3. The liposome suspension
15
16 172 was further dispersed in 40 %w/w dextran 500,000 solution in ratio of 1:2 v/v. This mixture was then
17
18 173 slowly added to 15 %w/w PEG 8,000 solution with a syringe under magnetic stirring (1100 rpm). To
19
20 174 this dispersion an aqueous CaCl₂ solution (60 mM) was added to reach the equimolar ratio of lipid and
21
22 175 calcium. After 2 hours of stirring, the resultant mixture was washed thrice by mixing with equal volume
23
24 176 of buffer (1 mM CaCl₂ and 150 mM NaCl) and centrifuged at 3000 rpm for 30 min. The resultant pellet
25
26 177 was resuspended with buffer and stored at 4°C. All samples were prepared in triplicate.
27
28
29
30 178
31
32
33 179 **Characterization of formulations**
34
35 180 Scanning electron microscopy:
36
37 181 A droplet of the sample was adhered on a perforated Formvar -coated copper grid (300 mesh,
38
39 182 Quantifoil Micro Tools GmbH, Germany). Excess liquid was removed with a lint-free filter paper and
40
41 183 examined in a LEO 1530 Gemini (Carl Zeiss, Germany) scanning electron microscope (SEM) at 4 kV
42
43 184 acceleration voltage. Images of randomly selected 110 particles of optimized formulation prepared
44
45 185 using NanoAssemblr™ were measured using Image J to estimate the average size (Rasband, 1997-
46
47 186 2014). The coefficient of variance or CV (%) corresponding to the particle size distribution was
48
49 187 calculated as described by Perez et al. (2015) using formula $CV (\%) = (\sigma / D) \times 100$ where σ is the standard
50
51 188 deviation (SD) of the particle size and D is their mean diameter.
52
53
54
55 189
56
57
58 190
59
60

1
2
3
4
5
6
7
8
9
10
11
12
13
14
15
16
17
18
19
20
21
22
23
24
25
26
27
28
29
30
31
32
33
34
35
36
37
38
39
40
41
42
43
44
45
46
47
48
49
50
51
52
53
54
55
56
57
58
59
60

191 Cryo-transmission electron microscopy:

192 A drop of formulation (2 μ l) was placed on a carbon-coated copper grid (Quantifoil Micro Tools GmbH,
193 Germany). The sample was subjected to plunge freezing in liquid ethane at -180 °C. The grids were
194 then transferred into a liquid nitrogen cooled ($T = -196$ °C) $\pm 70^\circ$ tilt cryo-holder (Gatan Inc., USA) and
195 inserted into the cryoelectron microscope Philips CM 120 cryo-TEM (Philips, Netherlands). Images
196 were captured using a TEM operating at 120 kV.

197

198 Investigation of cross section of resin-embedded cochleate composites:

199 Embedding was carried out using the procedure described previously by *Nagarsekar et al.*(2014).
200 Briefly, sample was redispersed in 100 mM cacodylate buffer (pH 7.2) containing 1% OsO₄ for 2 h.
201 Sample was centrifuged again and rinsed in buffer before dehydration in ethanol (50% v/v) for 15 min.
202 It was further subjected to 1% uranyl acetate solution for 1 h to improve contrast. The pellet was then
203 redispersed in an epoxy resin Araldite® used as an embedding medium. The mixture was polymerized
204 and ultramicrotomed in to thin (70–100 nm) slices using a diamond knife mounted on an Ultracut E
205 device (Reichert Labtec, Germany) at room temperature. The slices were transferred to copper grids
206 (Quantifoil, Germany) and examined by cryo-TEM.

207

208 Small angle X-ray scattering:

209 Small angle X-ray scattering (SAXS) measurements were performed at $\lambda=1.54$ Å using a Bruker
210 Nanostar (Bruker, Germany) equipped with a μ -focus X-ray source (I μ S, Incoatec, Germany), equipped
211 with a 2D position sensitive detector Vantec 2000 (Bruker GmbH, Germany). Sample-to-detector
212 distance was maintained at 107 cm. Samples were mounted on a metal rack and fixed using tape. All
213 measurements were carried out at room temperature and duration of measurement was 2 hours.
214 Prior to evaluations the scattering patterns were corrected for the background (Scotch tape) and
215 radially integrated to obtain the scattering intensity (using $q = (4\pi/\lambda) \sin \theta$, where 2θ =scattering angle

1
2
3 216 and λ = X-ray wavelength). All samples were centrifuged, washed and freeze dried before evaluation
4
5 217 and measurements were undertaken in triplicates.
6
7
8 218

9
10
11 219 **RESULTS AND DISCUSSION:**
12

13 220 The cochleate formation is a result of an instantaneous self-assembly induced by aggregation of
14 221 negatively charged lipid molecules interacting with a cationic binding agent such as calcium. So far
15 222 water and aqueous buffers have been widely reported for the preparation of cochleates. In our
16 223 preliminary studies, different solvent systems were compared for precipitation of cochleates to
17 224 investigate lipid-calcium interactions. We could show that spherical cochleate-composites were only
18 225 formed in aqueous-ethanolic mixtures (aqueous calcium chloride, ethanolic DOPS solutions). When
19 226 ethanolic DOPS was precipitated with ethanolic calcium in water-free environment, SEM analysis
20 227 revealed that the lipid precipitates formed did not exhibit any cochleates but showed aggregates of
21 228 lipid sheets or stacks (Fig. 1f). When ethanol was replaced with non-polar solvents such as chloroform,
22 229 dichloromethane and DMSO for dissolving DOPS, no cochleates or precipitates were formed. This
23 230 might be due to the high solubility of the lipid in these solvents and, therefore, ethanol was selected
24 231 as organic phase in our current study.
25
26
27
28
29
30
31
32
33
34
35
36
37
38
39
40

41 232

42
43 233 **Preparation of cochleate composites using microfluidic device:**
44

45 234 Microfluidic techniques provide a precise control over mixing of reactants and can be employed for
46 235 reproducible mixing. The following studies were carried out with the aim to optimize parameters with
47 236 respect to their effect on morphology and size of cochleate composites. Influence of solvent ratio,
48 237 flow rate and lipid concentration on final product was assessed with electron microscopy. The
49 238 conditions which allow most uniform formulation were identified based on the data obtained from
50 239 these experiments.
51
52
53
54
55
56
57
58
59
60

240

241

1
2
3
4
5
6
7
8
9
10
11
12
13
14
15
16
17
18
19
20
21
22
23
24
25
26
27
28
29
30
31
32
33
34
35
36
37
38
39
40
41
42
43
44
45
46
47
48
49
50
51
52
53
54
55
56
57
58
59
60

242 Influence of ratio of aqueous phase to organic phase:

243 In nanoprecipitation, solvent concentration is an important parameter. This experiment was carried
244 out in order to understand the influence of ratio of ethanol and water on the resulting morphologies
245 of the cochleate composites. For the precipitation experiment, calcium chloride was dissolved in 10
246 mM Tris buffer and DOPS was dissolved in ethanol. Care was taken to maintain a constant molar ratio
247 of calcium chloride : DOPS (1:1) for all experiments despite the changing flow ratios. Mixing was
248 carried out at flow rate of 12 ml/min. We prepared cochleate composites to achieve aqueous:
249 ethanolic phase ratios from 1:1, 1:2, 1:3, 1:5 and 1:9. In complete absence of ethanol, conventional
250 long cylindrical cochleates were obtained in preliminary studies. This observation did not change
251 significantly when high ratio of $\text{CaCl}_2_{(\text{aqueous})}$: $\text{DOPS}_{(\text{ethanolic})}$ (3:1) was used (data not shown). However,
252 when the ethanol fraction was increased beyond 75%, the morphology of the resulting particles
253 changed from large cochleate aggregates to spherical nanocochleate composites, as shown in Fig. 1.
254 At the ratio of 1:1 (Fig. 1a) large aggregated cylindrical cochleates were formed and their aggregation
255 lacked structure. These samples also showed presence of unrolled sheets. Increasing the amount of
256 ethanol (flow ratio 1:2) led to a big change in the morphology of aggregates. Agglomerates
257 approximately 6-12 μm in diameter consisting of large cochleates were formed as seen in Fig. 1b. At
258 both ratios cochleates formed were in micron range. Flow ratio of 1:3 produced particles containing
259 nanocochleates (Fig. 1c) which were roughly spherical and showed high tendency of aggregation.
260 Aggregates were usually made of at least 2-5 loosely packed cochleate-composites. It's important to
261 note that at this ratio microspheres clearly showed presence of nanocochleates which seemed to
262 indicate that increased ethanol content was important for the formation of cochleates with smaller
263 dimensions. Further increase in amount of ethanol (ratio 1:5) resulted in particles (Fig. 1d) which were
264 more spherical and uniform than before (approx. 3-6 μm diameter). These cochleate composites also
265 showed the tendency to aggregate and individual cochleate composites were made up of aggregated
266 nanocochleates. The ratio with minimum amount of water i.e. 1:9 produced cochleate composites
267 (Fig. 1e) which were spherical and were made up of densely packed nanocochleates. When the

1
2
3 268 precipitation was carried out in pure ethanol, ethanolic DOPS and ethanolic CaCl₂, the formation of
4
5 269 stacks was observed (Fig. 1f). However, these stacks did not form any cochleates even when the
6
7
8 270 samples were observed after 8 months of storage. From these results we suspect that the presence
9
10 271 of small amount of water is crucial for curling of bilayers into nanocochleate cylinders, however
11
12 272 further investigation is necessary to understand the exact underlying mechanism.
13
14

273

274 Influence of flow rate:

15
16
17
18
19 275 It is well known that size and morphology can be varied easily by changing the rate of mixing in a
20
21
22 276 microfluidic reactor. To evaluate this effect, we varied the flow rate from 1 ml/min to 18 ml/min
23
24 277 keeping a constant flow ratio for CaCl₂(aqueous phase) : DOPS(ethanolic phase) at 1:9. Resulting lipid aggregates
25
26 278 were analyzed using electron microscopy. Fig. 2 shows the influence of flow rate on the morphology
27
28 279 of resulting cochleate composites. In general, we found that lower flow rates formed particles arrested
29
30 280 and aggregated at intermediate stages of formation of cochleate composites. High flow rates due to
31
32
33 281 faster mixing formed spherical cochleate composites. At the slowest flow rate of 1 ml/min long
34
35 282 cylindrical cochleates were formed along with dense lipid precipitates as shown by arrows in Fig. 2a.
36
37 283 These precipitates may be non-bilayer structures formed as a result of interfacial deposition of lipid
38
39 284 due to displacement of ethanol. This result was an indication that not only high ethanol contents but
40
41
42 285 also high mixing rates are a prerequisite for the formation of nano-sized cochleates. When the flow
43
44 286 rate was increased to 3 ml/min, aggregates of 3-10 roughly spherical particles were observed (Fig. 2b).
45
46 287 Particles seemed to exhibit a higher aggregation tendency and large conventional cochleates were
47
48 288 also rarely observed. For samples prepared at 6 ml/min, dense isolated spherical particles with large
49
50 289 diameter were observed (Fig. 2c). The surface of these particles appeared much denser compared to
51
52 290 the cochleate composites. The dense nature of the particles was not completely clear and further
53
54 291 evaluation is required, but it was observed repeatedly for this flow rate. It appeared as if the growth
55
56 292 of particles was initiated before nucleation was completed. Which may result in competition between
57
58
59 293 growth of new nuclei and grown particles and causes high polydispersity. Flow rate of 12 and 18
60

1
2
3 294 ml/min gave rise to much more spherical and regular particles (Fig. 2d and 2e respectively) as
4
5 295 compared to those prepared at lower flow rates. Cochleate composites prepared at high flow rates
6
7 296 were made up of aggregated nanocochleates and stacks. At 18 ml/min particles seemed to vary in size
8
9 297 much more than that at 12 ml/min. Fig. 2e shows two particles, a completely formed particle (dark
10
11 298 arrow) and an incompletely formed particle (white arrow) which was often observed at flow rate of
12
13 299 18 ml/min. This morphological evolution was probably due to the high flow rate which does not give
14
15 300 enough time for aggregates to form spherical structures. Hence the flowrate of 12mL/min was chosen
16
17 301 as most appropriate for further experiments.
18
19
20

21 ~~302~~
22 304

23 24 305 Influence of Lipid Concentration:

25
26 306 Fig. 3 shows SEM images of cochleate composites at different lipid concentrations. We tested lipid
27
28 307 concentrations ranging from 1 mg/ml to 0.1 mg/ml while maintaining a flow rate of 12 ml/min and
29
30 308 flow ratio of $\text{CaCl}_2(\text{aqueous phase}) : \text{DOPS}(\text{ethanolic phase})$ at 1:9. All lipid concentrations produced spherical
31
32 309 cochleate composites made of nanocochleates. The morphology of the composites became more
33
34 310 regular and uniform in size with decreasing lipid concentration. For high lipid concentrations of 1 and
35
36 311 0.75 mg/ml, spherical cochleate composites were observed aggregated along with many small
37
38 312 inconsistent non-spherical cochleate composites (shown by arrows in Fig. 3a). Such morphology was
39
40 313 probably a result of very high nucleation and incomplete growth. Reducing the lipid concentration
41
42 314 further resulted in much more uniform and spheroid particles and had almost no signs of attached
43
44 315 aggregates (Fig. 3b). For smallest lipid concentration of 0.1 mg/mL the cochleate composites were
45
46 316 extremely regular (Fig. 3c). Hence it was chosen as 'optimized formulation' for further experiments.
47
48
49 317 In samples with high lipid concentrations, cochleate composites were made of a large number of
50
51 318 number of lipid stacks along with few nanocochleates. In our opinion, lipid stacks may be the primary
52
53 319 structures formed from nucleates when lipid solution encounters the binding agent. High lipid
54
55 320 concentrations probably gives rise to a large number of nucleates with small inter-particulate
56
57 321 distances. This high density of nucleates might cause aggregation before 'stacks to cochleate'

1
2
3 322 transformation is complete. Therefore the cochleate formation or curling of the stacks in these
4
5 323 particles seemed to be arrested at intermediate stages. For low lipid concentrations, cochleate
6
7
8 324 composites showed nanocochleates and highly curled stacks. This was probably because aggregation
9
10 325 was relatively gentle and allowed time for the stacks to evolve in to nanocochleates.

11 326

12 327

13 328 **Morphological evaluation and size distribution of cochleate composites:**

14
15
16
17 329 Optimized formulation of cochleate composites was further evaluated using SEM, cryo TEM and resin
18
19 330 embedding technique to understand the morphology of the aggregated subunits. Fig. 4a shows a high
20
21 331 magnification SEM micrograph of a cochleate composite showing many nanocochleates (white
22
23 332 arrows) along with few curled stacks (dark arrows). Cochleates have a tube like appearance and can
24
25 333 easily be identified by the hollow central channel. All of the aggregated nanocochleates and curled
26
27 334 stacks had sub-micron dimensions. Fig. 4b shows a cryo-TEM image of cochleate composite at higher
28
29 335 magnification where nanocochleates and curled stacks (dark arrow) can be clearly seen.
30
31 336 Nanocochleates had approximate diameter of 100 - 200 nm and were made up of 8-20 lipid bilayers.
32
33 337 Cross sections of cochleate composites obtained from the embedding study are as shown in Fig. 4c.
34
35 338 The cross sections confirmed that cochleate composites were mainly made up of hollow
36
37 339 nanocochleates which were aggregated to yield a spherical composite. Based on our EM studies,
38
39 340 cochleate composites were mainly made up of (1) nanocochleates with hollow central channel
40
41 341 (approx. length 400-600 nm) (2) curled bilayer stacks and (3) voids inside the cochleate composites
42
43 342 (few hundred nanometers). To investigate whether the microfluidic device had any influence on the
44
45 343 intrinsic structure of the nanocochleates, we also prepared cochleate composites using the 'modified
46
47 344 trapping method' as explained in the method section 2.2.2. EM studies of these samples revealed
48
49 345 formation of cochleate composites having irregular non-spherical shape (data not shown) which
50
51 346 confirmed our anticipation that efficient mixing achieved in the NanoAssemblr™ was responsible for
52
53 347 the spherical shape and uniformity of the cochleate composites.
54
55
56
57
58
59
60

1
2
3 348 The size distributions of cochleates obtained from trapping method and hydrogel isolation method
4
5 349 were compared with cochleate composites. The representative SEM images corresponding to
6
7
8 350 nanocochleates prepared by hydrogel isolation method and conventional trapping method are shown
9
10 351 in Fig. 5. The particle size distribution histograms of cochleates prepared by all three techniques are
11
12 352 shown in Fig. 6. The average diameter of optimized cochleate composites was about $4.4 \pm 0.3 \mu\text{m}$ with
13
14 353 CV (%) of 7.1. Compared to cochleates prepared by other methods, cochleate composites displayed a
15
16
17 354 very narrow size distribution. The mean particle size obtained from both trapping method and
18
19 355 hydrogel isolation method was $5.7 \pm 3.06 \mu\text{m}$ and $1.1 \pm 0.79 \mu\text{m}$ respectively. Their size distribution
20
21 356 histograms indicated a skewed size distribution profile (Fig. 6a and 6b). The total range of particle size
22
23 357 found for cochleates prepared by the trapping method ranged from 1.2 to $16.5 \mu\text{m}$ and for
24
25 358 nanocochleates, from 0.1 to $6.6 \mu\text{m}$. The CV (%) for cochleates prepared by trapping method was 53.3
26
27
28 359 and for nanocochleates it was 69.9, representing highly polydispersed samples. Considering CV (%)
29
30 360 values, the samples of cochleate composites were quite monodispersed when compared to the
31
32 361 conventional cochleates and nanocochleates. Hence the rate and homogeneity of mixing achieved
33
34 362 using microfluidic technique has a marked effect on the particle size of final cochleate formulation.
35
36
37 363 Similarly presence and amount of ethanol has a profound effect on the particle size distributions
38
39 364 obtained by reducing the probability of aggregation.
40
41
42
43
44

365

366 **Small angle X-ray scattering:**

46
47 367 To understand differences in the lamellar order between conventional cochleates prepared by
48
49 368 trapping method, hydrogel isolation method and cochleate composites presented in this study, SAXS
50
51 369 experiments were carried out. The SAXS patterns of both cochleate composites, prepared using
52
53 370 NanoAssemblr™ and 'modified trapping method' showed exactly the same pattern as conventional
54
55 371 DOPS cochleates and nanocochleates (Fig. 7). Diffractograms of cochleate composites,
56
57 372 nanocochleates and conventional cochleates yielded interlamellar repeat distance of 5.1 nm with
58
59 373 sharp reflexes at 2θ values of 1.7° and 3.4° . The SAXS data obtained for cochleate composites agrees
60

1
2
3 374 well with electron microscopy results and confirm that cochleate composites are in fact aggregates of
4
5 375 nanocochleates with high regularity.
6
7
8 376
9
10 377 **Formation mechanism of cochleate composites:**
11
12 378 Probable formation mechanism for the cochleate composites consists two steps, 1) nucleation, where
13
14 379 phosphatidylserine molecules bind calcium and grow longitudinally to form small lipid stacks which
15
16 380 can eventually roll into nanocochleates and 2) aggregation, where high mixing rates within the
17
18 381 microfluidic device gives rise to spherical cochleate composite formed by aggregation of
19
20 382 nanocochleates. From our observation, the nucleation process was heavily influenced by ethanol
21
22 383 concentration. Literature suggests that phospholipid bilayers can coexist in ethanol concentrations up
23
24 384 to 45 – 50 % (Touitou et al., 2000) and from our experiments it could be seen that when reaction
25
26 385 mixture had 50 % ethanol (solvent ratio 1:1) with 50 % aqueous calcium chloride, conventional long-
27
28 386 cylindrical cochleates were formed. Only when ethanol concentration was raised above 75 %
29
30 387 nanocochleates were formed. Ethanol forms hydrogen bonds with phosphate in the phospholipid
31
32 388 head groups and when present in high concentrations can increase alkyl chain disorder and can lead
33
34 389 to decrease in the bending energy in phospholipid bilayers (Patra et al., 2006, Feller et al., 2002,
35
36 390 Chanturiya et al., 1999). When cochleates are prepared in aqueous environment, stack formation is
37
38 391 caused by interaction between calcium and phosphatidylserine bilayers. This has a dehydrating effect
39
40 392 on the bilayers which results in highly condensed alkyl chains with high degree of order and interior
41
42 393 which is characterized by almost complete lack of water (Nagarsekar et al., 2014, Martin-Molina et al.,
43
44 394 2012). The resulting stacks would aggregate rapidly due to their hydrophobic surfaces leading to larger
45
46 395 planar sheets. These sheets further undergo curling to reduce their surface area to form cochleate
47
48 396 cylinders. However in ethanol rich environment, hydrophobic surfaces of stacks would be stabilized
49
50 397 by ethanol, resulting in smaller stacks. Stabilization coupled with lower bending energy could explain
51
52 398 the nanoscale dimensions of the cochleates found within the spherical cochleate composites.
53
54 399 Resulting nanocochleates and stacks further undergo aggregation to form cochleate composites.
55
56
57
58
59
60

1
2
3 400 Morphology of the composites was dictated by the mixing stage. This is a vital step and should be as
4
5 401 uniform and as fast as possible since any fluctuations in mixing can result in asymmetrical particles
6
7 402 with varying sizes. Poor mixing can also result in overlapping of nucleation and growth steps causing
8
9 403 formation of heterogeneous system. Ideal mixing conditions were difficult to reach by using
10
11 404 conventional mixing devices as we found out when we tried to replicate the composites using a
12
13 405 homogenizer. Where as in case of micro mixer of microfluidic device the mixing time is very small (in
14
15 406 milliseconds) which results in better control over process parameters and reproducibility (Kastner et
16
17 407 al., 2014).

18
19
20
21 408

22
23
24 409 **CONCLUSION:**

25
26 410 Polydispersity has always been the 'Achilles heel' of a cochleate system. In this study we report on
27
28 411 new monodisperse microparticulate system of nanocochleates. This method was developed to
29
30 412 fabricate cochleate composites with a simple microfluidic setup, which could easily be programmed
31
32 413 to transform for large scale production. We also propose strong influence of solvent conditions over
33
34 414 formation of the cochleate structures. The morphology of the microspheres prepared using
35
36 415 microfluidic device was strongly affected by flow rate and lipid concentration. Microfluidics could be
37
38 416 used further to tailor particle diameter of the formulation. Cochleate composites being made of
39
40 417 nanocochleates retain the basic advantages of cochleates. Hence the formulation of cochleate
41
42 418 composites may emerge with potential uses for pharmaceutical applications. We believe that our
43
44 419 study represents an important step forward to perceive processes governing the formation of
45
46 420 monodispersed cochleate drug delivery systems. Future outlook for our work would involve drug
47
48 421 loading and release experiments and to study the morphology when these composites are
49
50 422 manufactured from different cochleate forming lipids.

51
52
53
54 423

55
56
57
58 424

59
60

1
2
3
4
5
6
7
8
9
10
11
12
13
14
15
16
17
18
19
20
21
22
23
24
25
26
27
28
29
30
31
32
33
34
35
36
37
38
39
40
41
42
43
44
45
46
47
48
49
50
51
52
53
54
55
56
57
58
59
60

425 **ACKNOWLEDGEMENT**

426 A.F. and K.N. would like to thank the Phospholipid Research Center, Heidelberg for financial support.

427 F.H.S. is grateful to the Thuringian Ministry for Education, Science, and Culture (TMBWK; #B515-
428 11028, SWAXS-JCSM) for financial support.

429

430 **DECLARATION OF INTEREST**

431 The authors report no declarations of interest.

432

For Peer Review Only

1
2
3
4
5
6
7
8
9
10
11
12
13
14
15
16
17
18
19
20
21
22
23
24
25
26
27
28
29
30
31
32
33
34
35
36
37
38
39
40
41
42
43
44
45
46
47
48
49
50
51
52
53
54
55
56
57
58
59
60

433 REFERENCES

- 434 Belliveau NM, Huft J, Lin PJC, Chen S, Leung AKK, Leaver TJ, Wild AW, Lee JB, Taylor RJ, Tam YK,
435 Hansen CL & Cullis PR (2012). Microfluidic Synthesis of Highly Potent Limit-size Lipid Nanoparticles
436 for In Vivo Delivery of siRNA. *Mol Ther Nucleic Acids*, 1:e37.
437
- 438 Chanturiya A, Leikina E, Zimmerberg J & Chernomordik LV (1999). Short-chain alcohols promote an
439 early stage of membrane hemifusion. *Biophysical journal*, 77:2035-45.
440
- 441 Delmas G, Park S, Chen ZW, Tan F, Kashiwazaki R, Zarif L & Perlin DS (2002). Efficacy of Orally
442 Delivered Cochleates Containing Amphotericin B in a Murine Model of Aspergillosis. *Antimicrobial
443 Agents and Chemotherapy*, 46:2704-07.
444
- 445 Feller SE, Brown CA, Nizza DT & Gawrisch K (2002). Nuclear Overhauser Enhancement Spectroscopy
446 Cross-Relaxation Rates and Ethanol Distribution across Membranes. *Biophysical journal*, 82:1396-
447 404.
448
- 449 Garidel P, Richter W, Rapp G & Blume A (2001). Structural and morphological investigations of the
450 formation of quasi-crystalline phases of 1,2-dimyristoyl-sn-glycero-3-phosphoglycerol (DMPG).
451 *Physical Chemistry Chemical Physics*, 3:1504-13.
452
- 453 Gould-Fogerite S, Kheiri M, Zhang F & Mannino RJ (2000). Cochleate Delivery Vehicles: Applications
454 in Vaccine Delivery. *Journal of liposome research*, 10:339-58.
455
- 456 Gould-Fogerite S & Mannino RJ (2000). Cochleates for Induction of Mucosal and Systemic Immune
457 Responses #. T Vaccine Adjuvants. 179-96.
458
- 459 Huergo CC, Gonzalez VGS, Vazquez MMG, Jorin GB, Imia LGG, De La Caridad Puentes Rizo G,
460 Herrera MCS, Padron FS, Morales EXLR & Dominguez MaG 1997. Method of producing Neisseria
461 meningitidis B vaccine, and vaccine produced by method. Google Patents.
462
- 463 Jin TBSI, Mannino RUMDNJ, Segarra IBSI & Zarif LBSI 2001. Novel hydrogel isolated cochleate
464 formulations, process of preparation and their use for the delivery of biologically relevant molecules.
465 Google Patents.
466
- 467 Kastner E, Kaur R, Lowry D, Moghaddam B, Wilkinson A & Perrie Y (2014). High-throughput
468 manufacturing of size-tuned liposomes by a new microfluidics method using enhanced statistical
469 tools for characterization. *International Journal of Pharmaceutics*, 477:361-68.
470
- 471 Kulkarni VS, Boggs JM & Brown RE (1996). Modulation of nanotube assembly in simple sphingolipids.
472 *Progress in Biophysics and Molecular Biology*, 65:141-41.
473
- 474 Kulkarni VS, Boggs JM & Brown RE (1999). Modulation of Nanotube Formation by Structural
475 Modifications of Sphingolipids. *Biophysical journal*, 77:319-30.
476
- 477 Mannino RJ & Gould-Fogerite S 2002. Cochleate delivery vehicles. *In: Office CIP (ed.)*. Canada.
478
- 479 Martin-Molina A, Rodriguez-Beas C & Faraudo J (2012). Effect of calcium and magnesium on
480 phosphatidylserine membranes: experiments and all-atomic simulations. *Biophys J*, 102:2095-103.
481
- 482 Nagarsekar K, Ashtikar M, Thamm J, Steiniger F, Schacher F, Fahr A & May S (2014). Electron
483 Microscopy and Theoretical Modeling of Cochleates. *Langmuir*, 30:13143-51.

Journal of Liposome Research

- 1
2
3 484
4 485 Nie Z, Li W, Seo M, Xu S & Kumacheva E (2006). Janus and Ternary Particles Generated by
5 486 Microfluidic Synthesis: Design, Synthesis, and Self-Assembly. *Journal of the American Chemical*
6 487 *Society*, 128:9408-12.
7 488
8 489 Patra M, Salonen E, Terama E, Vattulainen I, Faller R, Lee BW, Holopainen J & Karttunen M (2006).
9 490 Under the Influence of Alcohol: The Effect of Ethanol and Methanol on Lipid Bilayers. *Biophysical*
10 491 *journal*, 90:1121-35.
11 492
12 493 Perez A, Hernández R, Velasco D, Voicu D & Mijangos C (2015). Poly (lactic-co-glycolic acid) particles
13 494 prepared by microfluidics and conventional methods. Modulated particle size and rheology. *Journal*
14 495 *of colloid and interface science*, 441:90-97.
15 496
16 497 Poste G, Papahadjopoulos D & Vail WJ (1976). Lipid vesicles as carriers for introducing biologically
17 498 active materials into cells. *Methods Cell Biol*, 14:33-71.
18 499
19 500 Rasband WS (1997-2014). ImageJ,. U. S. National Institutes of Health, Bethesda, Maryland, USA.
20 501
21 502 Sankar VR & Reddy YD (2010). Nanochchleates - a new approach in lipid drug delivery. *International*
22 503 *Journal of Pharmacy and Pharmaceutical Sciences* 2:220-23.
23 504
24 505 Sarig H, Ohana D, Epand RF, Mor A & Epand RM (2011). Functional studies of cochleate assemblies
25 506 of an oligo-acyl-lysyl with lipid mixtures for combating bacterial multidrug resistance. *FASEB journal :*
26 507 *official publication of the Federation of American Societies for Experimental Biology*, 25:3336-43.
27 508
28 509 Syed UM, Woo AF, Plakogiannis F, Jin T & Zhu H (2008). Cochleates bridged by drug molecules.
29 510 *International Journal of Pharmaceutics*, 363:118-25.
30 511
31 512 Tuitou E, Dayan N, Bergelson L, Godin B & Eliaz M (2000). Ethosomes - novel vesicular carriers for
32 513 enhanced delivery: characterization and skin penetration properties. *Journal of controlled release :*
33 514 *official journal of the Controlled Release Society*, 65:403-18.
34 515
35 516 Wang N, Wang T, Zhang M, Chen R & Deng Y (2014). Using procedure of emulsification-lyophilization
36 517 to form lipid A-incorporating cochleates as an effective oral mucosal vaccine adjuvant-delivery
37 518 system (VADS). *Int J Pharm*, 468:39-49.
38 519
39 520 Whitesides GM (2006). The origins and the future of microfluidics. *Nature*, 442:368-73.
40 521
41 522 Zarif L (2002). Elongated supramolecular assemblies in drug delivery. *Journal of Controlled Release*,
42 523 81:7-23.
43 524
44 525 Zarif L (2005). Drug Delivery by Lipid Cochleates. In: Nejat D ed. *Methods in Enzymology*. Academic
45 526 Press, 314-29.
46 527
47 528 Zarif L, Graybill JR, Perlin D, Najvar L, Bocanegra R & Mannino RJ (2000). Antifungal Activity of
48 529 Amphotericin B Cochleates against *Candida albicans* Infection in a Mouse Model. *Antimicrobial*
49 530 *Agents and Chemotherapy*, 44:1463-69.
50 531
51 532 Zarif L, Jin T, Segarra I & Mannino RJ 2003. Hydrogel-isolated cochleate formulations, process of
52 533 preparation and their use for the delivery of biologically relevant molecules. Google Patents.
53 534

Journal of Liposome Research

1
2
3
4
5
6
7
8
9
10
11
12
13
14
15
16
17
18
19
20
21
22
23
24
25
26
27
28
29
30
31
32
33
34
35
36
37
38
39
40
41
42
43
44
45
46
47
48
49
50
51
52
53
54
55
56
57
58
59
60

- 535 Zarif L & Mannino RJ (2000). Cochleates. Lipid-based vehicles for gene delivery-concept,
536 achievements and future development. *Advances in experimental medicine and biology*, 465:83-93.
537
- 538 Zayas C, González D, Acevedo R, Del Campo J, Lastre M, González E, Romeu B, Cuello M, Balboa J,
539 Cabrera O, Guilherme L & Pérez O (2013). Pilot scale production of the vaccine adjuvant
540 Proteoliposome derived Cochleates (AFCo1) from *Neisseria meningitidis* serogroup B. *BMC Immunol*,
541 14:1-5.
542
543

For Peer Review Only

1
2
3
4
5
6
7
8
9
10
11
12
13
14
15
16
17
18
19
20
21
22
23
24
25
26
27
28
29
30
31
32
33
34
35
36
37
38
39
40
41
42
43
44
45
46
47
48
49
50
51
52
53
54
55
56
57
58
59
60

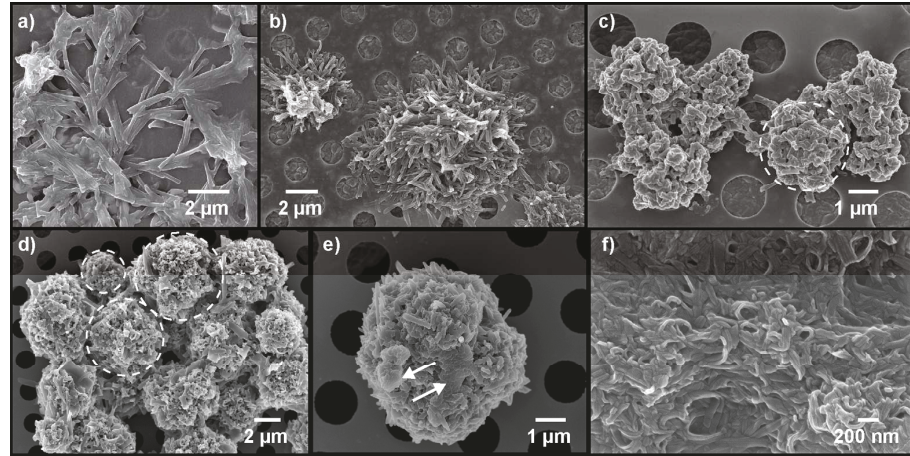


Figure 1: SEM images of DOPS cochleate composites obtained from NanoAssembler™ at CaCl₂ (aqueous phase) : DOPS (ethanolic phase) ratios of (a) 1:1 (b) 1:2 (c) 1:3 and (d) 1:5; dashed circles marks the spherical morphology of the aggregated cochleate composites (e) 1:9 ; arrows indicates planar sheets aggregated on a cochleate composite, and (f) DOPS lipid sheets precipitated from mixing of ethanolic solution of DOPS and ethanolic calcium chloride. Flow ratio was maintained constant at 12 ml/min.
164x82mm (300 x 300 DPI)

1
2
3
4
5
6
7
8
9
10
11
12
13
14
15
16
17
18
19
20
21
22
23
24
25
26
27
28
29
30
31
32
33
34
35
36
37
38
39
40
41
42
43
44
45
46
47
48
49
50
51
52
53
54
55
56
57
58
59
60

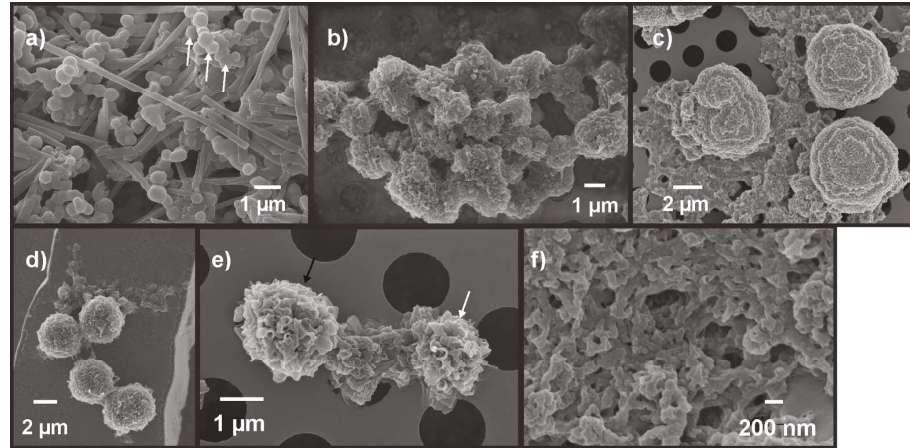


Figure 2: SEM images of DOPS cochleate composites obtained from NanoAssembler™ at different flow rates; (a) 1 ml/min; arrows showing non-bilayer structures (b) 3 ml/min (c) 6 ml/min (d) 12 ml/min (e) 18 ml/min and white arrow showing incomplete formation of particle (f) high magnification SEM image showing fused stacks formed in the dense particles obtained with flow rate of 6 ml/min. Constant flow ratio of 1:9 was maintained for all the samples.
168x83mm (300 x 300 DPI)

Journal of Liposome Research

1
2
3
4
5
6
7
8
9
10
11
12
13
14
15
16
17
18
19
20
21
22
23
24
25
26
27
28
29
30
31
32
33
34
35
36
37
38
39
40
41
42
43
44
45
46
47
48
49
50
51
52
53
54
55
56
57
58
59
60

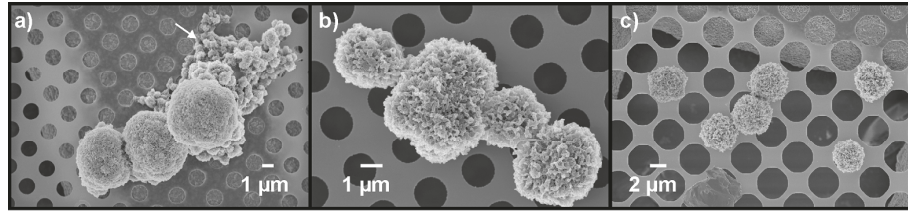


Figure 3: SEM images of DOPS cochleate composites obtained from NanoAssembler™ at lipid concentrations of (a) 0.75 mg/ml (b) 0.25 mg/ml (c) 0.1 mg/ml. Constant flow ratio of 1:9 and flow rate of 12 ml/min was maintained for all the samples.
180x41mm (300 x 300 DPI)

1
2
3
4
5
6
7
8
9
10
11
12
13
14
15
16
17
18
19
20
21
22
23
24
25
26
27
28
29
30
31
32
33
34
35
36
37
38
39
40
41
42
43
44
45
46
47
48
49
50
51
52
53
54
55
56
57
58
59
60

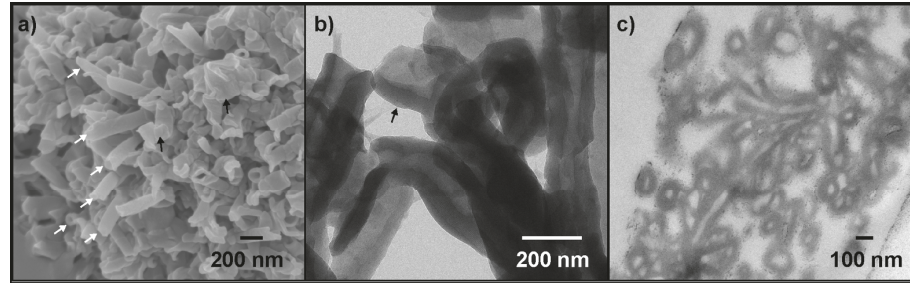


Figure 4: Morphology of optimized DOPS cochleate composites obtained from NanoAssembler™ a) SEM image showing nanocochleates (white arrows) and stacks (dark arrows) b) high magnification cryo-TEM image showing lamellar structure of the nanocochleates within the cochleate composites. Dark arrow shows a curling bilayer stack and c) TEM of cross section after resin embedding.
179x55mm (300 x 300 DPI)

1
2
3
4
5
6
7
8
9
10
11
12
13
14
15
16
17
18
19
20
21
22
23
24
25
26
27
28
29
30
31
32
33
34
35
36
37
38
39
40
41
42
43
44
45
46
47
48
49
50
51
52
53
54
55
56
57
58
59
60

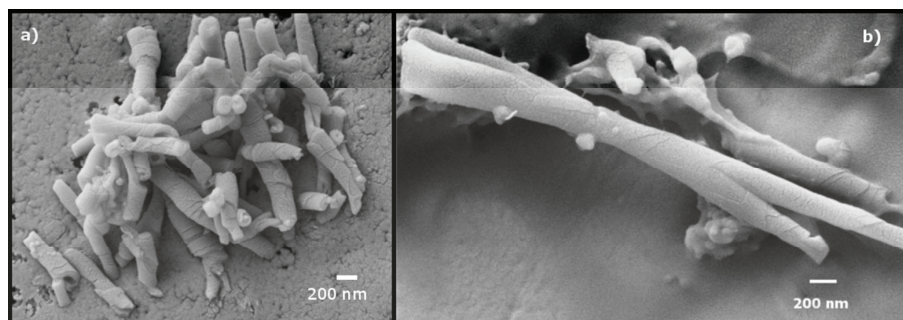


Figure 5: SEM images of DOPS, a) nanocochleates obtained by hydrogel isolation method b) conventional cochleates obtained by trapping method
86x30mm (300 x 300 DPI)

Peer Review Only

Journal of Liposome Research

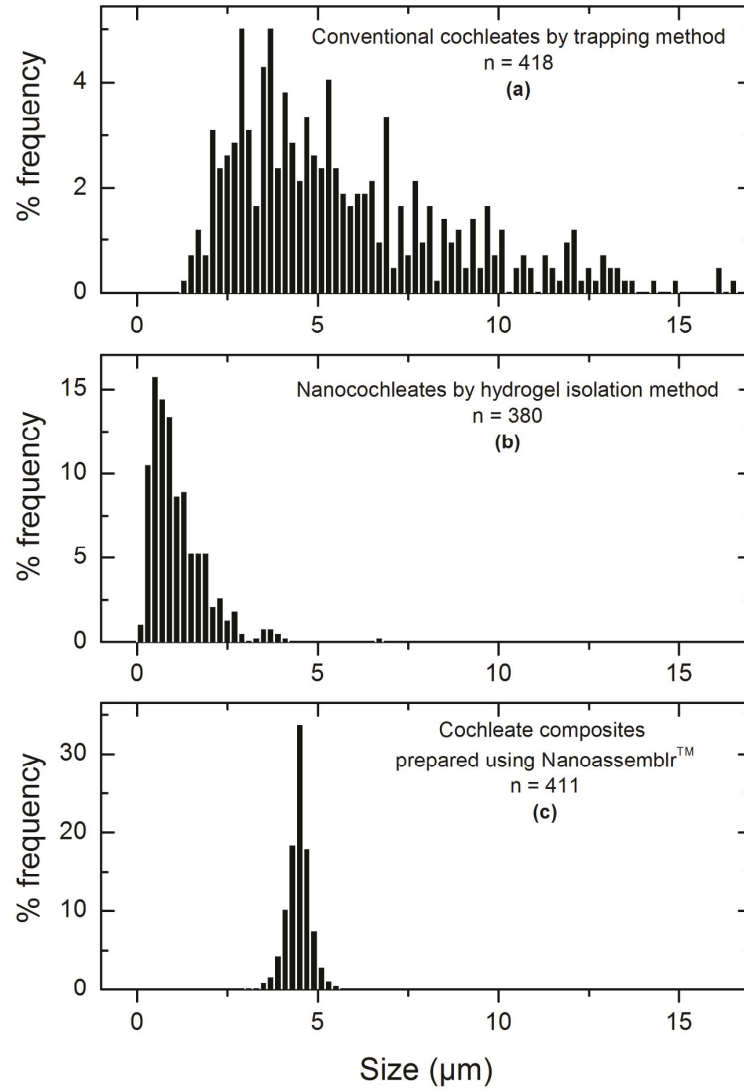
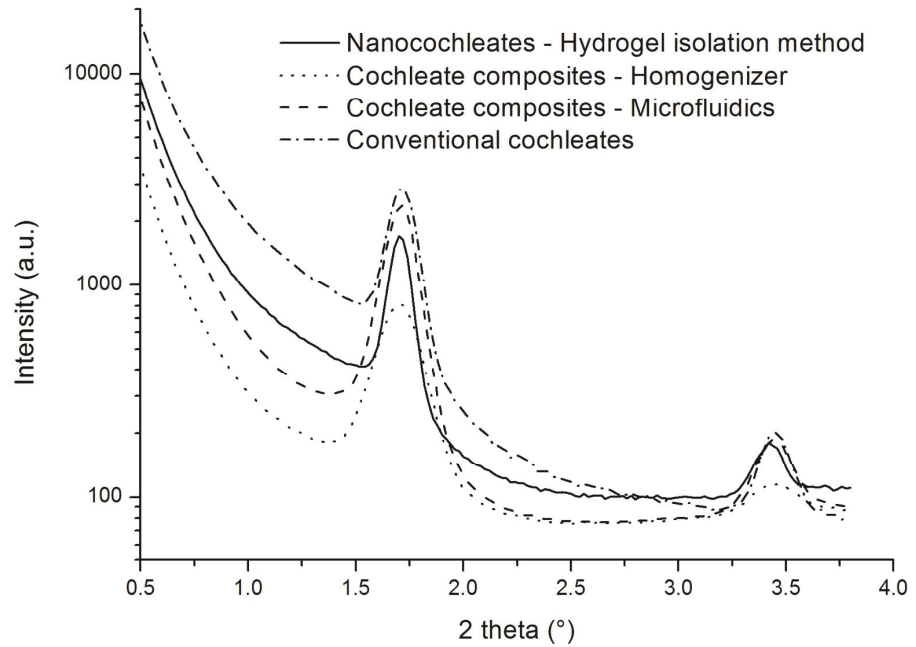


Figure 6: Particle size distribution determined from analysis of SEM images of a) conventional cochleates by trapping method b) nanocochleates by hydrogel isolation method c) optimized cochleate composites formulated using NanoAssembler™.
139x203mm (300 x 300 DPI)



31 Figure 7: SAXS patterns of DOPS cochleates obtained by (a) conventional trapping method (- · - · -) (b)
 32 nanocochleates by hydrogel isolation method (____) (c) cochleate composites prepared using
 33 NanoAssembler™ (- - -) and (d) cochleate composites prepared using a homogenizer (.....).
 34 149x105mm (300 x 300 DPI)

35
36
37
38
39
40
41
42
43
44
45
46
47
48
49
50
51
52
53
54
55
56
57
58
59
60

View Only

4 Discussion

4.1 General discussion:

It is apparent that recent developments in preparation methods, characterization and evaluation have allowed considerable improvements of cochleate formulations for drug delivery. However, in order to reach the market there is still need to carry out further research. We believe that the detailed knowledge of cochleates may contribute to tailor them for optimal use *in vivo* and reflect on the challenges that lie in this way. Therefore, in this dissertation cochleates were evaluated for their structure and formation using different microscopy techniques. Apart from this, the challenge of polydispersity of cochleate formulations has also been addressed by successfully combining the knowledge of solvent effect with the concept of controlled mixing using microfluidics to prepare a monodispersed system. In this section, we intend to discuss the details regarding the pathway of cochleate formation, effect of the building block on structural features of cochleates, feasibility of our new method for formulation of cochleates and potential applications of these new developments.

4.1.1 Investigation on formation of cochleates:

The mechanism of cochleate formation from PS has been speculated in brief by Papahadjopoulos et al. (1975). Their theory was based on results from freeze fracture-TEM and explains that on the addition of high affinity cations to negatively charged lipids, a formation of array of structures takes place. Presumably, bilayer fusion is believed to advance through several semi-stable intermediate structures such as discs, sheets which finally are converted into cochleates. Some investigations on intermediates arising during cochleate formation have been reported previously. Kachar et al. reported that pure PS vesicles may undergo fusion or violent rupture on interaction with calcium ions (Kachar et al., 1986). In 1981 Miller et al. showed the presence of flattened structures in microscopy within 10 ms after addition of cations to PS. Most of these studies involved bovine brain extract PS rather than pure PS which have not been studied in detail. Our major objective in **(Manuscript 1)** was to provide a sequence of the morphological changes that bilayers of PS with different saturation and carbon chain length undergo after interaction with calcium using experimental evidence. A number of variations on this interaction scheme have been exercised such as video-enhanced microscopy (Kachar et al., 1986), rapid mixing (Rand et al., 1985) and using a freezing device (Miller and Dahl, 1982) etc. However in this study we have focused on the influence of the process temperature. When the process temperature is above the transition temperature of the phospholipid the intermediate steps occur at tremendous speed i.e. within milliseconds and an appearance of intermediate structures seems to be synchronous. To deal with this issue we hypothesized that decreasing the process temperature below or around transition temperature (T_m) of lipid might decrease the speed

of reaction allowing us a measurable window of time to have a look at different intermediate stages taking place. As noted in **(Manuscript 1)** we evaluated cochleate samples of different phosphatidylserines using various electron microscopy techniques. Our interpretation for the sequence of events during cochleate formation is based on the comparison between observed morphology in these samples. The experimental data from **(Manuscript 1)** shows that different chosen phosphatidylserines exhibited similar morphologies during cochleate formation. Our results agree with previously reported early morphological changes where immediately after addition of calcium, primary structures like liposomes, micelles undergo mutual adhesion and fusion (Kachar et al., 1986). The intermediate multilamellar structures with dense packing were often observed after aggregation. The flat areas of contact resulting due to aggregation indicated that interaction may be sufficiently strong to deform primary structures indicating high values of adhesion energy. Such deformation may further result in bilayer rupture due to increased tension (Evans and Kwok, 1982; Evans and Parsegian, 1983). Our observations of cryo TEM showed that these aggregated structures further give rise to secondary bilayer fragments (which we named ribbons). We interpret that these structures result due to bilayer destabilization in intermediate multilamellar aggregates. This loss of stability might evolve from fusion particularly between the outer monolayers of aggregated bilayer structures. It was demonstrated that the repeat distance of such ribbon like structures by SAXS appeared to be much different as compared to both cochleates and primary structures like liposomes or micelles. This may result due to presence of calcium in these bilayers and was considered as an indication for intermediate structure.

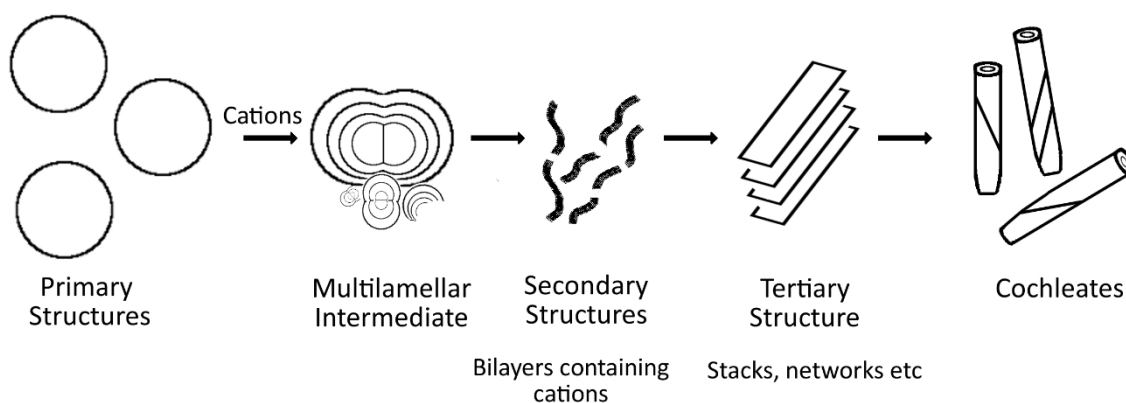


Figure 4.1: Diagrammatic representation of cochleate formation depicting sequence of intermediate structures during the process.

Our studies suggested that formation of cochleates directly from ribbons seems to be a demanding affair. This interpretation is based on the observation that no cochleate formation was observed in

DPPS and DSPS ribbon samples over long incubation times. This renders to possibility that formation of tertiary structures from ribbons requires energy. Our results show that ribbons further undergo aggregation to form an array of tertiary structures most characteristic of which are stacks. These structures had been previously also identified by Garidel et al. (2001) as bands in samples of DMPG cochleates. Stacks are multilamellar and generally have elongated trapezoidal shape (as depicted in Figure 4 of manuscript 1). Our results highlighted that stack formation may be essential in order to form cochleates. It was observed that stacks can also undergo fusion to form broad sheets or networks. Our SAXS experiments indicated that the tertiary structures do not reveal the same results for repeat distance as cochleates. Complete absence of tertiary structures was seldom observed in samples of cochleates prepared from PS. We interpret that these complex architectures composed of fused lipid networks, sheets and cochleates may be the final result of thermodynamic equilibrium during formation process. Such tertiary structures appear to be stable and may coexist with cochleates. The tertiary structures i.e. stacks or sheets further roll upon to form cochleates. Figure 4.1 displays diagrammatic representation of cochleate formation based on results from **(Manuscript 1)**. We presume that the rate of conversion of tertiary structures to cochleates is an important parameter which would influence polydispersity of the final cochleate formulation. This could be of interest from a pharmaceutical point of view considering the fact that for optimization of formulations, presence of intermediates can be an important issue as it can significantly influence physicochemical properties, drug loading, release properties etc.

Taken together **(Manuscript 1)** ascertained that cochleate formation is through evolution of well-defined hierarchical morphologies like ribbons, stacks, networks, sheets that leads to a stable cochleate structure. The most important conclusions from these studies are qualitative. Although cochleate formation may have more than one secondary pathway due to uncontrolled interactions, summary of our study in **(Manuscript 1)** provides enough support to speculate a fundamental order of probable intermediates arising during cochleate formation.

4.1.2 Structural features of cochleates:

Based on our microscopy results in **(Manuscript 1 and 2)**, the first point worth discussing about structure of cochleates is its central channel. As per Papahadjopoulos et al. cochleates are cigar like structures with folded morphology (1975) whereas Garidel et al. (2001) and Kodama et al. (1999) have mentioned the possibility of luminal opening in DMPG cochleates. All these arguments are based on freeze fracture TEM or TEM techniques, and need further research to support this observation completely. Hence to evaluate this issue the systematic observation of the internal structure of cochleates was carried out using 3D reconstruction from cryo electron tomography.

Figure 3 in **(Manuscript 2)** clearly depicts the presence of a continuous central channel that opens at both terminus of the cylindrical cochleate structure confirming the hypothesis of Garidel et al. (2001). Our observations suggested that unlike real cigars, cochleates do not possess a dense core. This observation was supported by other microscopy techniques such as SEM, TEM and evaluation of cross sections of resin embedded cochleates. Amongst all the evaluated cochleate particles, we very rarely came across some with absence of central channel as mentioned in **(Manuscript 2 Figure 4e)**. Investigation of cross section of resin-embedded Cochleates in **(Manuscript 2 Figure 4)** indicated that the majority of particles exhibited multilamellar scrolls folding into a compact, rolled-up structure as previously described by Papahadjopoulos et al. (1975). This study also confirmed the presence of central channel in cochleates. Based on these observations we deduced that cochleates have carpet roll like morphology and not cigar like structure. This structural feature might have a strong influence on physicochemical aspects of the drug delivery system. The parameters like mechanical stability, drug release pattern, area for surface chemistry modification or drug loading may change considerably depending upon presence or absence of the central cavity in the cochleate particle. Hence, one can anticipate that this knowledge can be casted to render an efficient drug carrier.

Evaluation of the effect of variation in acyl chains of phosphatidylserines on the structural features of cochleates was not carried out previously. We have used different phosphatidylserines to form cochleates in order to evaluate the effect of acyl chain length and saturation on structural features. In **(Manuscript 1 and 2)** we have analyzed electron micrographs with the help of the software Image J for determining dimensions of cochleates. We have specifically measured the width and length for a large ensemble of cochleate tubes. These measurements show apparent and statistically significant difference in dimensions with respect to the lipids used for preparation. Our microscopy studies showed that the width of inner channel of cochleates increased with presence of unsaturation. Changes in carbon chain length of lipids also resulted in change in dimensions of cochleates. Based on these results we suggest that the dimensions of cochleates are highly dependent upon their building blocks.

Considering the findings of electron microscopy studies, a theoretical model that was based on minimizing a phenomenological free energy expression was proposed. The calculations suggested that membrane bending and calcium induced bilayer–bilayer adhesion alone were insufficient to reproduce the observed relation between inner and outer cochleate tube radii. Yet, it could be reproduced by considering an additional free energy contribution that accounts for an area compression/expansion of the lipid bilayers within the cochleate. This modeling approach offers predictions for ratios of material constants, namely the ratio between the area compressibility and the bending modulus as well as the ratio between the bilayer adhesion energy and the bending

modulus. We believe that despite all approximations the theoretical model may succeed to capture some of the underlying principles of cochleate stability and may prove valuable for understanding of cochleates.

4.1.3 Effect of ethanol on formation of cochleates:

Since the preparation of cochleates by hydrogel-isolation method (Zarif et al., 2003), interest in their use for biomedical applications has been growing exponentially. In previously used preparation methods conventional techniques were used, for obtaining reaction conditions aimed at interaction of minimum number of bilayers with cations (Wang et al., 2014; Zarif et al., 2003). However cochleate formation is through process of continuous self-assembly which caters for coexistence of intermediates along with final product. Apart from this, the nature of cochleates to undergo continuous aggregation due to their hydrophobicity also makes control over final product a challenging task. Therefore, the approaches such as increasing viscosity of reaction medium or formulation of multiple emulsion did not help with issue of polydispersity even though they provided limited control over the size of final cochleate particles. Hence, we believe that although controlled mixing of reactants is a pivotal parameter for preparation of monodisperse cochleate system it is not the sole aspect that governs the final product.

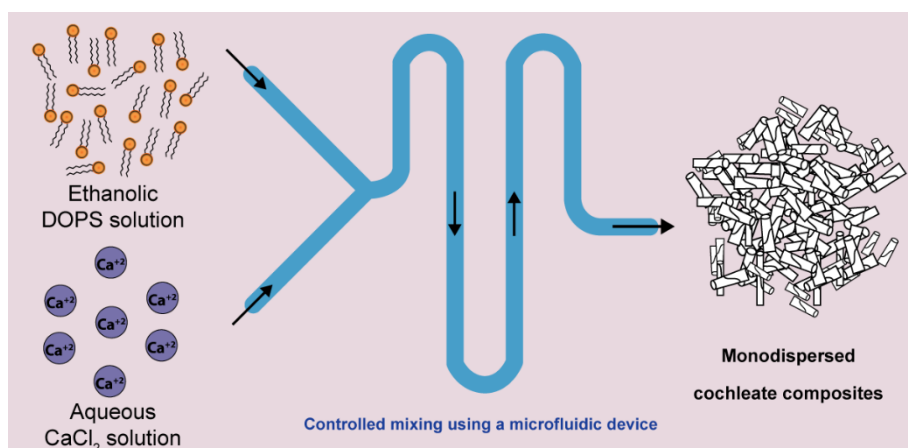


Figure 4.2: Diagrammatic representation of formation of monodisperse cochleate composites using microfluidic device after interaction of lipid solution with of calcium ions.

In **(Manuscript 3)** we have employed non-aqueous medium in combination with controlled mixing to formulate cochleates. The formation of lipid structures by nanoprecipitation in water-miscible organic solvents is not new. In this strategy using organic solvents along with aqueous phase aids in formation of nano-sized particles. Also as compared to aqueous environment it might aid in reducing surface tension at the interface of lipid particle and aggregation during preparation (Ramteke et al., 2012). Our dedication for this approach was supported by preliminary investigations which indicated

that the presence of water miscible organic solvent (>50% v/v) during precipitation gave rise to spheres made of nano-sized cochleates. To produce cochleates consistently, using microfluidic device was also a preferred choice. Microfluidics is a platform that has been known for its versatility regarding formulation of wide range of drug delivery systems (Zhang et al., 2013) and could exercise far greater control on the particle size than is possible by conventional methods.

In **(Manuscript 3)**, we have presented a microfluidics-based high through-put method for formation of microspheres (3-5 μm in diameter) made up of nano-cochleates. The formation of cochleates in a micromixer chip of microfluidic device is probably mediated by the diffusion of organic solvent into the miscible aqueous phase which causes nucleation, forming the lipid stacks. The high ethanol concentration during formulation of cochleates might stabilize the hydrophobic surfaces of stacks and assists in decreasing their bending energy (Feller et al., 2002; Patra et al., 2006). This may explain the formation of nano-scaled cochleates which further undergo aggregation to form microspheres. The process parameters such as flow rate and ratio of organic phase were optimized to produce monodispersed particles. Our results revealed that the particle size could be varied by changing the flow rate during preparation. The intermediates arising from overlapping of nucleation and growth phase could be minimized using optimized parameters. Particles obtained by this method were considerably uniform in size as compared to those obtained from conventional methods. This could be attributed to the fact that microfluidic device allowed for precise and reproducible mixing over micrometer length scales with controlled mechanical conditions. In comparison with conventional techniques, our approach offered easy handling and short formulation time. Microscopy studies and SAXS data confirmed the reproducibility of this technique and homogeneity of the products. Hence, development of this process could improve the quality attributes of cochleate formulations.

4.2 Conclusions and potential applications of this study

During current investigations of cochleates, findings regarding morphology and sequence of evolution of hierarchical structures have been made. The conclusions of this study may aid in finding missing links in previous literature on the formation mechanism of cochleates. Improved understanding of the formation mechanism could also allow for rectification of currently available formulation methods and the development new methods with higher reproducibility. The knowledge of different hierarchical structures and their possibility of coexistence might be of great interest considering their direct influence on physicochemical characteristics, stability, release kinetics etc. The high resolutions techniques used during this investigation availed gathering of additional information regarding peculiar structural features such as the hollow central channel. The detailed elucidation of structure of cochleates could help to establish a better perception regarding their

possible applications. This, in turn, would contribute to the design of cochleates for specific tasks. Developing a simple protocol to prepare monodisperse formulation of cochleates is a step ahead towards pharmaceutical industry and has several practical advantages. The described methodology availed reproducibility to the cochleate formulations. This would enable reproducibility of physicochemical characteristics of drug delivery system. Further a microfluidics device may allow for improved assistance in retaining the properties of sensitive drugs by providing controlled environment during preparation of cochleates as compared to conventional methods. The conventional approaches generate polydisperse aggregates of cochleates along with the intermediate morphologies. Given that stages like milling, homogenization, purification, washing of the final product cause an additional expense, using our strategy could prove cost effective. Cochleate microparticles synthesized using the microfluidic device can be easily modulated to produce higher yields. This can be of major advantage for expensive drugs considering the minimization of losses during production. So we postulate that our methodology described formation of monodisperse system that could widen the range of applications of cochleates. However, further studies are needed in order to reach the goal of incorporation of drug in formulation and further evaluation for efficiency. Nevertheless we hope that our study would contribute to advance the knowledge of cochleates and facilitate future research.

4.3 Future prospects of cochleates:

Cochleates are promising vehicles and are under investigation by companies like Matinas BioPharma in order to improve efficacy of some orally ineffective therapeutic agents. Considering medical applications, we can expect several drugs such as amphotericin B, ibuprofen etc. formulated into cochleate formulations in coming decades. Immunotherapy is another area in which researchers may expect progress. However to exercise potential of cochleates as drug delivery system *in vivo*, clear understanding of their mechanism of action at tissue and cellular level is required. More attention needs to be paid in understanding the effect of different building materials on systems efficiency *in vivo*. To design cochleates for successful drug delivery it is essential to carry out fundamental research to understand complex interactions such as drug release rates in different pathologies, effect of biological interactions like opsonization, and the barriers subjected while approaching target site etc. Given that the efficiency of cochleates is so far mainly gauged based on cell culture assays and murine models, the priority for future research should be to conduct bioavailability studies in humans. Apart from pharmaceutical industry cochleates may also prove to be useful in other areas such as food and nutrition industry, agricultural industry etc. Although during pharmaceutical investigations cochleates are made from pure and expensive raw materials using high technology, the low-purity

Discussion

lipid extracts may also be used for preparation. The growth of lipid based novel technologies in cosmetic products like skin creams, sunscreen lotions etc. have always helped in capturing the attention of customers making cochleates one of the favorable strategy.

5 Summary

Cochleates represent a unique and attractive platform for biomedical applications. Interest of pharmaceutical industries towards phospholipid based biodegradable drug delivery systems have propelled investigations on cochleates in recent years. While, evaluating versatility and efficiency of cochleates as a drug delivery vehicle remains the main focus of current research, cochleates still need to overcome some hurdles which stand in the way to reach the other side of a product pipeline. Better understanding of fundamental details such as structure and formation mechanisms will assist in improving performance of cochleates as a drug delivery vehicle. In this thesis we have carried out investigations on structural features and formation pathways of cochleates. Furthermore, we have employed our knowledge in developing novel methodology to produce improved cochleate formulation.

In the past most of the investigations related to structural features or formation of cochleates have relied heavily on freeze fracture techniques. In this study, we have investigated cochleates of phosphatidylserines using different microscopy techniques for searching metastable intermediates and their coexistence with cochleates. Based on our morphological exploration, we speculate a probable order of well-defined hierarchical structures in the pathway for cochleate formation. This mechanism may be through evolution of unstable intermediate aggregates that form ribbonlike structures containing calcium. Ribbons further aggregate to form stacks or sheets, which leads to the formation of stable cochleates. It was found that the structures such as stacks, sheets and their networks can coexist with cochleates up to 12 months. The highlight of our study was the observation that, stack formation was an essential stage in the formation mechanism, as in its absence cochleate formation was hindered. Data from tomographic evaluation demonstrated cochleates to be cylindrically curved bilayers enclosing an inner channel. The dimensions of a cochleate vary statistically with changes in building lipids. Specifically, the unsaturated lipid tends to form cochleates with larger dimensions as compared to the saturated lipid. We proposed a theoretical model based on these findings in order to predict dimensions of cochleates.

All the observations of microscopy studies pointed towards the fact that for achievement of desired cochleate formulation, controlled environment allowing a single morphology to prevail is very important. Hence, in the current investigation we have developed a simple method for preparation of monodisperse cochleate formulations. We used a combined approach employing solvent effect along with controlled mixing by a microfluidic device. For this purpose, the lipid solution in an organic solvent was subjected to fast mixing with very small amount of aqueous solution of binding agent. The novel formulation obtained by this method consisted of

Summary

microspheres (~4 μm in diameter) made up of nanocochleates and was suitable for large scale production. Our studies suggest that during controlled mixing, lipid stacks are generated within milliseconds. These stacks probably entangle and fuse into a micro spherical composite. We presumed that excess of ethanol reduced the bending energy and might have stabilized the interface of lipid stacks reducing the aggregation. This might aid in both, formation of nanocochleates and regular microspheres. The microspheres obtained were characterized using SAXS and electron microscopy and compared with cochleates obtained from preexisting methodologies. EM data confirmed that the cochleate composites were clustered matrices of nanoscale cochleates. Findings from characterization studies confirmed that our methodology eliminated elaborate preparation methods, while providing a monodispersed cochleate system with analogous qualities to nanocochleates.

In conclusion our project has managed to capture new information regarding the structural details and formation mechanisms of cochleates. Furthermore a simple, fast, efficient and highly reproducible method with strong control over process parameters was successfully developed for formation of monodispersed cochleate system. We believe our effort will provide a better understanding of formation of cochleates, which may help scientists to tailor their formulations by making rational alterations.

Zusammenfassung

Cochleate stellen ein einzigartiges und attraktives Konzept für biomedizinische Anwendungen dar. Das steigende Interesse der pharmazeutischen Industrie an bioabbaubaren Arzneistoffträgersystemen auf Basis von Phospholipiden hat in den letzten Jahren die Forschung über Cochleate vorangetrieben. Aktuell ist das Hauptanliegen der Forschung die Ermittlung der Leistungsfähigkeit und Vielseitigkeit der Cochleate als Arzneistoffträgersysteme. Allerdings müssen noch einige Hürden überwunden werden, bevor Cochleate den Sprung aus der Produktpipeline auf den Markt schaffen können. Ein tieferes Verständnis grundlegender Eigenschaften wie die Struktur und der Entstehungsmechanismus sollen helfen, die Leistung von Cochleaten als Arzneistoffträgersystemen zu verbessern. In dieser Arbeit haben wir Untersuchungen zu strukturellen Merkmalen und Entstehungsmechanismen von Cochleaten durchgeführt. Zusätzlich haben wir unsere Erfahrung in der Methodenentwicklung genutzt, um verbesserte Cochleatformulierungen herzustellen. In der Vergangenheit basierte die Mehrheit der Untersuchungen zu strukturellen Eigenschaften oder der Entstehung von Cochleaten auf Gefrierbruchtechniken. In dieser Arbeit haben wir Cochleate aus Phosphatidylserinen mit Hilfe verschiedener Mikroskopietechniken in Hinblick auf metastabile Zwischenzustände und deren Co-Existenz mit Cochleaten untersucht. Basierend auf unseren morphologischen Untersuchungen beschreiben wir die Entstehung der Cochleate als eine mögliche Abfolge klar abgegrenzter, hierarchischer Strukturen. Der beschriebene Mechanismus verläuft über die Entstehung instabiler Zwischenprodukte, die bandartige Strukturen mit Calcium darstellen. Diese bandartigen Strukturen verbinden sich weiter zu Folien oder Stapeln, was schließlich zur Bildung stabiler Cochleate führt. Es konnte gezeigt werden, dass die Strukturen wie Stapel und Folien bis zu 12 Monate mit Cochleaten co-existieren können. Der Höhepunkt dieser Studie war die Beobachtung, dass die Stapelbildung ein essentieller Schritt in der Entstehung der Cochleate ist, da in ihrer Abwesenheit die Cochleatbildung verhindert wurde. Tomographische Untersuchungen zeigten, dass Cochleate aus zylindrisch gekrümmten Bilayern bestehen, die einen inneren Kanal umschließen. Die Größe von Cochleaten variiert statistisch und hängt vom verwendeten Lipid ab. Besonders ungesättigte Phosphatidylserine tendieren im Vergleich zu ihren gesättigten Analoga dazu, größere Cochleate zu bilden. Auf Grundlage dieser Beobachtungen stellen wir ein theoretisches Modell vor, mit dessen Hilfe sich die Größe der Cochleate vorhersagen lässt. Unsere Beobachtungen belegen die Tatsache, dass für die Produktion einer speziellen Cochleatformulierung kontrollierte Bedingungen, die das Auftreten einer einzigen Morphologie begünstigen, sehr wichtig sind. Somit haben wir mit der vorliegenden Arbeit eine einfache Methode zur Herstellung monodisperser Cochleate entwickelt. Wir haben hierfür

Lösungsmittelleffekte, die durch Ethanol auf Cochleate¹ verursacht werden, mit einem kontrollierten Mischen durch einen Microfluidizer² kombiniert. Zu diesem Zweck wurden die Phosphatidylserine in einem organischen Lösungsmittel gelöst und schnell mit einer kleinen Menge einer wässrigen Lösung des Bindemittels gemischt. Die durch diese Methode erhaltene neue Formulierung besteht aus Mikrokugeln³ (~4 µm Durchmesser), die aus Nanocochleaten zusammengesetzt sind, und eignet sich für die Großproduktion. Unsere Studie legt nahe, dass während des kontrollierten Mischens Lipidstapel innerhalb von Millisekunden entstehen. Diese Stapel verfangen sich und fusionieren zu einem kugelförmigen Konstrukt im µm Bereich. Wir nehmen an, dass ein Überschuss an Ethanol die Biegeenergie reduziert und so möglicherweise die Grenzflächen der Lipidstapel stabilisiert und die Aggregation behindert. Dies kann sowohl bei der Entstehung der Nanocochleate als auch der regelmäßigen Mikrokugeln helfen. Die entstandenen Mikrokugeln wurden mit Hilfe von SAXS und Elektronenmikroskopie charakterisiert und mit Ergebnissen vorhandener Methoden verglichen, um die Bildung der Cochleate zu bestätigen. Durch Elektronenmikroskopie konnte belegt werden, dass die Cochleatverbände ein gebündeltes Netzwerk nanoskaliger Cochleate sind. Die Erkenntnisse aus den Charakterisierungsstudien bestätigen, dass unsere Methode etablierte Herstellmethoden verdrängt, indem eine monodisperse Cochleatformulierung mit vergleichbarer Qualität zu Nanocochleaten entsteht. Zusammenfassend konnte unser Projekt einige neue Informationen in Bezug auf die strukturellen Eigenschaften und den Entstehungsmechanismus der Cochleate aufdecken. Weiterhin wurde eine einfache, schnelle, effiziente und reproduzierbare Methode mit streng kontrollierten Prozessparametern zur Herstellung monodisperser Cochleate etabliert. Diese Arbeit trägt zu einem besseren Verständnis der Entstehung von Cochleaten bei und gibt Wissenschaftlern die Möglichkeit, ihre Formulierungen durch rationale Änderungen anzupassen.

6 References

Archibald, D.D., Mann, S., 1993. Structural studies of lipid fibers formed by sphingosine. *Biochimica et Biophysica Acta (BBA) - Lipids and Lipid Metabolism* 1166, 154-162.

Archibald, D.D., Yager, P., 1992. Microstructural polymorphism in bovine brain galactocerebroside and its two major subfractions. *Biochemistry* 31, 9045-9055.

Bangham, A.D., Papahadjopoulos, D., 1966. Biophysical properties of phospholipids. I. Interaction of phosphatidylserine monolayers with metal ions. *Biochimica et Biophysica Acta (BBA) - Biophysics including Photosynthesis* 126, 181-184.

Blaurock, A.E., 1982. Evidence of bilayer structure and of membrane interactions from X-ray diffraction analysis. *Biochimica et Biophysica Acta (BBA) - Reviews on Biomembranes* 650, 167-207.

Blaurock, A.E., McIntosh, T.J., 1986. Structure of the crystalline bilayer in the subgel phase of dipalmitoylphosphatidylglycerol. *Biochemistry* 25, 299-305.

Bozo, T., Brecka, R., Grof, P., Kellermayer, M.S., 2015. Extreme resilience in cochleate nanoparticles. *Langmuir* 31, 839-845.

Butler, K.W., Dugas, H., Smith, I.C.P., Schneider, H., 1970. Cation-induced organization changes in a lipid bilayer model membrane. *Biochemical and biophysical research communications* 40, 770-776.

Chellampillai, B., Yojana, B.D., Pawar, A.P., Shaikh, K.S., Thorat, U.H., 2014. Fisetin-loaded nanocochleates: formulation, characterisation, in vitro anticancer testing, bioavailability and biodistribution study. *Expert Opinion on Drug Delivery* 11, 17-29.

Cortial, A., Vocanson, M., Loubry, E., Briançon, S., 2015. Hot homogenization process optimization for fragrance encapsulation in solid lipid nanoparticles. *Flavour and Fragrance Journal*.

Del Campo, J., Lindqvist, M., Cuello, M., Bäckström, M., Cabrera, O., Persson, J., Perez, O., Harandi, A.M., 2010. Intranasal immunization with a proteoliposome-derived cochleate containing recombinant gD protein confers protective immunity against genital herpes in mice. *Vaccine* 28, 1193-1200.

Delmarre, D., Gould-Fogerite, S., Krause-Elmore, S.L., Mannino, R.J., 2004a. Cochleate preparations of fragile nutrients. Google Patents.

Delmarre, D., Lu, R., Tatton, N., Krause-Elmore, S., Gould-Fogerite, S., Manino, R.J., 2004b. Formulation of hydrophobic drugs into cochleate delivery vehicles: a Simplified Protocol & Bioral™ Formulation Kit, *Lyophilization Articles & Reports*, pp. 64–69.

References

Delmas, G., Park, S., Chen, Z.W., Tan, F., Kashiwazaki, R., Zarif, L., Perlin, D.S., 2002. Efficacy of Orally Delivered Cochleates Containing Amphotericin B in a Murine Model of Aspergillosis. *Antimicrobial agents and chemotherapy* 46, 2704-2707.

Dluhy, R., Cameron, D.G., Mantsch, H.H., Mendelsohn, R., 1983. Fourier transform infrared spectroscopic studies of the effect of calcium ions on phosphatidylserine. *Biochemistry* 22, 6318-6325.

Evans, E., Kwok, R., 1982. Mechanical calorimetry of large dimyristoylphosphatidylcholine vesicles in the phase transition region. *Biochemistry* 21, 4874-4879.

Evans, E.A., Parsegian, V.A., 1983. ENERGETICS OF MEMBRANE DEFORMATION AND ADHESION IN CELL AND VESICLE AGGREGATION. *Annals of the New York Academy of Sciences* 416, 13-33.

Feller, S.E., Brown, C.A., Nizza, D.T., Gawrisch, K., 2002. Nuclear Overhauser Enhancement Spectroscopy Cross-Relaxation Rates and Ethanol Distribution across Membranes. *Biophysical journal* 82, 1396-1404.

Flach, C.R., Mendelsohn, R., 1993. A new infrared spectroscopic marker for cochleate phases in phosphatidylserine-containing model membranes. *Biophysical journal* 64, 1113-1121.

Garidel, P., Blume, A., Hübner, W., 2000. A Fourier transform infrared spectroscopic study of the interaction of alkaline earth cations with the negatively charged phospholipid 1,2-dimyristoyl-sn-glycero-3-phosphoglycerol. *Biochimica et Biophysica Acta (BBA) - Biomembranes* 1466, 245-259.

Garidel, P., Richter, W., Rapp, G., Blume, A., 2001. Structural and morphological investigations of the formation of quasi-crystalline phases of 1,2-dimyristoyl-sn-glycero-3-phosphoglycerol (DMPG). *Physical Chemistry Chemical Physics* 3, 1504-1513.

Gibson, B., Duffy, A.M., Gould Fogerite, S., Krause-Elsmore, S., Lu, R., Shang, G., Chen, Z.W., Mannino, R.J., Bouchier-Hayes, D.J., Harmey, J.H., 2004. A novel gene delivery system for mammalian cells. *Anticancer Res* 24, 483-488.

Gould-Fogerite, S., Kheiri, M.T., Zhang, F., Wang, Z., Scolpino, A.J., Feketeova, E., Canki, M., Mannino, R.J., 1998. Targeting immune response induction with cochleate and liposome-based vaccines. *Advanced Drug Delivery Reviews* 32, 273-287.

Gould-Fogerite, S., Mannino, R., 2000. Cochleates for Induction of Mucosal and Systemic Immune Responses, in: O'Hagan, D. (Ed.), *Vaccine Adjuvants*. Springer New York, pp. 179-196.

Gould-Fogerite, S., Mannino, R.J., 1992. Targeted fusogenic proteoliposomes: Functional reconstitution of membrane proteins through protein-cochleate intermediates, in: Gregoriadis, G. (Ed.), *Liposome Technology*, 2nd ed. CRS press, pp. 261-276.

References

Gould-Fogerite, S., Mannino, R.J., 1996. Mucosal and systemic immunization using cochleate and liposome vaccines. *Journal of Liposome Research* 6, 357-379.

Gould-Fogerite, S., Mannino, R.J., 1999. Cochleate delivery vehicles. Google Patents.

Harris, J.R., Lewis, R.J., Baik, C., Pokrajac, L., Billington, S.J., Palmer, M., 2011. Cholesterol microcrystals and cochleate cylinders: Attachment of pyolysin oligomers and domain 4. *Journal of structural biology* 173, 38-45.

Hauser, H., Finer, E.G., Darke, A., 1977. Crystalline anhydrous Ca-phosphatidylserine bilayers. *Biochemical and biophysical research communications* 76, 267-274.

Jacobson, K., Papahadjopoulos, D., 1975. Phase transitions and phase separations in phospholipid membranes induced by changes in temperature, pH, and concentration of bivalent cations. *Biochemistry* 14, 152-161.

Jin, J.P., Zhang, W.V., Van Diepen, C., Curtis, J., Barrow, C.J., 2007. Microencapsulation of marine lipids as vehicle for functional food delivery, in: Barrow, C., Shahidi, F. (Eds.), *Marine nutraceuticals and functional foods*. CRC Press, pp. 115–154.

Jin, T., 2004. Cochleates without metal cations as bridging agents. Google Patents.

Jin, T., Mannino, R., Segarra, I., Zarif, L., 2001. Novel hydrogel isolated cochleate formulations, process of preparation and their use for the delivery of biologically relevant molecules. Google Patents.

Kachar, B., Fuller, N., Rand, R.P., 1986. Morphological responses to calcium-induced interaction of phosphatidylserine-containing vesicles. *Biophysical journal* 50, 779-788.

Kodama, M., Aoki, H., Miyata, T., 1999. Effect of Na⁺ concentration on the subgel phases of negatively charged phosphatidylglycerol. *Biophysical Chemistry* 79, 205-217.

Kouaouci, R., Silviu, J.R., Graham, I., Pezolet, M., 1985. Calcium-induced lateral phase separations in phosphatidylcholine-phosphatidic acid mixtures. A Raman spectroscopic study. *Biochemistry* 24, 7132-7140.

Kulkarni, V.S., Boggs, J.M., Brown, R.E., 1999. Modulation of Nanotube Formation by Structural Modifications of Sphingolipids. *Biophysical Journal* 77, 319-330.

Landge, A., Atmaram Pawar, shaikh, K., 2013. Investigation of cochleates as carriers for topical drug delivery. *International Journal of Pharmacy and Pharmaceutical Sciences* 5, 314-320.

References

- Lasic, D.D., 1997. Liposomes and niosomes, in: Rieger, M.M., Rhein, L.D. (Eds.), *Surfactants in cosmetics*, 2nd ed. Marcel Dekker, New York, pp. 264-281.
- Loomba, L., Scarabelli, T., 2013. Metallic nanoparticles and their medicinal potential. Part II: aluminosilicates, nanobiomagnets, quantum dots and cochleates. *Ther Deliv* 4, 1179-1196.
- Lu, R., Mannino, R., 2014. Cochleate compositions and methods of making and using same. Google Patents.
- Mannino, R., Gould-Fogerite, S., Krause-Elmore, S., Delmarre, D., Lu, R., 2005. Novel encochleation methods, cochleates and methods of use. Google Patents.
- Mannino, R.J., Gould-Fogerite, S., 1995. Lipid matrix-based vaccines for mucosal and systemic immunization. *Pharm Biotechnol* 6, 363-387.
- Mannino, R.J., Gould-Fogerite, S., Krause-Elmore, S.L., Delmarre, D., Lu, R., 2014. Encochleation methods, cochleates and methods of use. Google Patents.
- Mannino, R.J., Lu, R., 2014. Cochleates made with soy phosphatidylserine. Google Patents.
- Miclea, R.D., Varma, P.R., Peng, A., Balu-Iyer, S.V., 2007. Development and characterization of lipidic cochleate containing recombinant factor VIII. *Biochimica et biophysica acta* 1768, 2890-2898.
- Miller, D.C., Dahl, G.P., 1982. Early events in calcium-induced liposome fusion. *Biochimica et Biophysica Acta (BBA)-Biomembranes* 689, 165-169.
- Nasir, A., 2010. Nanovehicles: Topical Transportation of the Future, *The dermatologist*.
- Papahadjopoulos-Sternberg, B., 2012. Secondary Structure Formation by Bilayer-Active Peptides Studied by Freeze-Fracture Electron Microscopy: From Disc Micelles to Cochleate Cylinder. *Biophysical journal* 102, 290a.
- Papahadjopoulos, D., Kimelberg, H.K., 1974. Phospholipid vesicles (liposomes) as models for biological membranes: Their properties and interactions with cholesterol and proteins. *Progress in Surface Science* 4, 141-232.
- Papahadjopoulos, D., Portis, A., Pangborn, W., 1978. Calcium-induced lipid phase transitions and membrane fusion. *Annals of the New York Academy of Sciences* 308, 50-66.
- Papahadjopoulos, D., Poste, G., Schaeffer, B.E., 1973. Fusion of mammalian cells by unilamellar lipid vesicles: Influence of lipid surface charge, fluidity and cholesterol. *Biochimica et Biophysica Acta (BBA) - Biomembranes* 323, 23-42.

References

- Papahadjopoulos, D., Vail, W.J., Jacobson, K., Poste, G., 1975. Cochleate lipid cylinders: formation by fusion of unilamellar lipid vesicles. *Biochimica et biophysica acta* 394, 483-491.
- Papahadjopoulos, P.D., 1978. Large unilamellar vesicles (LUV) and method of preparing same. Google Patents.
- Patra, M., Salonen, E., Terama, E., Vattulainen, I., Faller, R., Lee, B.W., Holopainen, J., Karttunen, M., 2006. Under the Influence of Alcohol: The Effect of Ethanol and Methanol on Lipid Bilayers. *Biophysical journal* 90, 1121-1135.
- Pham, T.T., Gueutin, C., Cheron, M., Abreu, S., Chaminade, P., Loiseau, P.M., Barratt, G., 2014. Development of antileishmanial lipid nanocomplexes. *Biochimie* 107 Pt A, 143-153.
- Popescu, C., Adams, L., Franzblau, S., Zarif, L., 2001. Cochleates potentiate the efficacy of the antimycobacterial drug, clofazimine. , *The Interscience Conference On Antimicrobial Agents & Chemotherapy. EurekaMag*, p. 200.
- Portis, A., Newton, C., Pangborn, W., Papahadjopoulos, D., 1979. Studies on the mechanism of membrane fusion: evidence for an intermembrane Ca²⁺-phospholipid complex, synergism with Mg²⁺, and inhibition by spectrin. *Biochemistry* 18, 780-790.
- Poste, G., Papahadjopoulos, D., Vail, W.J., 1976. Lipid vesicles as carriers for introducing biologically active materials into cells. *Methods Cell Biol* 14, 33-71.
- Rahimpour, Y., Hamishehkar, H., 2012. Liposomes in cosmeceutics. *Expert Opin Drug Deliv* 9, 443-455.
- Ramani, K., Balasubramanian, S.V., 2003. Fluorescence properties of Laurdan in cochleate phases. *Biochimica et Biophysica Acta (BBA) - Biomembranes* 1618, 67-78.
- Ramasamy, T., Khandasamy, U., Hinabindhu, R., Kona, K., 2009. Nanocochleate - A new drug delivery system. *FABAD J. Pharm. Sci.* 34, 91-101.
- Ramteke, K., Joshi, S., Dhole, S., 2012. Solid lipid nanoparticle: a review. *IOSR Journal of Pharmacy* 2, 34-44.
- Ranck, J.L., Mateu, L., Sadler, D.M., Tardieu, A., Gulik-Krzywicki, T., Luzzati, V., 1974. Order-disorder conformational transitions of the hydrocarbon chains of lipids. *Journal of Molecular Biology* 85, 249-277.
- Rand, R.P., Kachar, B., Reese, T.S., 1985. Dynamic morphology of calcium-induced interactions between phosphatidylserine vesicles. *Biophysical journal* 47, 483-489.

References

- Rao, R., Squillante, I., Emilio, Kim, K.H., 2007. Lipid-Based Cochleates: A Promising Formulation Platform for Oral and Parenteral Delivery of Therapeutic Agents. *24*, 41-62.
- Ruocco, M.J., Graham Shipley, G., 1982. Characterization of the sub-transition of hydrated dipalmitoylphosphatidylcholine bilayers: X-ray diffraction study. *Biochimica et Biophysica Acta (BBA) - Biomembranes* *684*, 59-66.
- Sankar, R., Reddy, D., 2010. Nanocochleate - A new approach in lipid drug delivery. *Int J Pharm Pharm Sci* *2*, 220-223.
- Santangelo, R., Paderu, P., Delmas, G., Chen, Z.-W., Mannino, R., Zarif, L., Perlin, D.S., 2000. Efficacy of Oral Cochleate-Amphotericin B in a Mouse Model of Systemic Candidiasis. *Antimicrobial agents and chemotherapy* *44*, 2356-2360.
- Sarig, H., Ohana, D., Epand, R.F., Mor, A., Epand, R.M., 2011. Functional studies of cochleate assemblies of an oligo-acyl-lysyl with lipid mixtures for combating bacterial multidrug resistance. *FASEB J* *25*, 3336-3343.
- Silvius, J.R., Gagne, J., 1984. Lipid phase behavior and calcium-induced fusion of phosphatidylethanolamine-phosphatidylserine vesicles. Calorimetric and fusion studies. *Biochemistry* *23*, 3232-3240.
- Snyder, R.G., 1967. Vibrational Study of the Chain Conformation of the Liquid n-Paraffins and Molten Polyethylene. *The Journal of Chemical Physics* *47*, 1316-1360.
- Takahashi, H., Yasue, T., Ohki, K., Hatta, I., 1995. Structural and thermotropic properties of calcium-dimyristoylphosphatidic acid complexes at acidic and neutral pH conditions. *Biophysical journal* *69*, 1464-1472.
- Tardieu, A., Luzzati, V., Reman, F.C., 1973. Structure and polymorphism of the hydrocarbon chains of lipids: a study of lecithin-water phases. *J Mol Biol* *75*, 711-733.
- Tocanne, J.F., Ververgaert, P.H.J.T., Verkleij, A.J., Van Deenen, L.L.M., 1974. A monolayer and freeze-etching study of charged phospholipids II. Ionic properties of mixtures of phosphatidylglycerol and lysylphosphatidylglycerol. *Chemistry and physics of lipids* *12*, 220-231.
- Träuble, H., Eibl, H., 1974. Electrostatic Effects on Lipid Phase Transitions: Membrane Structure and Ionic Environment. *Proceedings of the National Academy of Sciences of the United States of America* *71*, 214-219.

References

- Verkleij, A.J., De Kruyff, B., Ververgaert, P.H.J.T., Tocanne, J.F., Van Deenen, L.L.M., 1974. The influence of pH, Ca²⁺ and protein on the thermotropic behaviour of the negatively charged phospholipid, phosphatidylglycerol. *Biochimica et Biophysica Acta (BBA) - Biomembranes* 339, 432-437.
- Ververgaert, J.T., De Kruyff, B., Verkleij, A.J., Tocanne, J.F., Van Deenen, L.L.M., 1975. Calorimetric and freeze-etch study of the influence of Mg²⁺ on the thermotropic behaviour of phosphatidylglycerol. *Chemistry and physics of lipids* 14, 97-101.
- Wang, N., Wang, T., Zhang, M., Chen, R., Deng, Y., 2014. Using procedure of emulsification-lyophilization to form lipid A-incorporating cochleates as an effective oral mucosal vaccine adjuvant-delivery system (VADS). *International Journal of Pharmaceutics* 468, 39-49.
- Wasan, K.M., Wasan, E.K., Gershkovich, P., Zhu, X., Tidwell, R.R., Werbovetz, K.A., Clement, J.G., Thornton, S.J., 2009. Highly Effective Oral Amphotericin B Formulation against Murine Visceral Leishmaniasis. *Journal of Infectious Diseases* 200, 357-360.
- Zarif, L., 2002. Elongated supramolecular assemblies in drug delivery. *Journal of Controlled Release* 81, 7-23.
- Zarif, L., 2005. Drug Delivery by Lipid Cochleates, in: Nejat, D. (Ed.), *Methods in Enzymology*. Academic Press, pp. 314-329.
- Zarif, L., Graybill, J.R., Perlin, D., Najvar, L., Bocanegra, R., Mannino, R.J., 2000. Antifungal Activity of Amphotericin B Cochleates against *Candida albicans* Infection in a Mouse Model. *Antimicrobial agents and chemotherapy* 44, 1463-1469.
- Zarif, L., Jin, T., Segarra, I., Mannino, R.J., 2003. Hydrogel-isolated cochleate formulations, process of preparation and their use for the delivery of biologically relevant molecules. Google Patents.
- Zarif, L., Mannino, R., 2002. Cochleates, in: Habib, N. (Ed.), *Cancer Gene Therapy*. Springer US, pp. 83-93.
- Zarif, L., Tan, F., 2003. Cochleates made with purified soy phosphatidylserine. Google Patents.
- Zhang, S., 2003. Fabrication of novel biomaterials through molecular self-assembly. *Nat Biotech* 21, 1171-1178.
- Zhang, Y.-P., Lewis, R.N.A.H., McElhaney, R.N., 1997. Calorimetric and Spectroscopic Studies of the Thermotropic Phase Behavior of the n-Saturated 1,2-Diacylphosphatidylglycerols. *Biophysical journal* 72, 779-793.
- Zhang, Y., Chan, H.F., Leong, K.W., 2013. Advanced Materials and Processing for Drug Delivery: The Past and the Future. *Advanced drug delivery reviews* 65, 104-120.

List of Abbreviations

AFM	→	Atomic force microscopy
Amb	→	Amphotericin B
DDPS	→	1,2-didecanoyl- <i>sn</i> -glycero-3-phospho-L-serine
DMPG	→	1,2-dimyristoyl- <i>sn</i> -glycero-3-phospho-(1'-rac-glycerol)
DMPS	→	1,2-dimyristoyl- <i>sn</i> -glycero-3-phospho-L-serine
DOctPS	→	1,2-dioctanoyl- <i>sn</i> -glycero-3-phospho-L-serine
DOPS	→	1,2-dioleoyl- <i>sn</i> -glycero-3-phospho-L-serine
DPPS	→	1,2-dipalmitoyl- <i>sn</i> -glycero-3-phospho-L-serine
DSC	→	Differential scanning calorimetry
DSPS	→	1,2-distearoyl- <i>sn</i> -glycero-3-phospho-L-serine
FTIR	→	Fourier transform infrared spectroscopy
Ms	→	Milliseconds
NMR	→	Nuclear magnetic resonance
PS	→	Phosphatidylserine
SAXS	→	Small-angle X-ray scattering
SEM	→	Scanning electron microscopy
WAXS	→	Wide-angle X-ray scattering
TEM	→	Transmission electron microscopy
T _m	→	Transition temperature

Curriculum Vitae

Personal Information

Name: Kalpa Nagarsekar
Date of Birth: December 25, 1984
Nationality: Indian
Address: Lessingstr. 8 (Pharm), 07743 Jena, Germany
Telephone: + 49 3641 949907 (office)
E-mail: kalpa.nagarsekar@uni-jena.de

Education

- PhD candidate (December. 2011 – Present) Friedrich-Schiller-University Jena, Germany
Thesis title: Cochleates: New insights into drug delivery system
- Masters of Pharmaceutical Sciences (October 2006 - October 2008) University of Mumbai, Mumbai, India
Thesis title: Preparation and Evaluation of leaf extract of *Vitex negundo* Linn ,
- Bachelor of Pharmaceutical Sciences (October 2002 - July 2006) University of Mumbai, Mumbai, India

Research Experience

Doctoral Research:

- Investigations on structural features of cochleates.
- Evaluation of intermediate morphologies generating during formation pathway of cochleates
- Developing novel methodology to produce improved cochleate formulation.

Master Research:

- Preparation and characterization of the supercritical fluid extract (SCF) and ethanolic extract of leaves of *Vitex negundo* Linn
- In-vivo and in-vitro evaluation for anti-lipid peroxidation activity of the extracts.

Other projects:

- Preparation, optimization and characterization of polymer-lipid composite nanoparticulate system of Amphotericin B for splenic targeting.
- In-vivo and in-vitro evaluation of Amphotericin B formulation for toxicity.

Publications

- **Nagarsekar K**, Ashtikar M, Steiniger F, Thamm J, Schacher F, Fahr A. Understanding cochleate formation: Insights into structural evolution *Soft matter* (2015) being revised.
- **Nagarsekar K**, Ashtikar M, Steiniger F, Thamm J, Schacher F, Fahr A. Micro-spherical cochleate composites: method development for monodisperse system *Liposome research* (2015) being revised.
- **Nagarsekar K**, Ashtikar M, Thamm J, Steiniger F, Schacher F, Fahr A, May S. Electron microscopy and theoretical modeling of Cochleates. *Langmuir* (2014) 30: 13143-51
- **Nagarsekar K**, Galdhar CN, Gaikwad RV, Samad A, and Devarajan PV. Amphotericin B LIPOMER for enhanced splenic delivery. *Drug Delivery Letters* (2014) 4(3): 208-220.
- **Nagarsekar K**, Nagarsenker MS, Kulkarni SR. Antioxidant and anti-lipid peroxidation potential of supercritical fluid extract and ethanolic extract of leaves of *Vitex negundo* Linn. *Indian J Pharm Sci* (2011) 73(4):422-9.
- **Nagarsekar K**, Nagarsenker MS, Kulkarni SR. Evaluation of composition and antimicrobial activity of supercritical fluid extract of leaves of *Vitex negundo*. *Indian J Pharm Sci* (2010) 72:641-3.

Presentations

1. Oral presentations

- Insight in Morphology of cochleates at 23rd Liposome workshop, Oberjoch, Germany, March 2014.
- Cochleates: A novel drug delivery platform at 22nd Liposome workshop at Ameland, Netherlands, September 2012.

2. Poster presentations

- Insights into the morphology of cochleates, poster presentation at Liposome Research Days, Copenhagen, Denmark (August 2014).
- Insights into the morphology of cochleates, Phospholipids in pharmaceutical research symposium; Heidelberg, Germany (September 2013).
- Amphotericin B cholesterol LIPOMER: Molecular aggregation and Characterization, Controlled Release Society German Chapter Annual Meeting & International Symposium of the Thuringian ProExcellence Initiative NanoConSens, Jena, Germany (March 2011).
- Formulation and in-vitro evaluation of amphotericin B LIPOMER. , Advances in Technology and Business Potential of New Drug Delivery Systems Organized By Controlled Release Society-Indian Chapter Mumbai, India (Feb 2010).
- Ethanolic extract of leaves of *Vitex negundo*: evaluation and feasibility of formulation development. Advances in Technology and Business Potential of New Drug Delivery Systems' Organized By Controlled Release Society-Indian Chapter Mumbai, India (Feb 2009).
- Composition and anti-lipid peroxidation activity of ethanolic extract and supercritical fluid extract of leaves of *Vitex negundo* Linn, 2nd international conference on drug discovery and development – south Asian perspective Mumbai, India (Oct 2008).
- Microscopy of Nirgundi and Nutmeg, National conference in Medicinal Botany Mumbai, India (Sept 2007).

Declaration

I would like to acknowledge that I am familiar with the 'Promotionsordnung' of the Faculty of Biology and Pharmacy in the Friedrich-Schiller-University Jena. All chapters of this dissertation were produced by myself. This dissertation does not contain any material previously submitted for any degree or diploma at any other University. Also this dissertation does not contain any material previously written or published by any other person, except where due acknowledgement or reference has been made in the text. I would also like to declare that I did not enlist the assistance of any 'dissertation-counseling agent' and that I did not provide any direct or indirect monetary benefit to any third party for work connected to my dissertation.

Kalpa Nagarsekar

Jena, 23.10.2015